Report No. FRA-OR&D 75-49

A METALLURGICAL ANALYSIS OF ELEVEN STEEL PLATES TAKEN FROM A TANK CAR ACCIDENT NEAR CALLAO, MISSOURI

C. G. Interrante
G. E. Hicho
D. E. Harne

SEPTEMBER 1972
FINAL REPORT

Prepared For
DEPARTMENT OF TRANSPORTATION
FEDERAL RAILROAD ADMINISTRATION
Office of Research and Development
Washington, D.C. 20590

NOTICE

This document is disseminated under the sponsorship of the Department of Transportation in the interest of information exchange. The United States Government assumes no liability for its contents or use thereof.

Technical Report Documentation Page

1. Report No.	2. Government Accession No.	3. Recipient's Catalog No.
FRA-OR&D 75-49		

4. Title and Subtitle	5. Report Date
A METALLURGICAL ANALYSIS OF ELEVEN STEEL PLATES TAKEN FROM A TANK CAR ACCIDENT NEAR CALLAO, MISSOURI	September 1972
	6. Performing Organization Code
7. Author(s) C.G. Interrante, G.E. Hicho, D.E. Harne	8. Performing Organization Report No. 312.01/51
9. Performing Organization Name and Address National Bureau of Standards Washington, D.C. 20234	10. Work Unit No. (TRAIS)
	11. Contract or Grant No. DOT-AR-10023
12. Sponsoring Agency Name and Address U.S. Department of Transportation Federal Railroad Administration Office of Research and Development Washington, D.C. 20590	13. Type of Report and Period Covered FINAL REPORT
	14. Sponsoring Agency Code

15. Supplementary Notes

16. Abstract

A metallurgical analysis of eleven steel plate samples designed as Callao samples K-1, K-2, K-3 and K-5 to K-12 was requested by the Bureau of Railroad Safety, Federal Railroad Administration, Department of Transportation. The Callao samples were removed from a tank car numbered GATX 94451 which had been involved in an accident near Callao, Missouri where the ambient temperature was reportedly 15°F.

An investigation was conducted at the National Bureau of Standards to determine if the plate sample conformed with the Association of American Railroads (AAR) Specification AAR-TC128-65 (flange quality, grade B, fine-grain practice) for high-tensile strength, carbon-manganese steel plates for tank cars, and to gather information pertinent to the question of the suitability of this type of steel for use as plate materials of tank cars.

17. Key Words	18. Distribution Statement
Metallurgical, Tank Cars	Document is available to the public through the National Technical Information Service, Springfield, Virginia 22161

19. Security Classif. (of this report)	20. Security Classif. (of this page)	21. No. of Pages	22. Price
Unclassified	Unclassified	184	

Form DOT F 1700.7 (8-72) Reproduction of completed page authorized

TABLE OF CONTENTS

TABLES

FIGURES

FIGURES

FIGURES

FIGURES

The temperature at the accident site was reported* by FRA officials to have been +15°F. For comparison, the U. S. Weather Bureau report indicates the temperature on January 8, 1971 at Columbia, Missouri Airport (about 56 miles south of Callao) was 20°F at 6:00 A.M., and 21°F at 9:00 A.M. The speed of the train at the time of the accident was 50 miles per hour.

It should be noted that, in the specification of AAR-TC128, the mechanical properties are specified for plates in the as-rolled condition, and that the shell-plate specimens taken from the Callao plate samples for this investigation were in the as-formed and stress-relieved condition. In the accident, these plates could have received some reforming during the rupturing of the tank car.

The shapes and appearances of the plate samples designated K-1, K-2, K-5, K-8, and K-11, which were used to determine mechanical properties, and the test results of this investigation indicate that the test plate samples, except for sample K-1, had only minor or negligible amounts of reforming. It is therefore believed that the observations and properties reported in this metallurgical analysis of the plate samples are germane to the plates in the tank car in service, except where noted in the report for some of the results for sample K-1.

PURPOSE

The principal purpose of this metallurgical analysis was to determine if the Callao plate samples, taken from the tank car numbered GATX 94451, conformed with the specification AAR-TC128-65 for high-tensile strength, carbon-manganese steel plates for tank cars. Another objective of the investigation was to gather information pertinent to the question of the suitability of this type of steel for use as the plate material of tank cars.

EXPERIMENTAL PROCEDURES

Chemical analyses, tensile and bend properties were determined for comparison with the requirements of the Specification AAR-TC128-65. Specimens for these tests were taken from samples K-1, K-2, K-5, and K-8. Other specimens taken from these samples were used for impact tests, inclusion content ratings, fracture-profile analyses, hardness surveys, thickness measurements, and other macroscopic and microscopic observations.

---

* Conversations, Mr. Q. Banks (FRA) and G. E. Hicho (NBS).

In this report, the designations longitudinal and transverse mean, respectively, parallel with and perpendicular to either the principal rolling direction (in the case of specimens of the plate materials) or the welding direction (in the cases of specimens of weld-metal and heat-affected-zone regions).

For the head and shell plates of samples K-1, K-2, and K-5, the rolling directions were determined by metallographic methods. For each of the two shell-plates K-8 and K-11, the rolling direction was estimated* to be the direction parallel with the welding direction of a circumferential weld contained in the plate.

Macroscopic Observations and Thickness Measurements

The fracture surfaces of samples K-1, K-3, K-5, K-6, K-7, K-9, K-10, and K-12 were macroscopically examined, and fracture-profile sections were taken perpendicular to the fracture lines on these samples at the locations designated in Figures 4,6,7,8,9,11,12 and 14. In some plate samples, as in sample K-1 (Figure 4), several fracture-profile locations were taken in order to obtain a more general representation of the fracture. In addition, at many fracture-profile location, thickness measurements were taken to determine the extent to which plate thinning occurred near the fracture sites.

The locations and orientations of the various other test specimens used in this report are shown together with their identification codes, in Figures 4,5,7,10, and 13. With the exception of head-plate K-1, each of the plate samples shown in these figures appear to have little or no deformation due to the rupturing of the tank car. Although it was somewhat flat, sample K-1 is not badly deformed except near the outer edges of the plate. Therefore, these outer edges were not used for specimens for tests of mechanical properties of the plate.

Chemical Analysis

Check chemical analyses (by the spectrometric method) were conducted at a quarterthickness position of the chemistry samples of weld metal** and rolled plates. The weld-metal

---

* See page 3 of Reference 10.

** Although the Specification of TC128 give no chemical requirements for weld metal, a chemical analysis was obtained on weld metal from plate K-2.

sample was taken from the weld that joined the "A" head and shell course number 1 in plate sample K-2. The base metal samples were head-plate and shell-plate samples taken respectively from K-1 and K-5. The locations from which the chemistry samples were taken on each of these plates are shown in Figures 4,5, and 7. The analyses were made by the Analytical Chemistry Division, NBS.

Tensile Testing

Tensile test specimens from samples K-1, K-2, K-5, and K-8 were prepared and tested in accordance with ASTM Methods and Definition A 370-71. The tensile test specimens were 0.250* inch in diameter and were taken as nearly as possible from the quarterthickness position of each plate. Two longitudinal and two transverse tensile specimens taken from each of the two plates K-1 and K-5 represented, respectively, the head-plate and shell-plate steels. One longitudinal (all weld-metal) specimen and one transverse (joint efficiency) specimen taken from the weld joint of each of two plates, K-2 and K-8, represented the weld joint of these plates.

Bend Testing

Two longitudinal and two transverse bend-test specimens taken from each of two plates, K-2 and K-5, represented respectively the head-plate and the shell-plate steels. These were prepared with dimensions of 3/8 x 1 1/2 x 6 inches. Six of these bend specimens, four from shell-plate K-5, and two from head-plate K-2,[one longitudinal (K2-8) and one transverse (K2-5)] were tested with the outside surface of the tank car being the outer curve of the bend specimen. The remaining two bend specimens from the plate K-2, one longitudinal (K2-7) and one transverse (K2-6), were tested with the outside surface of the tank car being the inner curve of the bend.

---

* The requirements of AAR-TC128 gives minimum elongation values for gage lengths of 8 inches (1970 and 1965 Specifications) and 2 inches (1970 Specification). The overall size of the Callao sample precluded the use of the standard tensile test specimens which are commonly used to obtain elongation in 2- and 8-inch gage lengths. Therefore, 0.250 inch diameter specimens were used with a 1-inch gage length so as to provide elongation values that are directly comparable with the values specified for the 0.500 inch specimens with 2-inch gage lengths [4,5].

In accordance with ASTM A 370-71 Methods and Definitions, specimens were bent through an inside diameter of 3/4 inch, so as to satisfy the requirement that the ratio of bend diameter (d) to specimen thickness (t) be equal to 2, as required by the AAR-TC128 Specification for plate materials.

In addition, two side-bend test specimens (taken from welds in plates K-2 and K-8) with dimensions 3/8" x 6" x plate thickness, were prepared with the cross-section of the weld placed at the center of the specimen. These specimens were bent through an inside diameter of 1 1/2 inches, so as to provide the required ratio of bend diameter (d) to specimen thickness (t) equal to 4 in accordance with ASTM E 190-64 for the quided-bend test for ductility of welds.

Impact Testing

Impact tests were conducted on specimens of base metal and weld heat-affected-zone material taken from the "A" head plate and shell course number 1. In addition, weld metal specimens were taken from circumferential welds between shell courses. The specimens were taken from head-plates K-1 and K-2, and from shell-plate K-5. Weld metal and heat-affected-zone specimens were taken from plates K-2, K-8 and K-11.

Two types of impact tests were used in this investigation: dynamic-tear tests, (DT) and standard Charpy V-notch (CV) tests. Specimens for the dynamic-tear tests were full-plate-thickness specimens (nominally 11/16 inches thick for the head-plate specimens, and 5/8 inches thick for the shell-plate specimens), with length and width dimensions of 7.125 and 1.6 inches, respectively, and with a saw-cut and cold-pressed notch with a depth of 0.375 inch. The Charpy specimens were standard size and they were machined from the quarterthickness location nearest to the inside of the tank car. Dynamic-tear tests were conducted on both head-plate and shell-plate steel specimens, and the CV tests were conducted on these same steels, as well as on weld-metal specimens and on weld heat-affected-zone regions of the head-and shell-plate steels.

For all sets of impact specimens, tests were conducted over a temperature range selected to show the transition from ductile to brittle fracture. In addition, the DT test specimens* were tested at elevated temperatures up to 1300 F. This was done to simulate the response of the steel to fracture under the broad range of temperatures likely to be encountered when a tank car is engulfed in a fire.

---

* These specimens were at temperature for about 25 minutes prior to testing.

Test methods used for the DT tests were those developed [6,7] by the Naval Research Laboratory and the test methods for the CV tests were in accordance with ASTM Designation E 23-66. The experimental data were analyzed by a computer method, which calculated the curves of best fit for the available data using a least-squares method, and which then plotted the calculated curves and the experimental data with an incremental digital plotter. The scales used on the axes for these plots are those established in earlier reports [9,10]. Therefore comparisons of the various data collected to date can be readily made by overlaying two or more plots.

The orientations of specimens and notch configurations used in the impact tests and the orientation codes for these various types of impact-test specimens are given in Figure 15. Each type of specimen has a 2-letter code. The first letter of the orientation code represents the long axis of the test specimen and the second letter represents the direction of crack propagation; the letters L, T, and S were used in these codes to represent three orthogonal plate directions: longitudinal, transverse, and short-transverse (or thickness) direction. The longitudinal direction is the principal rolling direction and the standard longitudinal and transverse configurations were therefore respectively designated LT and TL. Thus, the LT specimen has its long axis in the rolling direction of the plate and the notch is oriented so as to produce crack propagation in the transverse direction (perpendicular to the rolling direction) of the plate.

The LT and TL specimens are the standard longitudinal and transverse orientations used in previous reports [8,9,10] prepared for FRA. In this report, the LT and TL specimens were used for CV tests of head-plate, shell-plate and weld-metal steels*, as well as for DT tests of head-plate and shell-plate steels. Specimens of these orientations relate to the cases involving growth of through-thickness cracks in directions parallel to the plate surfaces, and these results are generally considered to be most important.

---

* In addition, TL specimens of the weld heat-affected-zone (HAZ) regions of the head-plate and shell-plate steels were tested. It is noted later in this report that the HAZ head-plate specimens are not of the true TL orientation as defined here.

The LS and TS specimens are respectively longitudinal and transverse specimens that are notched to give crack propagation in the short-transverse (or thickness) direction of the plate. Head-plate and shell-plate CV specimens with these orientations were tested. Specimens with these orientations relate to cases involving cracks that propagate in a direction perpendicular to the plate surfaces, such as in the initial rupture of a plate in a tank car that is impacted by some external force.

The SL and ST specimens are short-transverse specimens with notches that give crack propagation in the longitudinal and transverse plate directions, respectively. CV specimens with these orientations were tested only for the head-plate steel. These orientations may relate in a general sense to cases involving fracture along planes parallel with the plate surfaces, such as occurred along the fracture edge of plate K-7 (the edge of the area marked #7 in Figure 9 and area N in Figure 26). This type of fracture is commonly called tearing.

Metallographic Observations and Hardness Testing

Representative photomicrographs (at X100) were obtained on metallographic samples taken from samples K-1 to K-3, and K-5 through K-12.

On one head-plate sample (from K-1) and on one shell-plate sample (from K-5), metallographic observations were made on three mutually perpendicular planes as defined in Figures 16 and 17. Plane A is parallel to the plate surface, plane B is a transverse plane perpendicular to the rolling direction and plane C is a longitudinal plane parallel to the rolling direction.

Two methods were used for rating inclusions in the steels: (1) ASTM E 45-63, Method A, which provides for the ratings of the JK field number of the worst field for four different types of inclusions observed in an area of 0.25 square inches on longitudinal "C" planes, and (2) a method which uses a quantitative television microscope (QTM) to determine the area percentage of inclusions at approximately X338 magnification. For this QTM method, a total of 100 fields were observed on each specimen with 50 fields taken at the center of the plate thickness, and with the remaining 50 fields taken at the two quarterthickness locations. In general, the QTM methods described in the literature [11] were used.

Rockwell B hardness measurements were taken on various plate and weld samples taken from plates K-1, K-2, K-5 and K-8. In addition, Knoop microhardness measurements were taken in the heat-affected-zone (HAZ) region near a weld of shell course number 1.

RESULTS AND DISCUSSIONS

Chemical Composition

The chemical compositions, as determined by the NBS laboratory check analyses of the chemistry samples taken from Callao samples K-1 ("A" head plate), K-5 (shell course number 1) and K-2 (weld metal), are given in Table I along with the producers ladle analyses and the chemical requirements for M128-65 and -70, Grade B steel. The results of the laboratory check analysis and the producers ladle analysis are in good agreement and they indicate that the composition of Callao samples K-1 and K-5 meet the chemical requirements for M128-65 Grade B steel.

Although the value of 0.26 percent carbon, as given for the NBS check analysis for head-plate K-1, is greater than the specified maximum ladle analysis of 0.25 percent carbon, this check analysis is within the product analysis tolerance for carbon steel plates given recently by ASTM Designation A6-70. However, it should be noted that the carbon and manganese contents of head-plate K-1 are at or near the top of the range permitted for this grade of steel.

In keeping with good welding practice, the carbon content in the weld metal is considerably lower than that of these plates.

The aluminum content of the chemical sample taken from shell-plate K-5 was determined to be less than 0.005 percent by weight (total Al). This indicates* that the steel apparently was not made to fine-grain practice [12], in an apparent violation of the requirement of AAR-TC128-65 that "the steel shall be made to fine-grain practice". Shell-plate K-5 was taken from Bethlehem Steel Corporation heat number 649Y352, which has a reported [by Bethlehem (3b)] McQuaid-Ehn Grain Size Number of 5-7. This grain size does not seem to us

---

* For fine grain practice, the expected value of total aluminum is a minimum of 0.02 t0 0.015 percent.

to be consistent with the low aluminum content of this steel.

It should be noted that the fine-grain practice requirement is somewhat unrealistic for plates that are to be used in the as-rolled condition; i.e. whenever a subsequent heat treatment above the critical (transformation) temperature for the steel will not be given, as is the case for this tank-car shell plate. The fine-grain practice is used to govern austenite grain size and is normally specified to prevent or retard grain coarsening during an annealing or a normalizing heat treatment. To a limited extent the austenite grain size may effect the resulting ferrite grain size of the product. Apart from this consideration, the fine-grain practice does not seem to us to bear directly on the question of the expected mechanical properties of the steel. The ferrite grain size is more directly correlated with the mechanical properties of the steel, whereas the fine-grain practice tends to govern the austenite grain size, which is measured in the McQuaid-Ehn test. Thus, the apparent failure to meet the requirement seems to us to be of minor significance.

Metallographic Analysis

Microstructures and inclusions of samples from the "A" head plate and from shell course numbers 1, 2 and 4 were examined. The results of these examinations are discussed below.

In addition, metallographic methods were used to determine the principal rolling direction in the two plate samples of the "A" head plate (plates K-1 and K-2) and in one of the samples of shell course number 1 (in plate K-5). The results of these determinations are shown on these plates by the rolling direction arrows in Figures 4, 5, and 7. The rolling directions were used as the references for the metallographic analysis of inclusions and microstructures of head plate K-1 and shell plate K-5. The results of this metallographic analysis are shown in Figures 16 through 23 and a discussion of these results follows.

Inclusion Morphology —— Unetched samples of head-plate K-1 and shell-plate K-5, as viewed on three mutually perpendicular planes, are shown in Figures 16 and 17, respectively. The figures show the morphology of the inclusions in these steel plates. The inclusions in the C planes (longitudinal planes) are much longer than inclusions in the B planes, indicating that the C planes are approximately aligned with the principal rolling direction for each plate. The lengths of inclusions

on the B planes of shell-plate K-5 are very short and this indicates that this shell plate received very little or no cross rolling. For the head plate K-1, the B-plane inclusions were long in comparison with those observed in the B planes of shell-plate K-5. Thus, the "A" head plate appears to have been cross rolled, but the relative lengths of inclusions on its B and C planes indicates that this plate was not extensively cross rolled.

In comparison with the appearances of inclusions on the B and C planes —— these inclusions are either lines or points —— inclusions on the A planes are planar in shape. This is not particularly evident in the photomicrographs presented here (partly due to the difficulty of preparing an A plane specimen), but it is shown in Figure 4 of reference number 9.

Microstructures of the "A" Head Plate —— The microstructures of the "A" head plate, as observed on samples from K-1 and K-2, are variable. This is shown in Figures 18 through 21. Figure 18 is a montage of the microstructures at X30 taken from one plate surface to the other. The microstructures of the outside half of the thickness of the plate, (given in the bottom part of this figure) are generally fine, and similar to that given in Figure 19. The microstructures of the inside half are coarse, with much larger pearlite colonies and comparatively coarse ferrite, similar to that given in Figure 20. This duplex of microstructures was observed in plate K-1 on three full-thickness metallographic specimens but none of the other metallographic specimens from this plate had the finer microstructure. The observed non-uniformity of microstructures is surprising to us, as we would expect a relatively uniform microstructure in plates that have been uniformly heat treated at 1650 F prior to hot forming.

This nonuniformity is important because test specimens used for determinations of mechanical properties, except for dynamic-tear specimens, were quarterthickness specimens, which means for plates of 5/8 to 11/16 inch in thickness that the specimens represent only half of the plate thickness.

The microstructure observed on a single full-thickness sample taken from plate K-2 is given as Figure 21. This structure, which is similar to that shown in Figure 20, was observed throughout the thickness of this specimen. These figures show the large pearlite colonies and ferrite of about

grain-size number 8. In addition, this steel shows some microstructural banding, particularly at locations between the plate quarter points.

Microstructures of Shell Course Number 1 —— The microstructures observed on samples from shell course number 1 were less variable than those observed in the samples from the "A" head plate. Figure 22 shows the microstructures of sample K-5 on three mutually perpendicular planes at magnifications of X 100 and X 240. These microstructures are mixtures of ferrite and pearlite. Some bands of alternate layers of ferrite and pearlite are observable at various locations on the B and C planes and they are apparent only at the lower magnification level in this figure. The ferrite was estimated to be an ASTM grain size No. 7 for samples from K-5 and K-10v, and ASTM grain size No. 8 for samples from K-6, K-3, and K-10u. The microstructures of plate K-5 are not unexpected for a carbon-manganese steel in the as-rolled condition produced in accordance with AAR-TC128-65 specifications.

Microstructures of Shell Course Number 2 —— The microstructures of samples from shell course number 2 are very similar to those observed in samples taken from course number 1. Typical microstructures taken from plates K-7 and K-8 are presented in Figure 23. These microstructures are also typical of those observed in the samples taken from K-9 and K-10w, which were also taken from shell course number 2.

Microstructures of Shell Course Number 4 —— The microstructure given for sample K-12 in Figure 23 typifies the microstructures of samples from K-11 and K-12 from shell course number 4, and it is similar to the microstructures observed in samples taken from course numbers 1 and 2, except that the pearlite colonies in this sample are larger (about ASTM grain size No. 4) and similar to the size of the coarse grained parts of the "A" head plate. The ferrite grains are estimated to be ASTM grain size No. 7 and in this photomicrograph they appear to surround or outline the coarse pearlite colonies in this steel. This microstructure is not unexpected for a carbon-manganese steel in the as-rolled condition produced in accordance with the AAR-TC128-65 specifications.

Macroscopic Observations

The macroscopic examination of the Callao samples revealed that the outside surfaces of all plates contained black and/or white paint and there was no evidence of exposure to fire on any of the plates as received at NBS although the fracture surfaces were somewhat rusted.

The results of the examinations of the fracture profiles of plate samples that contained fractures are discussed below for the "A" head plate and for plates and welds from shell course numbers 1, 2, and 4. Photographs of the fracture-profile samples are shown in Figures 24 through 28.

A tabulation of the fracture modes observed in the samples taken from tank car GATX 94451 is given in Table II. This Table indicates that twenty fracture samples were examined; sixteen have fractures which are nearly perpendicular to the plate surfaces; three have a "mixed" fracture mode; and one (through a weld) has a shear-like fracture mode.

Sixteen profile specimens have a fracture mode that is nearly perpendicular to the plate surfaces, indicating that, in general, the plates of this tank car failed in a brittle manner. Three fracture surfaces have a "mixed" fracture mode containing some combination of this perpendicular mode along with a tearing mode and a shear fracture mode. The weld specimen with the shear fracture mode is shown in Figure 28a, which is a photograph of the weld section taken from plate K-6 of shell course number 1. Photographs of fractures through the heat-affected-zone (HAZ) regions of weldments from plate K-10 of shell course number 2, are shown in Figure 28b and 28c. These photographs indicate that these HAZ regions also failed in a brittle manner.

An unusually wide circumferential weld between shell courses numbered 4 and 5 was examined and is shown in Figure 29 in a cross-sectional view.

The figure shows that at this location, a total of seven weld passes were used to join these two 5/8 inch-thick shell plates: three small weld passes, and four large weld passes which are presumably submerged-arc weld. It also shows the large and significant misalignment of these plates.

The NBS measurement of this misalignment indicates that the plates are offset approximately 0.203 inch, and this value is about 0.047 inch greater than that which is presently allowed for a circumferential weld of a 5/8 inch-thick plate.*

Hardness Measurements

The results of the hardness survey taken on samples of the "A" head plate, shell courses numbered 1 and 2, two weld-metal samples and a heat-affected zone sample are given in Table III.

The average hardness for the "A" head plate as measured on samples from plate K-1, is R_B 91.4. This value corresponds to an approximate tensile strength of 91,000 psi. In comparison, the average tensile strength obtained in tension tests of this steel is 95,600 psi.

The average hardness obtained for the shell course number 1, as measured on samples from plate K-5, is R_B 91.3 and this value corresponds to a tensile strength of 91,000 psi. The average for the tensile test results for this steel is 87,000 psi.

The average hardness for the weld metal between shell course numbers 1 and 2 is R_B 92.8. The results of micro-hardness measurements of the heat-affected zone (HAZ) of this weldment indicate that the average Knoop hardness value for the coarse-grained HAZ region is 273, and this value converts to about R_C 24 (about R_B 100). These hardness results indicate that, in keeping with good practice, this weldment was stress relieved after fabrication.

Thickness Measurements

The results of the thickness measurements taken on 16 fracture profile samples are given in Table IV. These results indicate that substantial plate thinning did not occur in any of the fracture profile samples measured.

---

* This conclusion is based on the tolerance prescribed in Appendix W, Table 15.03(a) of the AAR SPECIFICATIONS FOR TANK CARS, January 1, 1970 Ed.

Inclusion Content Ratings of Samples K-1 and K-5

The results of the inclusion content ratings for the head and shell plates of samples K-1 and K-5 are given in Table V. The Quantitative-Television-Microscope (QTM) area-percentage ratings indicate that the head and shell plates have overall inclusion contents of 0.35 and 0.33 area percent, respectively, and both steels have not more than 21 observed fields with an inclusion area equal to or greater than 0.5 percent. These results indicate that the inclusion content of this head-plate steel is slightly greater than that of the shell-plate steel, but slightly less than that of the South Bryon shell-plate sample [9].

A summary table showing the comparative cleanliness of the steels investigated to date follows:

		Overall Inclusion Content (Area %)		Number of Fields with Inclusion Area ≥ 0.5 Area %	
Accident Site	Steel	Head	Shell	Head	Shell
South Byron	M128	-	0.40	-	29
Crescent City	A212	0.19	0.13	0	2
Callao	M128	0.35	0.33	21	15

Although the literature gives very little information on the inclusion area percent expected in steel plate [10], some data is given [11] for the number of fields with an inclusion area ≥ 0.5, in 100 fields examined at X338. For production heats this number is between 1 and 28: The values obtained from the QTM observations of the Callao specimens are at the high end of this range.

The results of inclusion rating by ASTM E-45, Method A indicates that manganese sulfides are the principal types of inclusions in the plates investigated.

Bend Tests on Samples K-2, K-5, and K-8

The results of the bend tests of the shell plate from sample K-5, head plate from sample K-2 and weldments from samples K-2 and K-8 are given in Table VI and Figures 30 and 31. The side-bend specimens of the weldments passed the guided-bend tests for ductility of welds. The head-plate and shell-plate specimens that were tested with the outside surface of the

tank car being the outer curve of the bend, passed the AAR-TC128-65 bend requirement.

The transverse head-plate specimen that was tested in a non-standard manner, with the outside surface of the tank car being the inner curve of the bend, failed the bend test for plates. In this head-plate sample, K2-6, cracks were visible at an angle of bend of approximately 120°. With further bending the cracks extended until the specimen fractured into two pieces at 180° of bend. While this failure is not considered a failure of the bend requirement for this steel, the failure is instructive. This transverse specimen failed at a relatively low angle of 120° and the longitudinal specimen did not fail, indicating that the tendency for bend-test failure will be greater for transverse bend specimens.

The failed specimen was different from the specimens tested in the standard manner in that the outer curve of the bend represents the steel near the center of the plate for the non-standard test whereas it reprsents the plate surface in the standard test. In addition, the inclusion content near the plate center is greater than that near the plate surfaces. Thus, these tests indicate that the tendency to fail in the bend test increases with the inclusion content, which is dependent upon the thickness location within the plate.

Tensile Properties

The results of the tensile tests of the specimens from head plate K-1, shell plate K-5, and the weldments from plates K-2 and K-8 are given in Table VII. The results of the longitudinal and transverse head and shell-plate specimens, and the weld specimens indicate that the plates and the weldment meet the AAR-TC128-65 requirements of 19 percent minimum elongation, 50,000 psi minimum yield point, and 81,000 to 101,000 psi tensile strength. The results of the transverse weld tensile tests indicate that the strength of the weldment exceeds the required minimum; hence the weldment has a joint efficienty of 1.0 and meets the AAR requirements.

The observed strength levels of the longitudinal and transverse specimens of the "A" head plate K-1 are similar. However, the ductility of the plate, as measured by the reduction of area and the elongation, is anisotropic, with the ductility of the longitudinal specimens being greater than that of the transverse specimens. These observations also apply to the specimens of shell plate K-5.

The absence of both a distinct yield point and a lower-yield strength in specimens taken from the "A" head plate indicates that these specimens had been cold deformed prior to tensile testing. We believe that this deformation was most likely the deformation that accompanied the failure of the tank car and not deformation associated with the machining of the test specimens.

Figure 32a and 32b, respectively, show the fracture surfaces of the transverse and longitudinal tensile test specimens. All of the specimens show a cup-and-cone fracture mode in the outer surface with a region of flat fracture in the center of the specimens. The fracture appearances of the flat-central regions are somewhat lamellar for the transverse shell-plate specimens K5-1 and -2, but for all other specimens the flat-central regions are not lamellar.

Impact Test Results

The results of Charpy V-notch (CV) and dynamic-tear (DT) impact tests are given in Figures 33 through 38 and Appendices B through G for the following categories of specimens representing the "A" head plate and shell course number 1: longitudinal head-plate (Fig. 33, Appendix B), transverse and short-transverse head-plate K-1 (Fig. 34, Appendix C), longitudinal shell-plate K-5 (Fig. 35. Appendix D), transverse shell-plate K-5 (Fig. 36, Appendix E), heat-affected-zone regions of head plate and of shell plate (Figure 37, Appendix F), and weld-metal of circumferential welds (Fig. 38, Appendix G). In addition, the results of the elevated-temperature DT tests of head-plate K-1 and shell-plate K-5 are given, respectively, in Figures 39 and 40 and in Appendices H and I.

Thus, each figure represents one of these categories of specimens and shows all of the observed values and the calculated curves for the category that the figure represents. There are three lettered frames for each figure number with one letter for each of the fracture criteria: Percent shear fracture appearance is the A frame, energy absorption is the B frame and lateral expansion is the C frame. The scales of the three frames of each data set have been standardized in this and in previous [9,10] reports, so that any set of frames can be overlayed to compare various results. The values of energy-absorption obtained in the DT tests are about 10 times the values obtained in CV tests (due to the larger areas of fractures in DT tests). Therefore these energy values were divided by 10

so that they could be plotted on the standard energy scale of 100 ft-lb and in the same frame with the comparable CV data, as shown in Figures 33B, 34B, 35B and 36B. However, in Figures 39 and 40, the DT test results for elevated temperatures are plotted with a full-scale value of 1000 ft-lb, so that on these plots the energy values may be read directly.

Each appendix gives the observed and calculated results for the category that it represents. These results are given as a series of tables. The sequence of presentation of the tables within an appendix is the same as that given in the corresponding figure for that category. This sequence is given in the figures under the words SPECIMEN IDENTIFICATION shown in the upper left-hand corner of each frame. The tables in the appendices are numbered 1A, 1B, 1C, 2A, 2B, etc., with the A,B, and C designations representing the three fracture criteria, as discussed above.

Fracture Criteria —— For the CV tests, a complete data set includes results for three fracture criteria: percent shear fracture appearance, energy absorption, and lateral expansion. For the DT tests, a complete data set includes results for only the first two of the three criteria (i.e. lateral expansion is not measured in the DT tests).

Temperature Limits of the Transition Zone —— The impact test results given in this report indicate that within a given data set, the transition zone* begins and ends over roughly the same range of temperatures irrespective of the fracture criteria (A,B, or C). Furthermore, with increasing temperature over the transition zone, the magnitude of the values of energy absorption in DT and CV tests (and of lateral expansion in the CV tests) is linearly related to (nearly proportional to) the percent shear fracture appearance.

Transition-Zone Limits of Temperature: CV Tests vis-a-vis DT Tests —— The temperature limits of the transition zone differ for the two test methods, DT vs. CV. This is observed by comparing CV and DT results of tests conducted on specimens with similar orientations (i.e. either LT or TL specimens may be compared). These comparisons may be made on each of eight different frames; four of these frames contain percent-shear-fracture-appearance plots given as Figures 33A through 36A, and four contain energy-absorption plots given as 33B through 36B.

---

* The transition zone begins at the highest temperature on the lower shelf and it extends to the lowest temperature of the upper shelf.

For a given steel, the transition zone for each of the sets of CV specimens occurs over about the same range of temperatures. This is observed by comparing, for example the A frames of Figures 33 and 34. This is true for CV tests of either head-plate or shell-plate specimens. Similarly, the transition zones of the sets of DT tests of longitudinal and transverse shell-plate specimens occur over the same range of temperatures but this temperature range is about 35 F higher than that for CV tests of shell-plate specimens. This difference is not unexpected.

For the head-plate tests, the variability of test results is somewhat unexpected. The results of tests on transverse specimens indicate tht the transition occurs at higher temperatures in DT tests (by about 45 F), whereas the results of longitudinal tests indicates that the transition occurs at higher temperatures in CV tests (by about 40 F).

The impact-test behavior of this head-plate steel is unexpected in that the transition zone of HDTL* specimens occurs at lower temperatures than expected. This is believed to be due to the combined influences of microstructural inhomogeneity of the plate and of possibly cold deformation that occurred when the tank car ruptured. However, it is our view that the microstructural heterogeneity of this plate is of dominant importance in governing the variability of the behavior of these impact tests.

This view is based in part of our findings that metallographic specimens taken from impact specimens (HLI-24, HLH-10, HTG-46, HTF-63)* that had been tested in the transition zone of each of four sets of CV specimens had similar microstructures and these microstructures were similar to the microstructures of a transition-zone specimen (HDTT-38) representing the set of transverse DT specimens. However, these microstructures, as represented in Figure 20, were observed to be quite different from the microstructure of a transition-zone specimen (HDTL-60) representing the set of longitudinal DT specimens. This longitudinal specimen had the variable microstructure shown as a montage of photomicrographs in Figure 18A. The finer microstructure observed throughout the majority of the thickness of this specimen, as shown in Figure 19, is believed to have effected a decrease in the temperature of the transition zone for the HDTL set of specimens. Thus, the transition zone of the HDTL specimens occurs over a range of temperatures that is relatively low in relation to that of the CV sets of impact specimens taken from the "A" head plate.

---

* Identification codes for impact specimens are shown in Figures 4,5,7, and 13.

Transition-Zone Limits of Temperature for Various CV Orientations —— The results given in Figures 33 through 36 and 38 indicate that, for a given steel, the Charpy V-notch transition zone begins and ends over roughly the same range of temperatures irrespective of the orientation of either the specimens or the notches. This is particularly evident in the 50-percent-shear-fracture data given in Table VIII. This general behavior is also evident in Figures 33 through 36, and 38. Overlays of Figures 33 and 34, or Figures 35 and 36 show the similarities of the behaviors as a function of orientation of specimen and notch. The plots of shear-fracture appearance show this behavior most clearly. For example, an overlay of Figures 33A and 34A show that the shear-fracture appearance behaviors of the longitudinal, transverse, and short-transverse head-plate specimens are similar.

One exception to the above behavior is observed for the case of shell-plate specimens designated STB, which have the LS orientation (longitudinal specimens with crack propagation in the short-transverse direction). The results for these specimens were so highly variable that the transition curves could not be defined from the available data sufficiently to render them meaningful.

Lower-Shelf Behavior —— The lower shelf extends from very low temperatures up to the temperature at the lower limit of the transition zone of impact curves. For all orientations of specimens tested, in this region the percent-shear-fracture appearance is zero or nearly zero and the values of energy absorption vary only over a very narrow range of low values (i.e. low in relation to upper-shelf energy values) for both CV and DT tests. Similarly, in the CV tests the lateral expansion values in the lower-shelf region are low in magnitude and narrow in range.

Upper-Shelf Behavior —— The upper shelf begins at the higher temperature limit of the transition zone and extends to all higher temperatures used in the tests. In this region, the fracture appearance is 100 percent shear for both DT and CV tests and for all orientations of specimens and notches. The magnitudes of the upper-shelf values of energy absorption and lateral expansion are governed in part by the directionality of the microstructure of the material, and therefore the effect of this directionality on impact properties can be assessed by tests with specimens having various orientations of axes and notches.

The results indicate that the effects of orientation of specimens and notches on the energy-absorption behavior in DT tests are similar to the effects in CV tests. (However, the magnitude of the energy-absorption values are about 10 times greater for the DT tests and this is principally due to the larger cross sectional area of the DT specimens.) Therefore, in the discussion to follow the CV test results will be given as the principal examples, with the understanding that (where corresponding DT data is available) the results are similar in character for the DT tests.

The results indicate that, in general, the trends observed for measurements of energy-absorption data are similar to the trends observed for lateral-expansion data. Thus, for brevity, only energy-absorption data will be discussed in detail.

The shelf-energy-absorption values obtained on a given steel vary with orientation of the specimen and with orientation of the notch. As shown in Table VIII, for a given steel, the values for CV tests decrease in the order LS, LT, TS, TL, ST, SL, with the values for the ST and SL orientations being nearly equal.

As a function of Charpy V-notch specimen orientation, the shelf-energy values thus decrease in the order: longitudinal specimens, transverse specimens, short-transverse specimens. Similar results are shown in Table IX, given for the selected DT tests, in which the energy values decrease in the same order: LT, TL. This general behavior is believed to be due principally to the morphology of inclusions in the steel. An inclusion can be thought of as an orthogonal parallelepiped, with 3 orthogonal directions L, T and S as defined earlier. With this model, the dimensions of the inclusion in these directions are greatest in the L direction and smallest in the S direction. If the "plane" of the inclusion is defined as that plane which contains the L and T directions (the longest dimensions), then the effect of inclusions on the observed results of these impact tests is consistent with the following explanation for the energy absorption and lateral expansion data.

Fracture of short-transverse specimens (ST and SL orientations) occurs with the least amount of energy absorption because the fracture plane in these specimens is parallel with

the "plane" of the inclusions (i.e. it contains the L and T axes of the inclusions). In addition, the fracture plane is parallel with alternate layers of a banded microstructure and this may detract from the energy absorption in short-transverse specimens. In the other orientations, the fracture plane is perpendicular to the alternate layers of the microstructure.

In transverse specimens (TS and TL orientations), the fracture plane is perpendicular to the "plane" of the inclusions and it contains only the longest and shortest (L and S) axes of the inclusions; thus, in these specimens the progress of the crack front is damped more frequently with the tough metal matrix which contains the inclusions, and energy absorption is accordingly increased.

In the longitudinal specimens (LS and LT orientations), the fracture plane is perpendicular to the "plane" of the inclusions and the fracture plane must cut across or bisect the inclusions. Thus the fracture plane contains only the two shorter axes (T and S) of the inclusions, with the results of a further comparative enhancement of the damping action from the tough metal matrix and a concomitant increase in the energy-absorption value required for fracture.

For a given specimen orientation, either longitudinal or transverse, crack propagation in the short-transverse (S) direction requires more energy than in the corresponding transverse (T) or longitudinal (L) direction, i.e. LS compared with LT, and TS compared with TL. This occurs despite the fact that the pair of inclusion axes contained in the fracture plane is the same for both orientations (for LS and LT or for TS and TL). Therefore this effect is believed to be principally due to microstructural banding in the steel. In a banded steel, there exist alternate layers of tough ferrite and a comparatively brittle ferrite-pearlite mixture. Crack propagation in the S direction, in the LS and TS specimens, occurs by fracture which progresses through alternate layers of brittle and tough materials, with the net result of an enhanced damping action from the tough material in the alternate layers; this would be expected to give rise to greater energy-absorption values when compared with the values for the corresponding fracture along the T or L directions. Crack propagation in the T and L directions occurs through all layers of the material simultaneously and this would be expected to require comparatively less energy for fracture.

Cross-Rolling Indices for Plate Steels —— If the extent of cross-rolling of plate materials is assessed by a cross-rolling index defined here as the ratio of the maximum shelf-energy absorption in transverse specimens of TL orientation to the maximum shelf-energy absorption of longitudinal specimens of LT orientation. Then a value of 1 represents a completely cross-rolled plate and lower values represent lesser degrees of cross rolling. This index is tabulated below for the head-plate and shell-plate steels.

	Cross-Rolling Index	
	Head Plate K-1	Shell Plate K-5
CV Tests	38/54 = .70	38/75 = .51
DT Tests	420/650 = .65	377/746 = .51

It is apparent from this table that the head plate was cross rolled to a greater extent than the shell plate. However, the head plate was not fully cross rolled.

The DT results for the head plate indicate a lower index than expected, but this too might be related to the anomalous effects attributed above to microstructural differences between the longitudinal and transverse DT specimens.

Upper-shelf Behavior of Weldments —— The shelf-energy absorption values of the weld-metal (LT and TL) specimens, and of the heat-affected-zone (HAZ) specimens of both the head-plate and the shell-plate tests, are adequate and they reflect good welding practice*.

---

* We suspect that the CV values obtained for the HAZ region might not be representative of the behavior of the plate in service. This suspicion is based on our finding that the shape of the HAZ region precludes the placement of the notch uniformly along the coarse-grained region of the HAZ. (This region is considered to be the brittlest region in many weldments.) For this reason it is believed that the DT test might be a more suitable test method for determining the impact characteristics of the HAZ of weldments of plate material of thickness levels similar to those of the plate materials tested in this work. This belief is based on the presumption that while the problem of the initial placement of the notch would not be alleviated for the DT test, the crack path in the DT test is much longer than in the CV test. Then, perhaps at longer crack propagation distances, the crack front would seek and follow the brittlest region along a weldment in a manner similar to that which would obtain in the fracture along a weldment in a large plate.

Transition Temperatures in CV Tests —— As was discussed above, for a given steel the limits of the transition occur at the approximately same temperatures irrespective of the fracture criteria and irrespective of the orientations of the specimens or of the notches. In addition, the value of the fracture criteria in the lower shelf is independent of the orientations. With this in mind it becomes apparent that the 15 ft-lb or the 15 mil transition temperatures will be in the inverse order of the upper-shelf values of either energy absorption or lateral expansion. For example, the shelf-energy absorption values for the head plate K-1 decrease in the order LS, LT, TS, TL, ST, SL and the corresponding 15 mil transition temperatures for these specimens are respectively 10, 41, 64, 64, 170, and 175 F. The other series of transition temperatures for a given steel, as shown in Table VIII, follow this same trend for their various orientations of specimens and notches.

In addition, the results given in Table VIII indicate that the transition zone for the shell plate occurs at lower temperatures than that for the head plate. Taking into account only the more conventional longitudinal (LT) and transverse (TL) specimens, the transition temperature for the shell plate is about -1°F based on a 15 ft-lb criteria and it is 6°F based on a 15 mil criteria. The corresponding values for the head-plate steel are respectively 64 and 52°F. The 50-percent-shear fracture transition temperatures are 92°F for the head and 56°F for the shell. The various transition temperatures are within the range of temperatures in which tank cars are normally used in service.

The behavior of weld-metal and heat-affected-zone* specimens shown in Table VIII indicate that the impact characteristics of these weldments are much more favorable, e.g. 15 ft-lb av. values of -37 and -48°F, respectively. These values reflect good welding practice.

Transition Temperatures in DT Tests —— The results of dynamic-tear tests given in Table IX indicate that the nil-ductility-transition (NDT) temperatures are about 40 F for the head plate and about 34 F for the shell plate; and that the average temperatures for 50-percent-shear-fracture appearance and 50-percent-maximum-energy absorption are respectively 90 F and 82 F for the head-plate steel and 92 F and 87 F for the shell-plate steel. It is noted that for the

---

* See footnote on page 22 for a comment on these HAZ tests.

head-plate specimens, all of these temperatures are much higher for the transverse than for the longitudinal determinations and these differences are believed to be due to the microstructural variability of this head-plate steel.

Elevated-Temperature Dynamic-Tear Tests —— These results are given in Figures 39 and 40, in Appendices H and I and in Appendix B Table 3, Appendix C Table 6, Appendix D Table 3, Appendix E Table 3, and in Table IX. The results indicate that the linear relationship* between percent-shear-fracture appearance and energy absorption holds only for tests conducted at temperatures up to the beginning of the upper shelf. With further increases in temperature, the fracture mode continues to be 100 percent shear, but the energy-absorption values are variable and the energy-absorption plots have minimum values at temperatures near 1050 F (see Figures 39 and 40).

For each of the four sets of tests shown in these plots, a minimum value of energy absorption occurs in the range of temperatures from 850 to 1100 F, depending on the steel and the specimen orientations. For three of these sets, the minima fall within a narrow range of 1000-1100°F. The fourth set, HDTL, gave a minimum at 850°F, which may be misleading because a measurement was not taken at 1100°F.

The results of tests of transverse head-plate specimens indicate that the magnitude of the decrease in upper-shelf energy-absorption values at elevated temperatures can be greater than 50 percent of the maximum energy absorption as measured over the usual range of impact test temperatures.

General Discussion

The purposes of this investigation were to determine if the plate samples taken from tank car GATX 94451, involved in an accident near Callao, Missouri, conformed with specifications for tank car materials, and to gather information pertinent to the more general question of the suitability of these materials for use in this application in the future.

For the most part the materials meet the required specifications. The results of the NBS laboratory check chemical analyses indicated that all samples tested meet their respective chemical requirements. However, plate sample K-5, taken from the shell course number 1, apparently was not made to fine-grain practice. The results of mechanical tests on specimens taken from the "A" head plate, weld metal and shell course number 1,indicate that all of these steels meet the bend and tensile requirements for M128 steel, and the weld joint efficiency is 1.

---

* See the earlier discussion of "Temperature Limits of the Transition Zone" given on page 17.

Additional information obtained from fracture surface analyses, metallographic sections, hardness traverses, and impact tests may be useful in later analyses of the general question mentioned above. The tests of impact properties were most extensive and they may be of great importance in the final analysis of the general question.

Our examinations of the fracture edges of the Callao plate samples indicated that shear fracture was predominant only on a fractured weld-metal sample, indicating a ductile fracture mode in this weldment. In general, little or no shear fracture and/or plate thinning were observed in the case of the base-metal and heat-affected-zone fractures, indicating brittle modes of fracture predominated in almost all of the failed parts of the tank car that were examined.

The fracture modes observed on fracture edges of these plate samples are consistent with the measurements of the impact characteristics (given in this report) for the head-plate, shell-plate and weld-metal steels tested. The tank car apparently failed upon impact with a part of a bridge and it is estimated that the temperature of the steel of the tank car was about 15°F when this occurred. Steels with nil-ductility-transition (NDT) temperatures at and above this temperature would be expected to fail in a fast, brittle-fracture mode under severe impact conditions. The averages of estimated NDT temperatures of the head-plate and shell-plate steels tested were about 40 F and 38F respectively. Thus, brittle failure was virtually assured for these steels under severe impact conditions at 15°F.

The multiplicity of orientations of Charpy V-notch tests conducted on the head-plate and shell-plate steels can be used in a more general way, to understand the behavior of these steels under the variety of conditions that lead to failure. The results indicate that anisotropy of the upper-shelf energy absorption is three dimensional. Furthermore, it was found that, for a given steel tested under various orientations of specimens and notches, the transition temperatures (such as those for 15 ft-lb or 15 mil criteria) are in inverse order to the upper-shelf values of these criteria, as measured for the various notch and specimen configurations.

In contrast with this behavior, the shear-fracture-appearance criteria was much less affected by orientation of either the specimen or the notch, at least for tests conducted by a given test method, either Charpy V-notch (CV)

or dynamic tear (DT). The observed differences in the shear-fracture-appearance data for various orientations of specimens and notches seem to be related only to gross microstructural variations in the steel tested. This was demonstrated for the case of the DT tests and it is believed to be true in a general sense for CV tests as well.

The results of impact tests and metallographic examinations of numerous specimens taken from the "A" head plate indicate that this plate is very heterogeneous. Gross microstructural heterogeneity was observed in this plate, and this heterogeneity was used to explain the anomalous relation between the CV and DT impact results for the plate. It is believed that this heterogeneity would give rise to heterogeneity in some of the mechanical properties of the plate in service. It is believed furthermore that the thermal treatment associated with the hot forming process was principally responsible for the observed heterogeneity in the microstructural and impact characteristics of this steel plate.

The results of the CV and DT impacts tests indicated to us that the effects of heterogeneity of microstructure in steel plates can be detected more readily in DT tests because (1) the full plate thickness can be tested in DT tests of steels of the thickness levels commonly used in tank car construction and (2) in a given set of specimens used to establish the ductile-to-brittle transition, the area of fracture surface generated in the DT tests is greater than that for the CV tests. It is also noted that for the "homogeneous" steels tested the transition zone occurs at higher temperatures for DT tests than for CV tests.

The results of DT tests conducted at elevated temperatures in the range of temperatures from 300 to 1300 F indicated that there is a minimum in the energy-absorption behavior of both the head-plate and the shell-plate steels, with this minimum occurring at temperatures near 1050 F. At this minimum, the magnitude of the measured value of energy absorption can be less than 50 percent of the usual value of upper-shelf energy absorption as measured at temperatures below 300 F. The importance of these findings is not clear at this time, but they may warrant further investigations of the effect of time at elevated-temperatures on impact properties of these steels.

In previous reports [9,10], energy-absorption values for longitudinal specimens of the LT orientation, for steel of various strength levels were taken from the literature [14] for comparison with the values obtained in our exploratory studies of the impact properties of tank car steels. The results to date are summarized in Figure 42. Analyses given in the previous reports [9,10] seem to be sufficient for explaining the data added from the results of the present work. However, it is noted that the comparatively low value of energy absorption of the M128 steel of head plate K-1 is to be explained in part by the fact that this steel was somewhat cross-rolled and this process is expected to decrease the value for LT specimens while it increases the value for TL specimens.

SUMMARY AND CONCLUSIONS

1. The Callao samples investigated in this report include a total of 11 steel plates of M128-B steel. These samples were designated K-1 to K-3 and K-5 to K-12, all of which were taken from a failed tank car designated GATX 94451. The samples selected for tests of mechanical properties and of chemical composition were taken from the "A" head plate, from shell course number 1, and from circumferential weldments of the tank car.

2. The chemical compositions of the samples taken from the "A" head plate and from shell course number 1 meet the chemical requirements of AAR-TC128-65, Grade B steel. However, the results of a determination of the aluminum content of a chemical sample taken from shell course number 1 indicates that this plate was apparently not made to fine-grain practice, in an apparent violation of the requirements of AAR-TC128-65.

3. The results of tensile tests indicated that the head plate, the shell plate and the weldment meet the tensile requirements for M128 steel, and that the weld joint efficiency is 1.

4. The results of bend tests indicated that the head-plate and shell-plate steels passed the AAR-TC128 bend requirements for plates and the weldment passed the guided-bend test for welds.

5. Results of bend and tensile tests and chemical analyses of weld samples indicated that, in general, good welding practices were used in the fabrication of the welds examined. However, one exception was observed: The misalignment of a circumferential weld was measured to be offset by about .05 inch greater than that allowed in the AAR SPECIFICATIONS FOR TANK CARS, 1970 Edition.

6. Although the head-plate steel meets the mechanical property requirements, the results of metallographic examinations and impact tests indicate that the thermal treatment used in the hot forming of this head plate resulted in an undesirable nonuniformity in some of the mechanical properties of this plate.

7. Both the calculated nil-ductility-transition (NDT) temperatures from dynamic tear-tests and the transition temperatures from Charpy V-notch tests were higher for the "A" head plate than for shell course number 1, and for both steels these temperatures are within the range of temperatures in which tank cars are normally used in service and above the temperatures at which this tank car reportedly failed.

8. The results of thickness measurements and the appearances of fracture profile samples of failed parts of the tank car indicated that the steels examined had fractured with predominantly brittle fracture modes, except for a failed weld-metal sample.

9. The measurements of the impact characteristics of the head- and shell-plate steels indicated that under conditions of severe impact and at the reported temperature of the tank car at the time of the accident, these steels would be expected to fail in a brittle manner.

10. The results of impact tests indicated that:

    a. The transition from ductile to brittle failure occurs at temperatures that in general are higher in dynamic-tear (DT) tests than in Charpy V-notch (CV) tests.

    b. With a given test method for each of two steels tested, the transition from ductile to brittle failure occurs over roughly the same temperature range irrespective of the orientations of the specimens and the notches in the specimens and this invariance holds for each of three fracture criteria used in the CV tests and for each of two fracture criteria used in the DT tests.

c. Upper-shelf energy absorption, as measured at temperatures below 300 F has a three-dimensional anisotropy in the steels tested. An explanation of the nature and causes of this anisotropy in terms of inclusion shape and banding is given in this report.

d. The relationship between upper-shelf energy absorption, as measured in DT tests, versus temperature, in the range from 300 to 1300 F, has a minimum value at temperatures estimated to be near 1050 F for both the head-plate and shell-plate steels tested.

e. This minimum value can be less than 50 percent of the energy absorption value of upper-shelf energy as measured at temperatures below 300 F.

ACKNOWLEDGMENT

The dynamic-tear tests of specimens reported here were conducted at the Naval Research Laboratory. The authors wish to thank W. S. Pellini, E. A. Lange and their fellow workers for their kind cooperation and assistance.

REFERENCES

1. Correspondence between Mr. A. J. Eiber, Battelle Memorial Institute, Columbus Laboratories, and Mr. E. A. Phillips, Project Director, Association of American Railroads, Chicago, Illinois, entitled "Preliminary Data on Macon, Missouri, Tank Car Failure."

2. Memorandum, dated March 10, 1971, from Mr. Mac E. Rogers, Director, Bureau of Railroad Safety, Department of Transportation to Mr. George E. Hicho, NBS.

3a. United States Steel Corporation, Homestead Works, Metallurgical Report dated April 19, 1969.

3b. Bethlehem Steel Corporation, Johnstown Works, Metallurgical Report dated April 12, 1969.

4. George E. Dieter, "Introduction to Ductility", Ductility, ASM, Metals Park, Ohio, 1968.

5. The Making, Shaping and Treating of Steel, U. S. Steel Seventh Edition, 1957, p. 892.

6. E. A. Lange and F. J. Loss, "Dynamic Tear Energy - A Practical Performance Criterion for Fracture Resistance", Naval Research Laboratory, November 17, 1969.

7. E. A. Lange, P. P. Puzak, and L. A. Cooley, "Standard Method for the 5/8 Inch Dynamic Tear Test", Naval Research Laboratory Report 7159, August 27, 1970.

8. G. E. Hicho, D. E. Harne, "Hazardous Materials Tank Cars - Evaluation of Tank Car Shell Construction Materials", U. S. Department of Commerce, National Bureau of Standards, September 28, 1970.

9. C. G. Interrante, G. E. Hicho, "Metallurgical Analysis of A Steel Shell Plate Taken From A Tank Car Accident Near South Byron, New York, U. S. Department of Commerce, National Bureau of Standards, October 22, 1971.

10. C. G. Interrante, G. E. Hicho, and D. E. Harne, "A Metallurgical Analysis of Five Steel Plates Taken From A Tank Car Accident Near Crescent City, Illinois", U. S. Department of Commerce, National Bureau of Standards, March 10, 1972.

11. R. A. Rege, W. D. Forgeng, Jr., D. H. Stone, and J. V. Alger, "Microcleanliness of Steel-A new Quantitative TV Rating Method", Application of Modern Metallographic Techniques, ASTM ASP 480, American Society for Testing and Materials, 1970, pp. 249-272.

12. Basic Open Hearth Steelmaking, Physical Chemistry of Steelmaking Committee, Iron and Steel Div. AIME, 1951, p. 361.

13. E. A. Lange and L. A. Cooley, Factors Determining the Performance of High-Strength Structural Metals (Nil-Ductility Transition Temperature in 5/8-Inch Dynamic Tear Energy for Steels). Report of NRL Progress, May 1971, p. 33.

14. J. H. Gross, "The Effective Utilization of Yield Strength", Journal of Engineering for Industry, 1971, ASME Paper No. 71-PVP-11.

Table I. Chemical Composition* of the Callao Samples

Element		Percent by Weight: Specification AAR-M128-Grade B Ladle Analysis 1965	Specification AAR-M128-Grade B Ladle Analysis 1970	NBS Laboratory Check Analysis K-1 (Head)	NBS Laboratory Check Analysis K-5 (Shell)	NBS Laboratory Check Analysis K-2 (Weld)	Producer's Ladle Analysis* K-1**	Producer's Ladle Analysis* K-5***
Carbon	Max	0.25	0.25	0.26	0.23	0.15	0.24	0.20
Manganese	Max	1.35	1.35	1.25	1.15	1.09	1.30	1.18
Phosphorus	Max	0.040	0.040	0.012	0.012	0.014	0.011	0.014
Sulfur	Max	0.050	0.050	0.028	0.014	0.019	0.026	0.028
Silicon	Max	0.30	0.30	0.21	0.20	0.55	0.26	0.24
Vanadium	Max	(+)	0.08	0.035	< 0.01	0.016	0.05	(+)
Copper	Max	0.35	0.35	0.10	0.27	0.17	0.11	(+)
Nickel	Max	0.25	0.25	0.06	0.16	0.08	0.19	0.09
Chromium	Max	0.25	0.25	0.18	0.10	0.11	0.05	0.15
Molybdenum	Max	0.08	0.08	0.020	0.010	0.018	0.05	(+)
Aluminum	(+)	(+)	(+)	0.026	< 0.005	0.008	(+)	(+)
Columbium	(+)	(+)	(+)	< 0.01	< 0.01	< 0.01	(+)	(+)
Zirconium	(+)	(+)	(+)	< 0.01	< 0.01	< 0.01	(+)	(+)
Titanium	(+)	(+)	(+)	< 0.01	< 0.01	< 0.01	(+)	(+)

* These values were obtained by optical emission spectrometric analysis.

** The U.S. Steel Corporation heat number for head plate K-1 is 69E247 (McQuaid-Ehn grain size 8).

*** The Bethlehem Steel Corporation heat number for shell plate K-5 is 649Y352 (McQuaid-Ehn grain sizes 5-7).

(+) Not specified or not determined.

Table II. Fracture Modes Observed in Specimens Taken from Tank Car GATX 94451

Sample	Head or Shell Plate	Corresponding Figures	Profile Area	Fracture Mode
K-1	"A" Head	4, 24	A	NP(a)
		4, 24	B	NP
		4, 24	C	NP
K-3	Shell Course 1	6, 25	D	NP
		6, 25	E	NP
		6, 25	F	NP(b)
K-5	Shell Course 1	7, 25	I	NP
		7, 25	J	NP
K-6	Shell Course 1	8, 25	K	NP
		8	L (weld metal)	Shear
K-7	Shell Course 2	9, 26	M	NP
		9, 26	N	Mixed
K-9	Shell Course 2	11, 26	Q	NP
		11, 26	R	NP
		11, 27	S	Mixed
		11, 27	T	Mixed
K-10	Shell Course 2	12, 27	U	HAZ(c)
		12, 27	V	NP
		12, 27	W	NP
K-12	Shell Course 4	14, 27	X	NP

(a) Brittle fracture which propagates in a plane that is nearly perpendicular (NP) to plate surfaces.
(b) This specimen appears to have been slightly bent prior to fracture.
(c) Brittle fracture that propagates along the heat-affected zone of a weld.

Table III. Results of Hardness Surveys Taken on Specimens from Tank Car GATX 94451

Specimen	Sample Location	Hardness (Rockwell B)	Averages R_B	
K-1 ("A" Head Plate)	Figure 4, Area F	88.0, 88.0, 93.0, 94.0, 88.0, 92.0, 91.0, 90.0, 91.0	(90.6)	91.4
K-2 ("A" Head Plate)	Figure 5, "Hardness Survey Area"	92.5, 91.5, 90.5, 94.5, 94.0, 92.0, 92.5, 91.0	(92.3)	
K-5 (Shell Course Number 1)	Figure 7, Area G	89.5, 90.5, 91.0, 88.0, 88.0, 88.0, 90.0, 90.0, 90.5	(89.5)	91.3
K-8 Shell Course 1	Figure 10, "Hardness Survey Area"	92.0, 91.5, 94.5, 96.0, 95.0, 93.0, 92.5	(93.5)	
K-8 Shell Course 2	Figure 10, "Hardness Survey Area"	90.0, 89.5, 88.5, 87.5, 89.0, 89.0, 90.5, 90.0, 90.0		89.3
Weld of K-2	Weld Between Shell Course Number 1 and the "A" Head Plate	94.0, 94.0, 91.5, 92.5, 92.0		92.8
Weld of K-8	Weld Between Shell Course Numbers 1 and 2	89.0, 89.0, 94.0, 96.0		92.0
Heat-Affected Zone of K-8	Weldment of Shell Course 1	Average of 15 Knoop hardness determinations was 273, which converts to Rockwell "C" 24		R_C 24

Table IV. Thickness Measurements Taken on the Fracture Profile Samples From Tank Car GATX 94451

Distance from the Fracture Surface (in.)	Samples from K-1, "A" Head Plate			Shell Course Number 1							Shell Course Number 2					
				Plate K-3			Plate K-5		Plate K-6		Plate K-7			Plate K-9		
	Area A	Area B	Area C	Area D	Area E	Area F	Area I	Area J	Area K	Area L	Area M	Area N	Area Q	Area R	Area S	Area T
0	.660	.670	-*	.631	.642	.642	-	.627	.643	.641	.638	.646	.635	.641	.636	.643
0.1	.662	.674	-	.631	.642	.642	.630	.627	.643	.641	.638	.647	.637	.643	.636	.645
0.2	.662	.677	.650	.634	.643	.643	.634	.627	.644	.641	.638	.649	.637	.643	.637	.646
0.3	.662	.677	.652	.634	.644	.644	.635	.628	.645	.641	.638	.650	.638	.644	.637	.647
0.4	.666	.675	.654	.632	.643	.644	.636	.630	.645	.642	.638	.650	.639	.645	.637	.647
0.5	.666	.672	.653	.632	.644	.645	.637	.630	.645	.642	.638	.651	.639	.646	.637	.648
0.6	.668	.673		.633	.644	.645	.639	.631	.646	.643	.638	.651	.639	.646	.638	.648
0.7	.668	.674		.632	.644	.645	.639	.631	.647	.643	.638	.652	.638	.647	.639	.649
0.8	.668	.674			.645		.641	.631	.648	.644	.638	.652	.639	.648	.640	.649
0.9	.668	.674			.645		.642	.632		.644	.641	.652	.639		.641	
1.0							.643	.634		.644	.644	.653			.641	
1.25							.643	.637			.646				.642	
1.50							.643	.639			.648					
1.75								.641			.649					
2.0								.641			.651					

* No measurements taken due to deformation near fracture edge after the failure.

Table V. Inclusion Content Ratings of Head Plate K-1 and Shell Plate K-5

QTM Ratings (inclusion area percent)

Specimen Identification	1/4 Thickness Position	Midthickness Position	3/4 Thickness Position	Number of Fields with Inclusion Area > 0.5*	Worst Field	
					Quarter thickness	Mid-thickness
A: Magnification X338						
1. Head Plate K-1 (see Fig. 4)						
Area K1-IA	0.32	0.34	0.18	14	0.58	0.71
Area K1-IB	0.28	0.15	0.25	5	0.96	0.44
Area K1-IC	0.54	0.34	0.77	45	1.30	1.05
Averages	0.38	0.28	0.40	21	0.95	0.73
2. Shell Plate K-5 (see Fig. 7)						
Area K5-I5D	0.34	0.35	0.39	16	0.99	0.70
Area K5-I5E	0.26	0.25	0.42	14	0.98	0.68
Averages	0.30	0.28	0.41	15	0.98	0.69

ASTM E-45 Method A Ratings (in JK Field Number)
(Based on worst field in 0.25 square inch per specimen)

Specimen Identification	Type A**		Type B		Type C		Type D	
	Thin	Heavy	Thin	Heavy	Thin	Heavy	Thin	Heavy
Area K1-IA	2.3	0	1.3	1.8	0	0	0	0
Area K1-IB	2.5	0	1.2	0	0	0	1.6	0
Area K1-IC	2.7	0	1.6	0	0	0	0	0
Area K5-I5D	2.7	0	1.2	1.0	0	0	0	0
Area K5-I5E	2.7	1.4	1.0	1.3	0	0	1.0	0

* per 100 fields at X338 magnification.
** Type A, B, C, D inclusions are defined in ASTM E-45.

Table VI. Bend Test Results of Specimens Taken from Tank Car GATX 94451

Orientation	Sample Number	Ratio of Bend Diameter to Thickness	Angle of Bend	Comments
Plate Specimens Tested in Accordance with Bend Test Requirements for Plates				
Shell Plate				
Longitudinal	K5-3	2.0	180°	Passed
Longitudinal	K5-4	2.0	180°	Passed
Transverse	K5-1	2.0	180°	Passed
Transverse	K5-2	2.0	180°	Passed
Head Plate				
Longitudinal	K2-7	2.0	180"	Passed*
Longitudinal	K2-8	2.0	180°	Passed
Transverse	K2-5	2.0	180°	Passed
Transverse	K2-6	2.0	120°	Cracks at 120°, fractured completely at 180°.*
Side Bend Specimens Tested in Accordance with Requirements of Guided-Bend Test of Welds				
Plate #2	K2	4.0	175°	Passed
Plate #8	K8	4.0	175°	Passed

* Unlike the other plate specimens, these specimens were tested with the outside surface of the tank car being the inner curve of the bend. Failure of these specimens is not considered to be evidence for failure of the bend requirements of the specification.

Table VII. Tensile Properties of Specimens Taken From Tank Car GATX 94451

Code	Orientation	Yield Point (psi)	Lower Yield Strength (psi)	Yield Strength, 0.2% Offset (psi)	Tensile Strength (psi)	Reduction of Area (percent)	Elongation (percent)
M128 Head-Plate Steel Taken from Sample K-1							
HL-7	Longitudinal	none	none	62,500	98,200	61.3	25.2
HL-8	Longitudinal	58,200	57,000	58,100	88,700	63.4	29.8
Average	Longitudinal			(60,300)	(93,450)	(62.4)	(27.5)
HT-5	Transverse	none	none	54,200	96,400	56.9	23.8
HT-6	Transverse	none	none	62,300	99,000	52.0	23.9
Average	Transverse			(58,250)	(97,700)	(54.5)	(23.9)
M128 Shell-Plate Steel Taken from Sample K-5							
ST-3	Longitudinal	58,800	57,000	57,400	87,200	69.2	30.7
ST-4	Longitudinal	57,500	55,700	56,000	86,700	69.8	30.6
Average	Longitudinal	(58,150)	(56,350)	(56,700)	(86,950)	(69.5)	(30.7)
ST-1	Transverse	57,400	54,800	54,800	86,600	56.3	28.1
ST-2	Transverse	57,100	55,700	56,100	87,300	58.2	28.0
Average	Transverse	(57,250)	(55,250)	(55,450)	(86,950)	(57.3)	(28.1)
Weld Metal Taken from Samples K-2 and K-8							
W9	Longitudinal	none	none	61,700	84,100	62.1	30.0
W10	Longitudinal	60,400	59,200	59,200	82,500	62.3	17.8
Average	Longitudinal			(60,450)	(83,300)	(62.2)	(23.9)
W11	Transverse	60,800	60,000	58,400	83,000	63.2	18.6
W12	Transverse	none	none	62,400	86,500	59.5	18.5
Average	Transverse			(60,400)	(84,750)	(61.4)	(18.6)
TC 128-65 Specification	(a)	(a)	(a)	51,000 minimum	101,000 max. 81,000 min.	(a)	19.0 minimum (b)

(a) Not specified.

(b) TC 128-65 specifies elongation in 8 inches only. However, TC 128-70 specifies values for both 2 inches and 8 inches, with the 2 inch value representing the standard 0.500 inch diameter round specimens. Values were obtained in these tests with 0.250 inch-diameter specimens and the gage length was adjusted to 1-inch so as to give results that are directly comparable with specified elongation requirements.

Table VIII. Charpy V-Notch Impact Test Results for Specimens From Tank Car GATX 94451

Specimen Orientation (a)	Specimen Identification and Location (b)	Transition Temperatures, F			Maximum Shelf Energy Absorption, ft-lb
		15 ft-lb Energy Absorption	15 Mil Lateral Expansion	50 Percent Shear Fracture	
Steel From "A" Head Plate					
Longitudinal Specimens					
1 LS	HLI	4.0	10.1	83.0	85.9
2 LT	HLH	55.6	40.7	85.8	54.0
Steel From "B" Head Plate					
Longitudinal Specimens					
1 LS	STB	(e)	(e)	(e)	>120.2
2 LT	STA	- 4.8	- 4.4	60.6	74.5
Transverse Specimens					
3 TS	SLD	- 1.8	3.0	46.8	54.8
4 TL	SLC	3.3	14.8	52.3	57.8
Weld Metal					
Longitudinal Specimens					
1 LT	WL	- 34.3	- 30.0	60.8	74.7
Transverse Specimens					
2 TL	WT	- 39.1	- 35.5	59.2	60.1
Heat-Affected Zone					
Head-Plate K-2					
TL (d)	HT	- 49.4	- 52.0	- 16.5	69.1
Shell Plate K-5					
TL	HK	- 45.6	- 45.3	- 3.8	44.8

Footnotes (a) through (e) are given on the next page.

Table VIII. (Continued)

(a) Orientation Code is given in Figure 15.
(b) See Figures 4, 5, 7, 10, and 13 for locations of specimens.
(c) Upper shelf values for these specimens are
13.9 ft-lb at 210 F and
13.5 ft-lb at 160 F.
(d) The orientation code for these HAZ specimens of the head-plate steel applies to the direction of welding. The angle between specimen axis and the principal direction of rolling of the plate is about 45° as shown in Figure 5, and thus these results should be intermediate between the values that would obtain with true longitudinal and true transverse specimens.
(e) This set of specimens has highly variable impact characteristics, and no valid estimate could be derived from the available data.

Table IX. Results of Dynamic-Tear Tests for Specimens from Tank Car GATX 94451

	Specimen			Estimated NDT[c] Temperature (F)		50 Percent Shear Fracture	50 Percent Maximum En. Abs.		Maximum Shelf En. Absorption[d]	Approximate Minimum Along Upper Shelf[e]	
	Thickness (inch)	Orientation (a)	Designation (b)	(@ 100 ft-lb)	(@ 75 ft-lb)	Temp. (F)	(ft-lb)	Temp. (F)	(ft-lb)	(ft-lb)	Temp (F)
"A" Head Plate											
Longitudinal	11/16	LT	HDTL	12	3	47	325	43	650	445	850
Transverse	11/16	TL	HDTT	83	61	133	210	121	420	195	1050
Average				48	32	90	268	82	535	320	950
Shell Plate K-5											
Longitudinal	5/8	LT	SDTL	42	17	96	373	95	746	425	1000
Transverse	5/8	TL	SDTT	47	29	87	189	79	377	257	1100
Average				45	23	92	281	87	562	341	1050

(a) Orientation codes are given in Figure 15.

(b) Designations as given in Figures 4 and 7.

(c) Based on recommendations given in Reference 13.

(d) For temperatures below 300 F only.

(e) For temperatures above 300 F only.

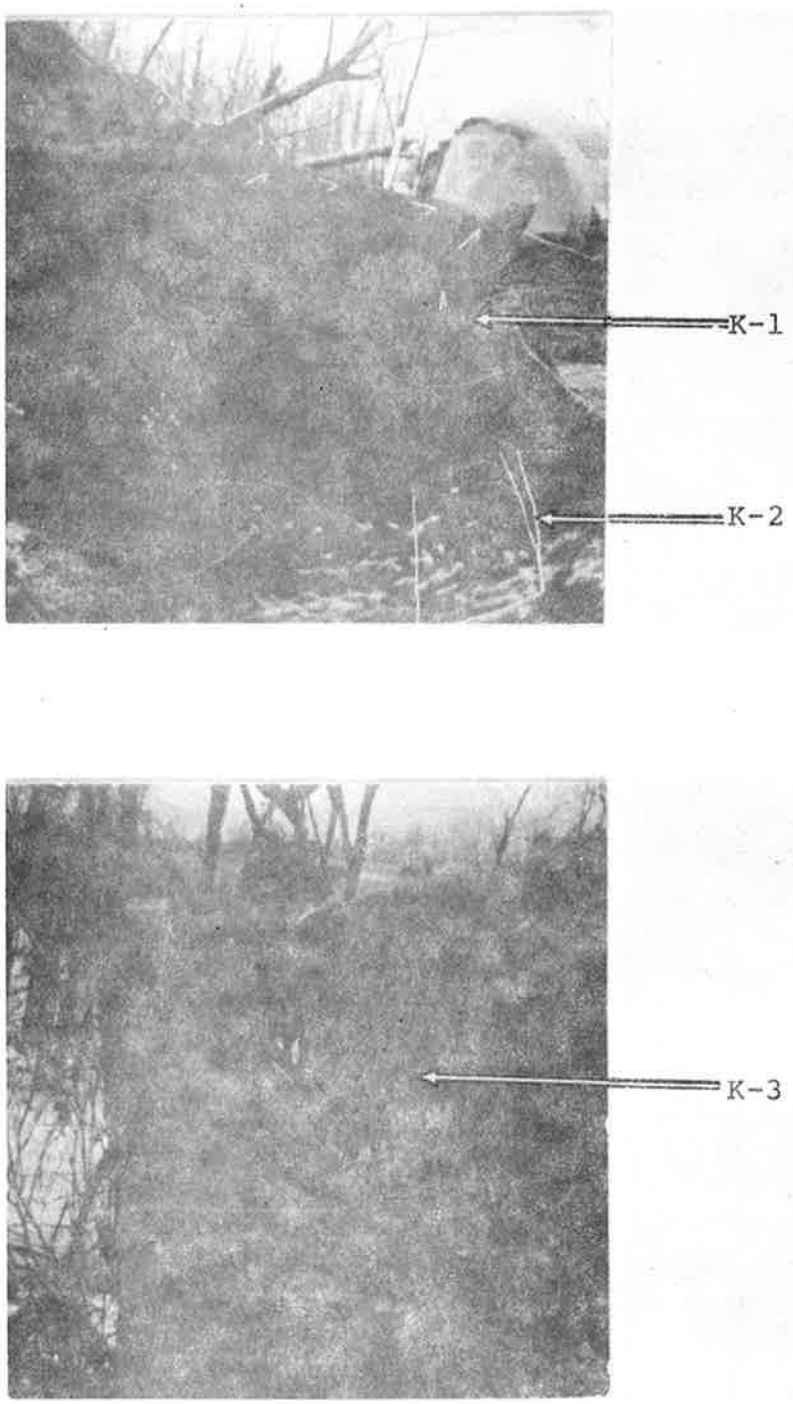

Figure 1. Photographs Showing Samples K-1, K-2, and K-3 at the Scene of the Accident.

Both photographs were taken from the inside of the tank car.

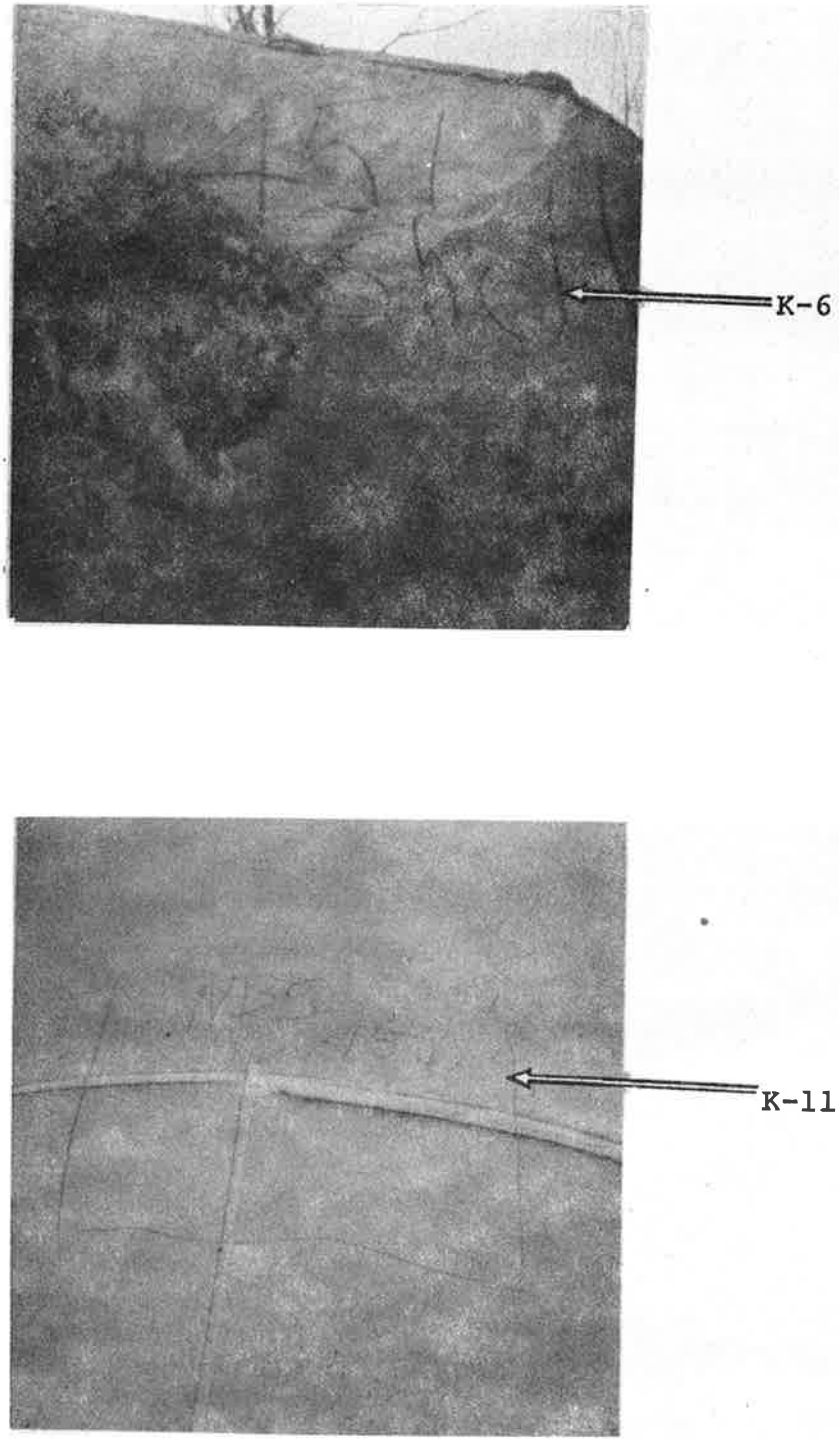

Figure 2. Photographs Showing Samples K-6, and K-11 at the Scene of the Accident.

Both photographs were taken from the outside of the tank car.

Figure 3. Schematic Diagram Showing the Location of Samples In Tank Car GATX 94451, Viewed From the Outside.

The shaded areas represent the locations of the samples sent to NBS for investigation. The sample locations selected by the AAR investigators are those outlined with the dashed lines and marked AAR.

The symbols, T.S. and ⟶, were placed on the drawing by AAR investigators. T.S. refers to a tearing shear fracture and ⟶ is an arrow which points in the same direction as the chevrons on the fracture surface and in a direction opposite to the direction of fracture propagations.

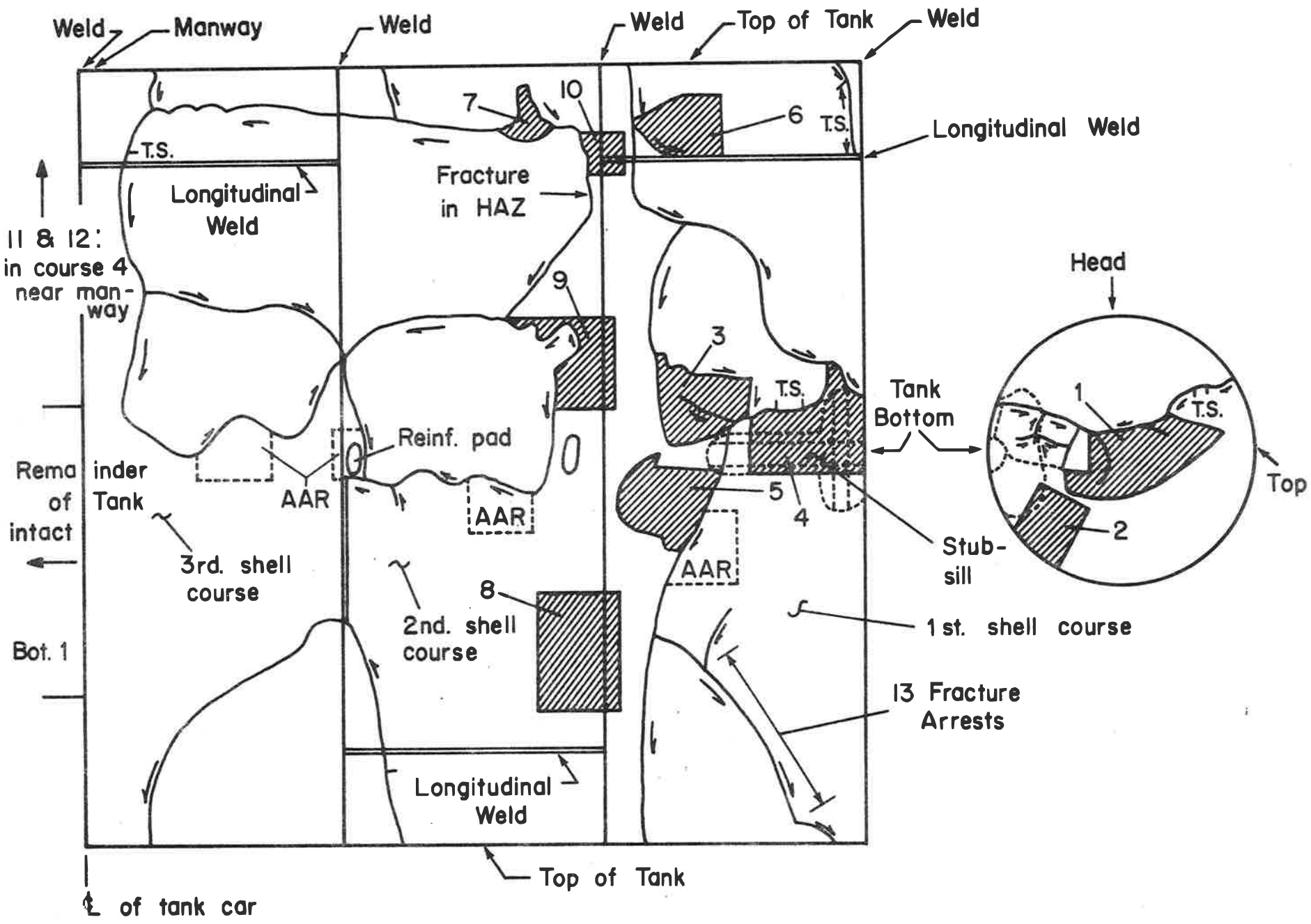
Weld
Manway
Weld
Weld
Top of Tank
Weld
7
10
6
T.S.
Longitudinal Weld
T.S.
Longitudinal Weld
Fracture in HAZ
11 & 12: in course 4 near manway
9
3
T.S.
Tank Bottom
Head
1
T.S.
Top
Reinf. pad
Rema inder of intact Tank
AAR
AAR
5
4
Stub-sill
2
3rd. shell course
AAR
8
2nd. shell course
1st. shell course
Bot. 1
13 Fracture Arrests
Longitudinal Weld
Top of Tank
℄ of tank car

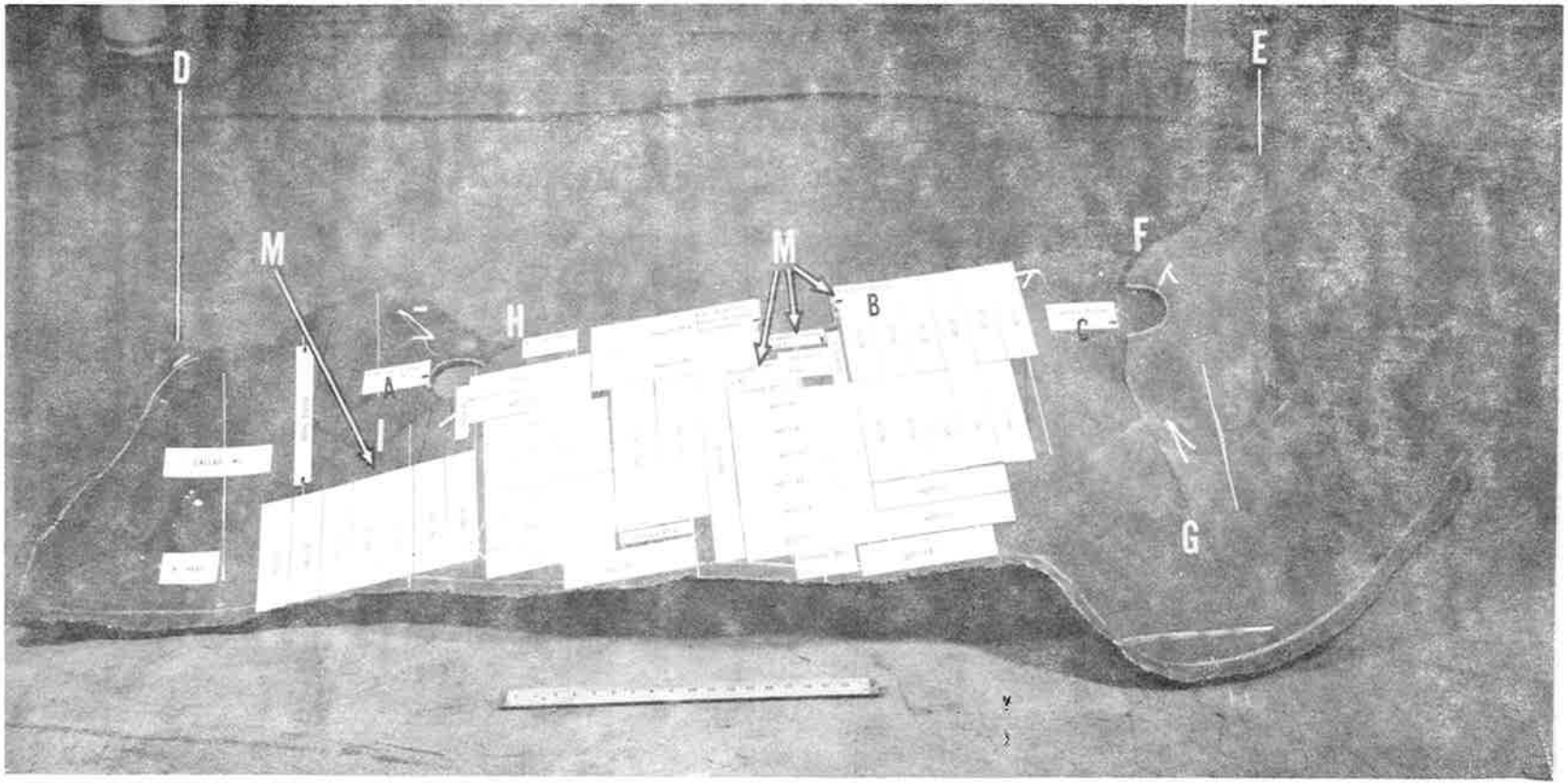

Figure 4. Location of Test Specimens on Head-Plate Sample K-1.

Location of test specimens was established prior to photographing. Fracture profiles were taken at A and C, along the fracture lines IH and GF respectively, and at B along the fracture line DE. Metallographic observations were made on the plate at the areas marked M. The specimens marked HDTL and HDTT were used for dynamic-tear tests. The other impact specimens were used for Charpy V-notch tests. Black and white paint was visible on the outside surface of this sample. Photograph of the inside surface at approximately 1/9 magnification.

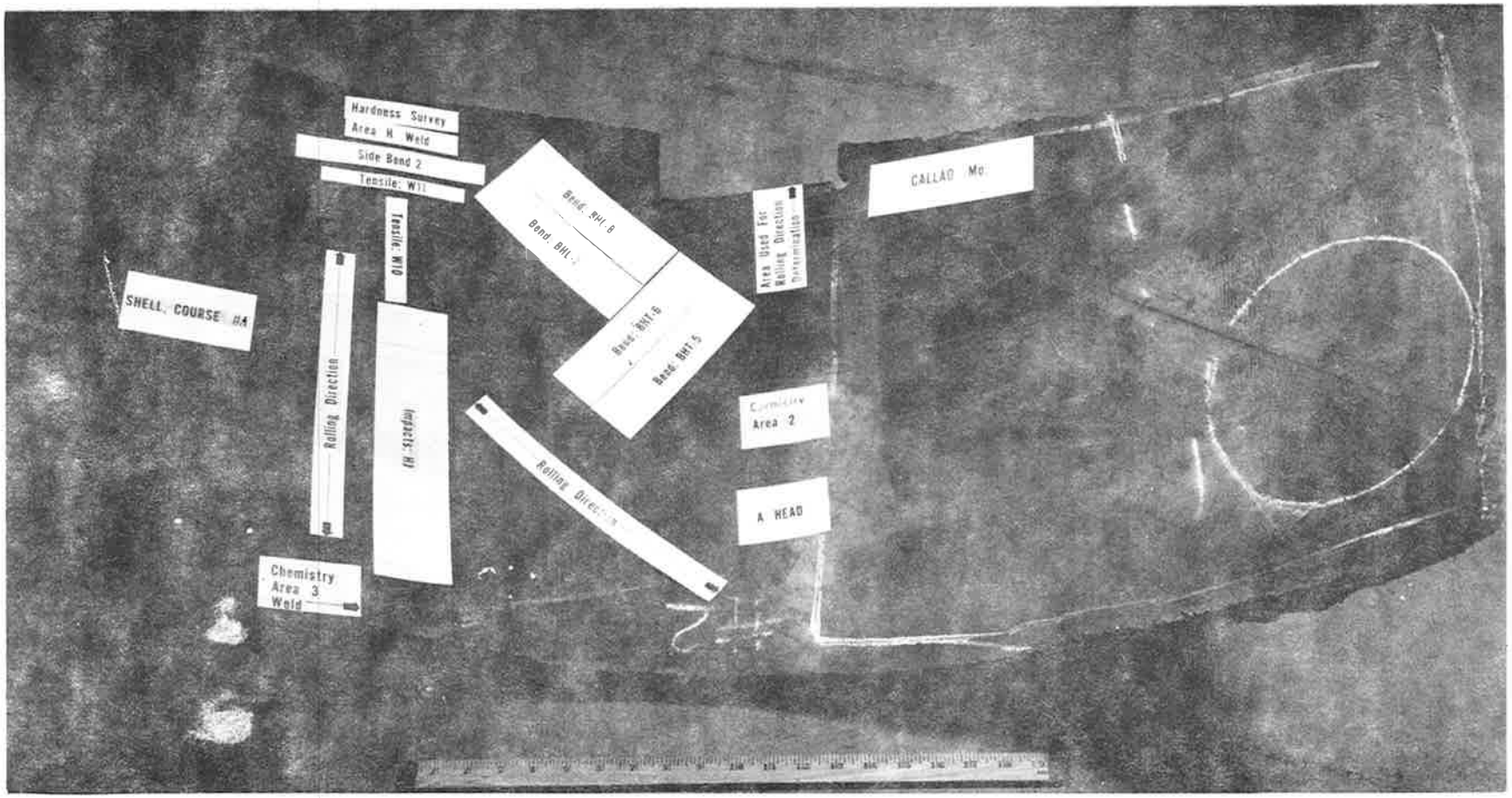

Figure 5. Location of Test Specimens on Sample K-2.

This sample contains part of the "A" head plate and a small part of shell course number 1. The location of each test specimen was established prior to photographing. Black and white paint were visible on the outside surface of this sample. Photograph of the inside surface at approximately 1/9 magnification.

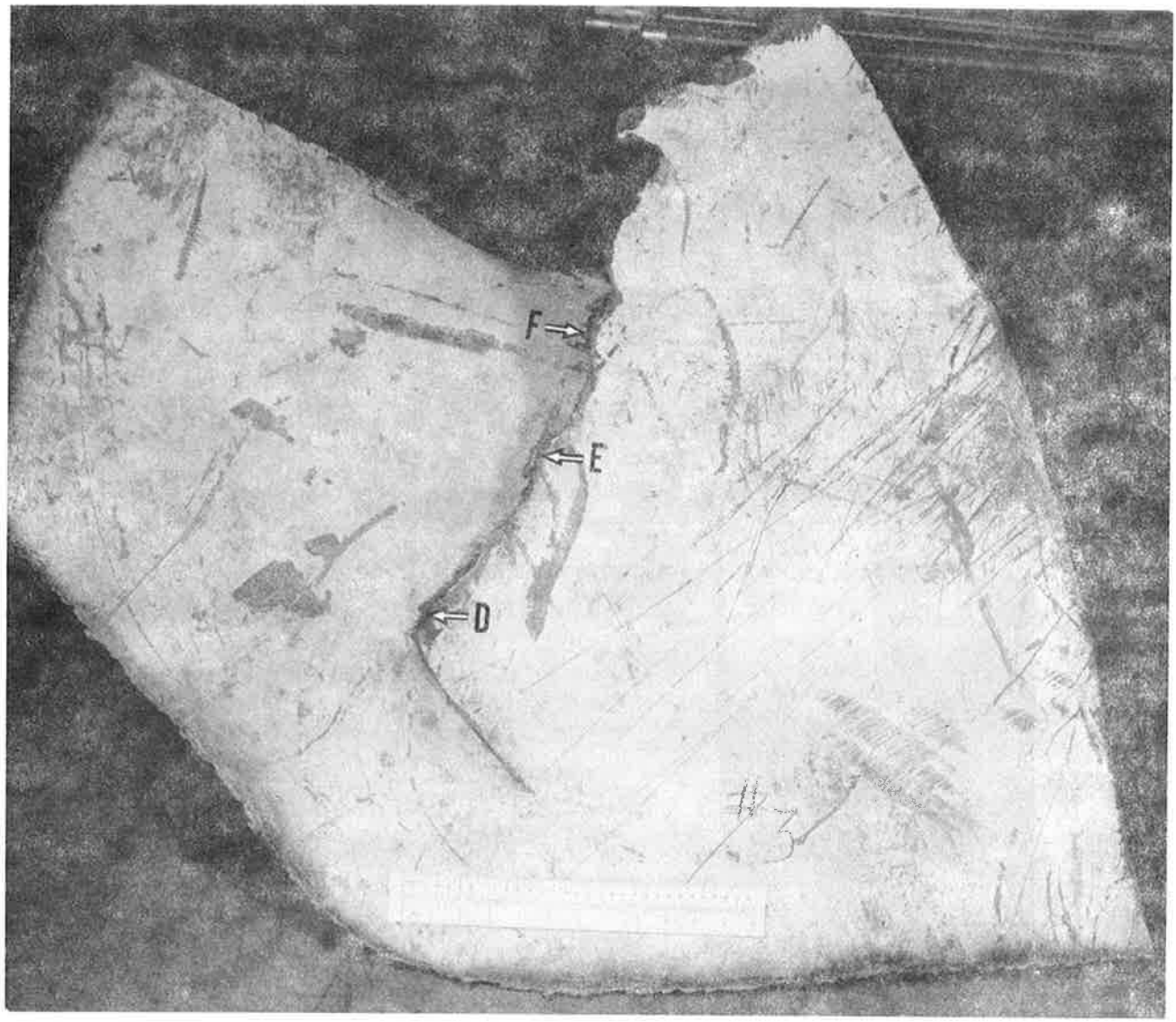

Figure 6. Shell-Plate Sample K-3 Taken from Shell Course Number 1.

Fracture profiles and thickness measurements were taken at D, E, and F. Note that the white paint on the plate surface has been abraded but it has not been burnt. Photograph of the outside surface at approximately 1/6 magnification.

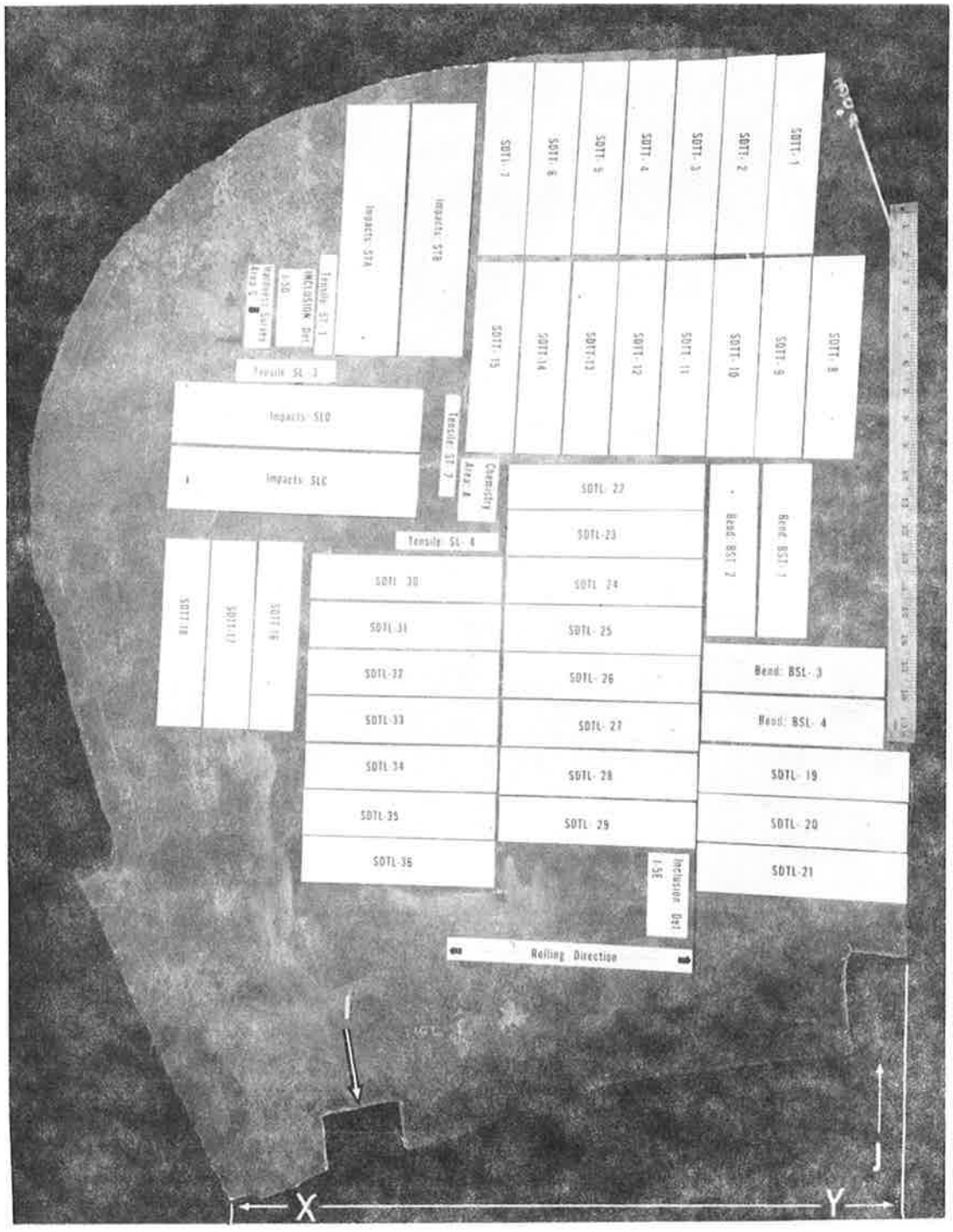

Figure 7. Shell-Plate Sample K-5 Taken from Shell Course Number 1.

The location of each test specimen was established prior to photographing. Fracture profile photographs and thickness measurements were taken at I and J, along the line of fracture which extends from X to Y. Specimens marked SDTT and SDTL were used for the dynamic-tear tests. White and black paint was present on the outside of this plate specimen. Photograph of the inside surface at approximately 1/6 magnification.

Figure 8. Shell-Plate Sample K-6 Taken from Course Number 1.

Fracture profile photographs and thickness measurements were taken at K and L, along the fracture line which extends from A to C. The fracture from C to L occurred along the heat-affected zone of the longitudinal weld in shell course number 1. In figure 3, we have added plate K-6, the fracture line A-C and the arrows indicating crack propagation in plate K-6. None of these were in the original AAR diagram. The region marked W represents an area of weld metal observed along the fracture line below L. The straight line segment, which contains W, is believed to be a heat-affected zone fracture line. White paint is visible on the plate, abraded but not burnt. Photograph of the inside surface at approximately 1/6 magnification.


A
K
L
W
C

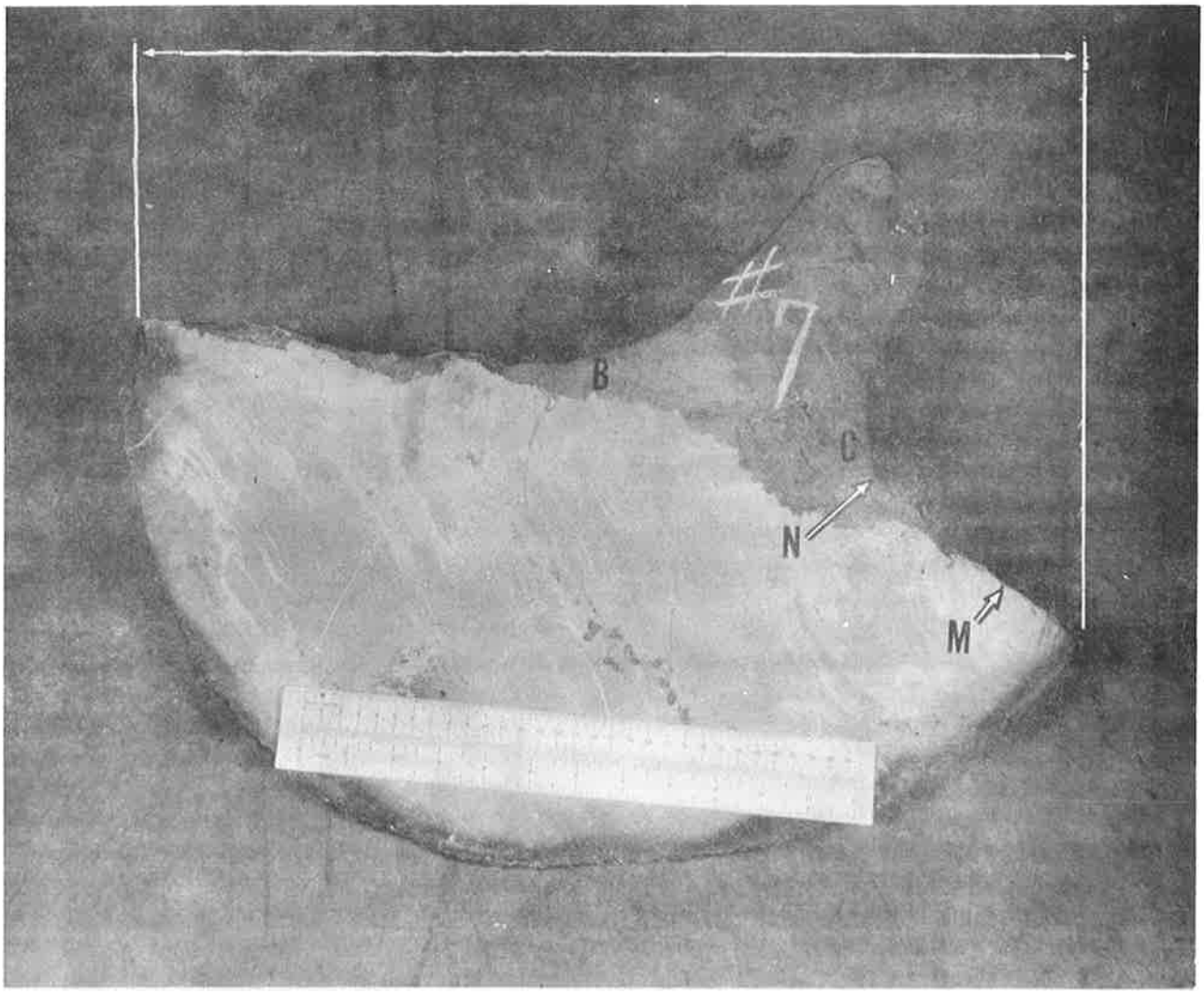

Figure 9. Shell-Plate Sample K-7 Taken from Course Number 2.

Fracture profiles and thickness measurements were taken at M and N. These areas were also used for metallographic observations. The fracture extends from A to D. Between B and C lies a "tongue" which developed in the fracture process. White paint is visible on this sample; however, in the region of the "tongue", the white paint was removed. This was believed to be due to the fracturing process. Photograph of the outside surface at approximately 1/4 magnification.

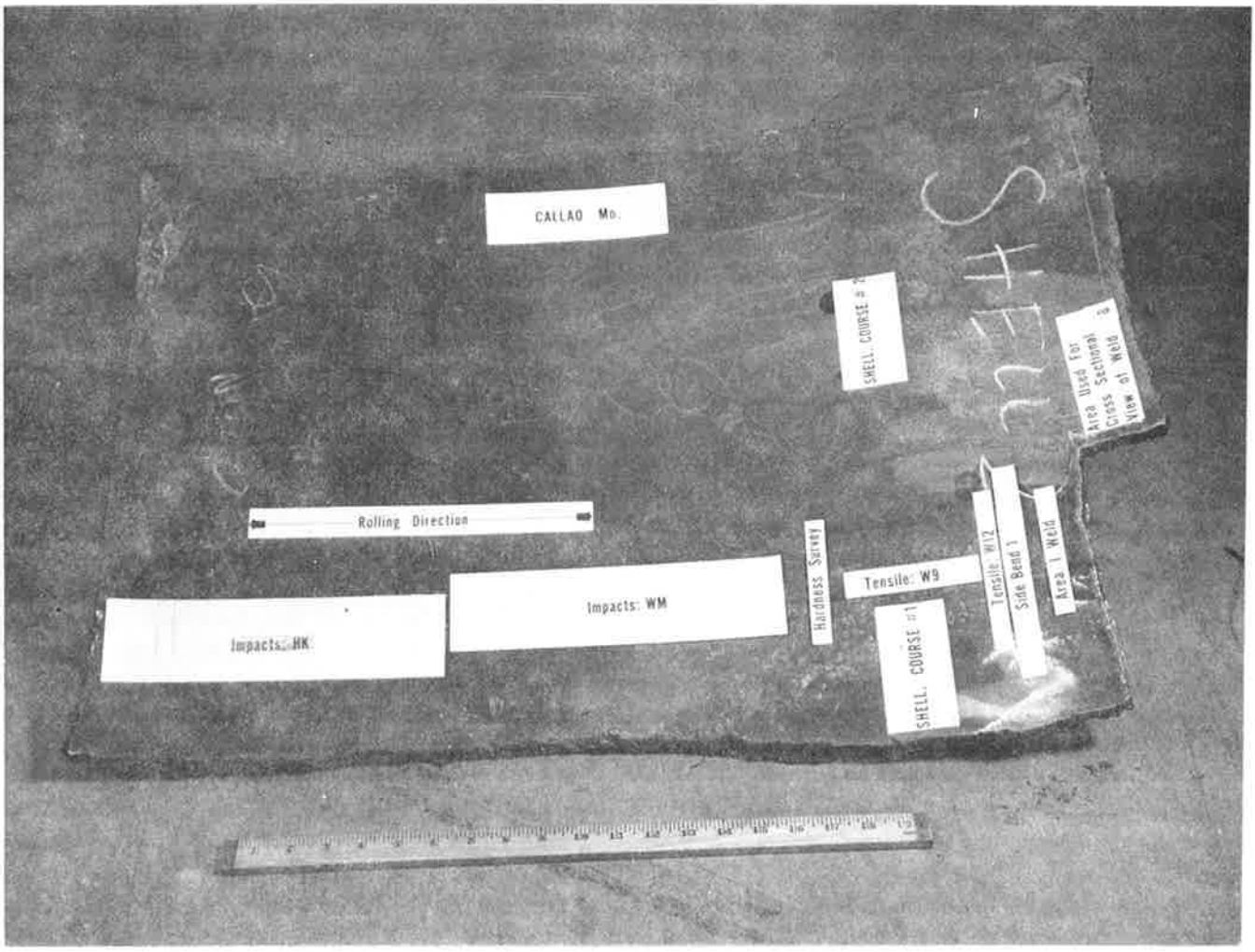

Figure 10. Shell-Plate Sample K-8 Taken from Course Numbers 1 and 2.

This sample contains no fracture. The location of each test specimen was established prior to photographing. Black paint was present on the plate. Photograph of the inside surface at approximately 1/5 magnification.

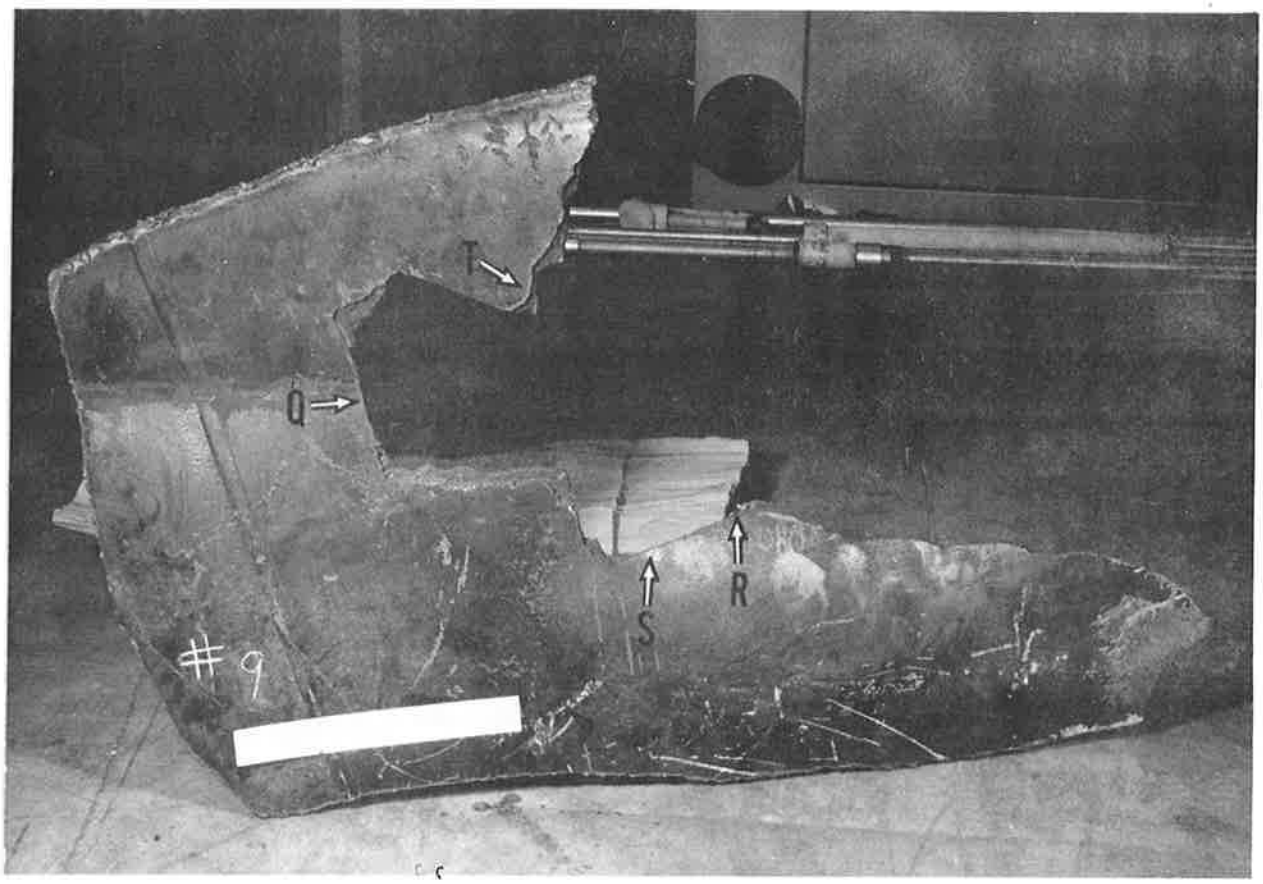

Figure 11. Shell-Plate Sample K-9.

Fracture profiles and thickness measurements were taken at areas Q, R, S, and T. Black paint is visible on the surface of this sample. The paint is abraded but not burnt. Photograph of the outside surface at approximately 1/5 magnification.

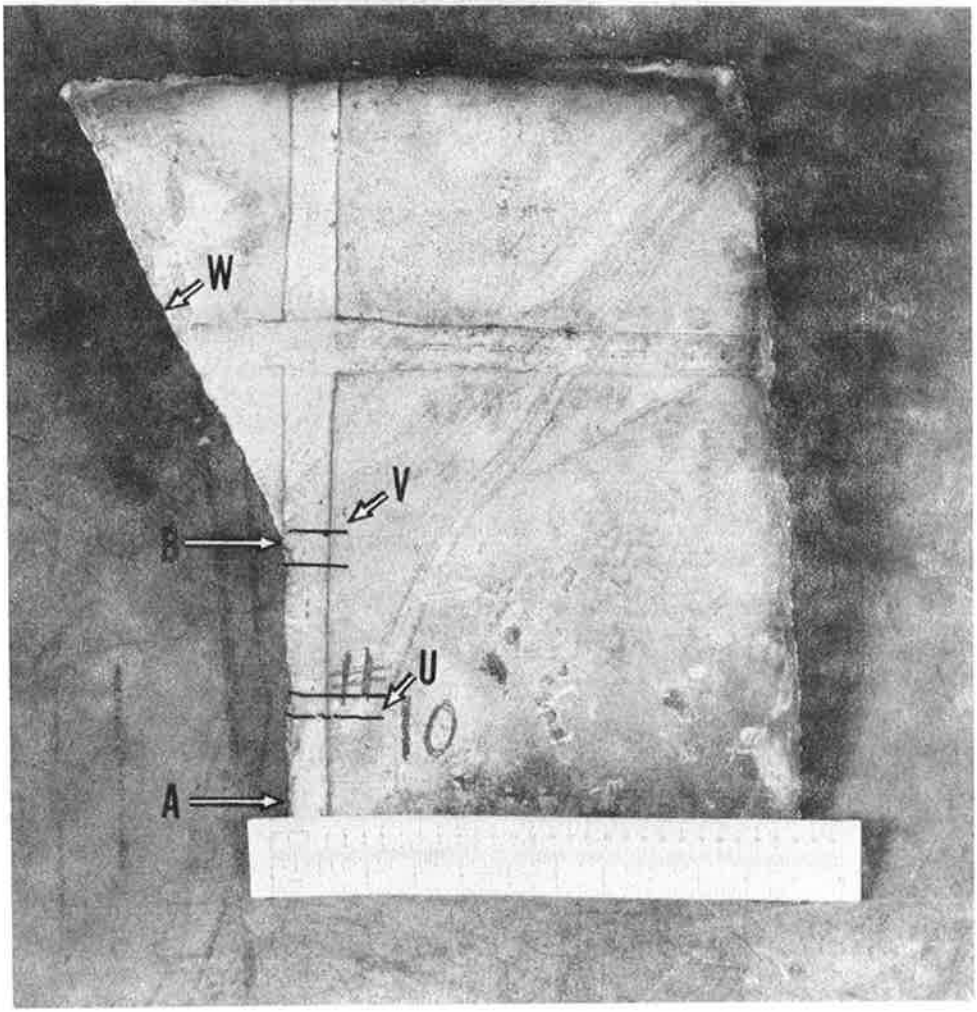

Figure 12. Shell-Plate Sample K-10.

Fracture profile photographs and thickness measurements were taken at U and W. The fracture line proceeds along the edge of the weld from A to B, then abruptly turns approximately 26° to the left. The abraded but unburnt white paint is visible on the sample. Photograph of the outside surface at approximately 1/4 magnification.

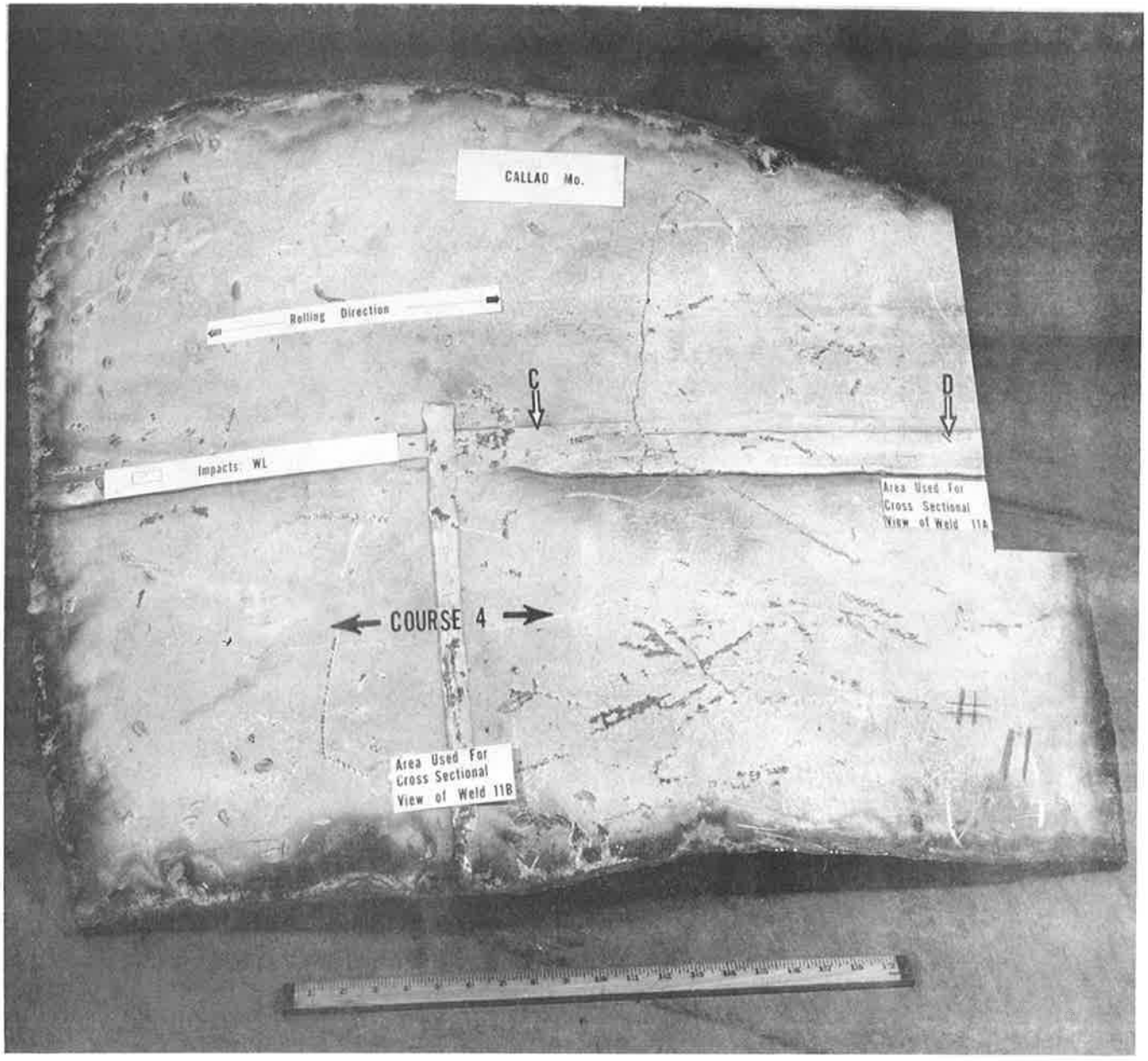

Figure 13. Shell-Plate Sample K-11 Taken from Course Number 4.

Arrows at C and D show the rather large weld region which existed in this sample. A cross-sectional photograph of this area is given in Figure 29 in this report. The abraded but unburnt white paint is visible on the sample. Photograph of the outside surface at approximately 1/4 magnification.

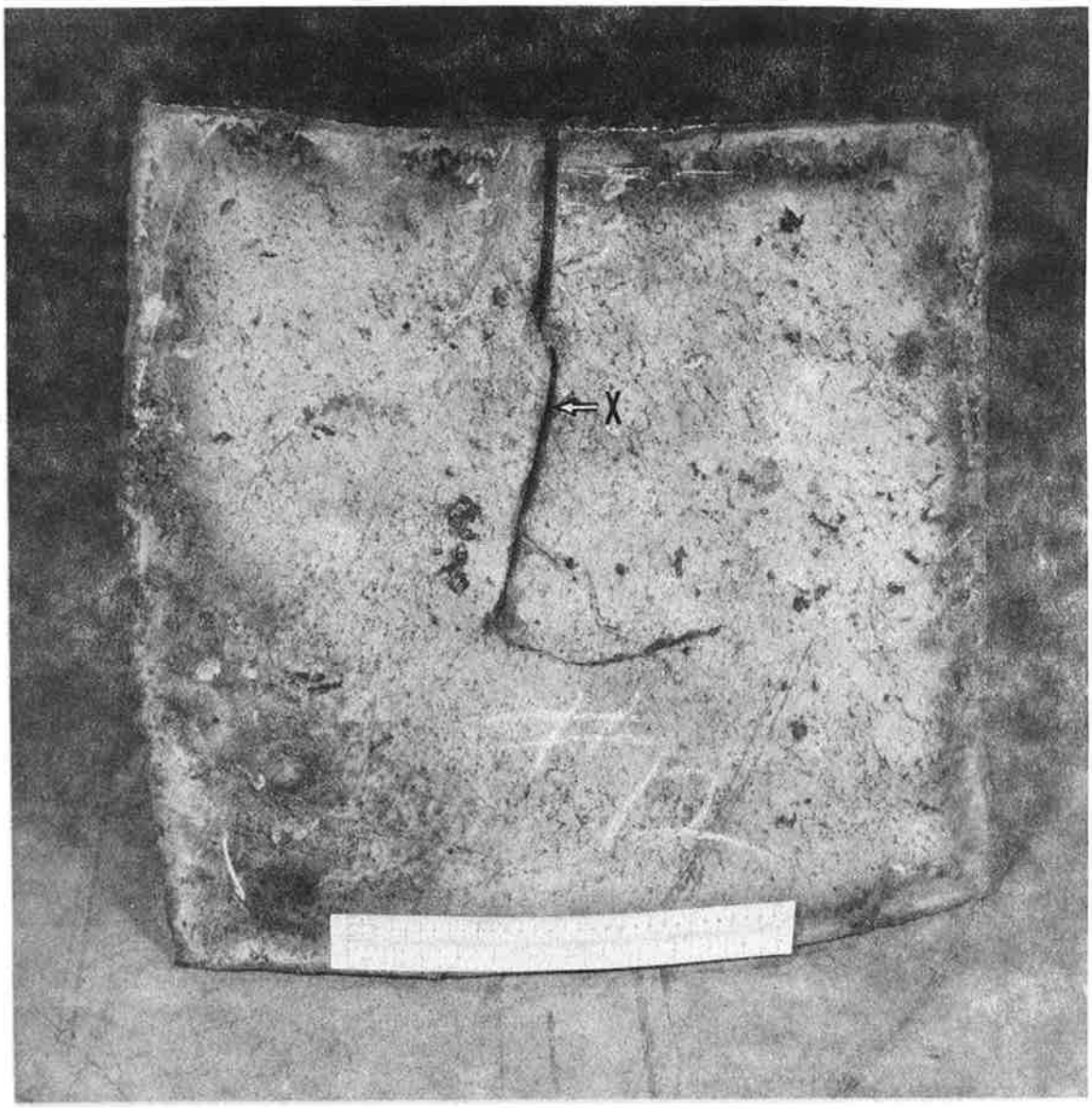

Figure 14. Shell-Plate Sample K-12 Taken from Course Number 4.

The photograph shows a fracture near the dome of the tank car. A fracture-profile photograph and thickness measurements were taken at X. Abraded but unburnt white paint is visible on the sample. Photograph of the outside surface at approximately 1/5 magnification.

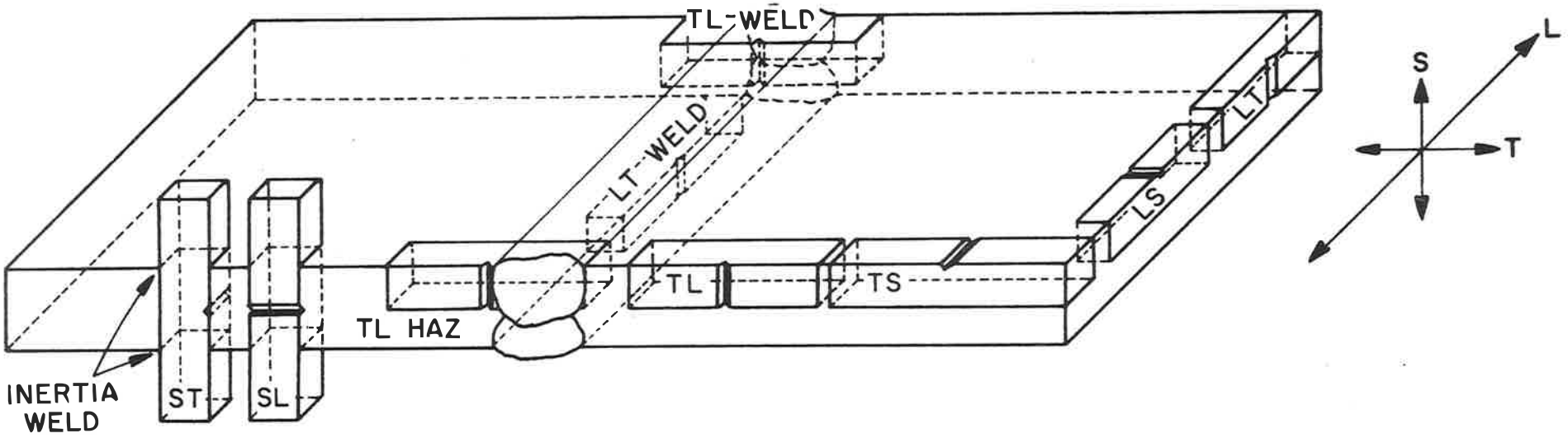

Figure 15. Orientation Codes of Various Impact Test Specimens.

Specimen Orientation Code: The two letter code gives direction of the long axis of the specimen (L, T, or S) followed by the direction of crack propagation (L, T, or S). The letters L, T, and S refer to the three orthogonal plate directions, as defined below:

- L Longitudinal or rolling direction of plate. For weld-metal specimens, this refers to the direction of welding.
- T Transverse direction: perpendicular to rolling direction but in the plane of the plate. For weld-metal and heat-affected-zone specimens, this refers to the perpendicular to the welding direction.
- S Short-transverse direction: perpendicular to L and T.

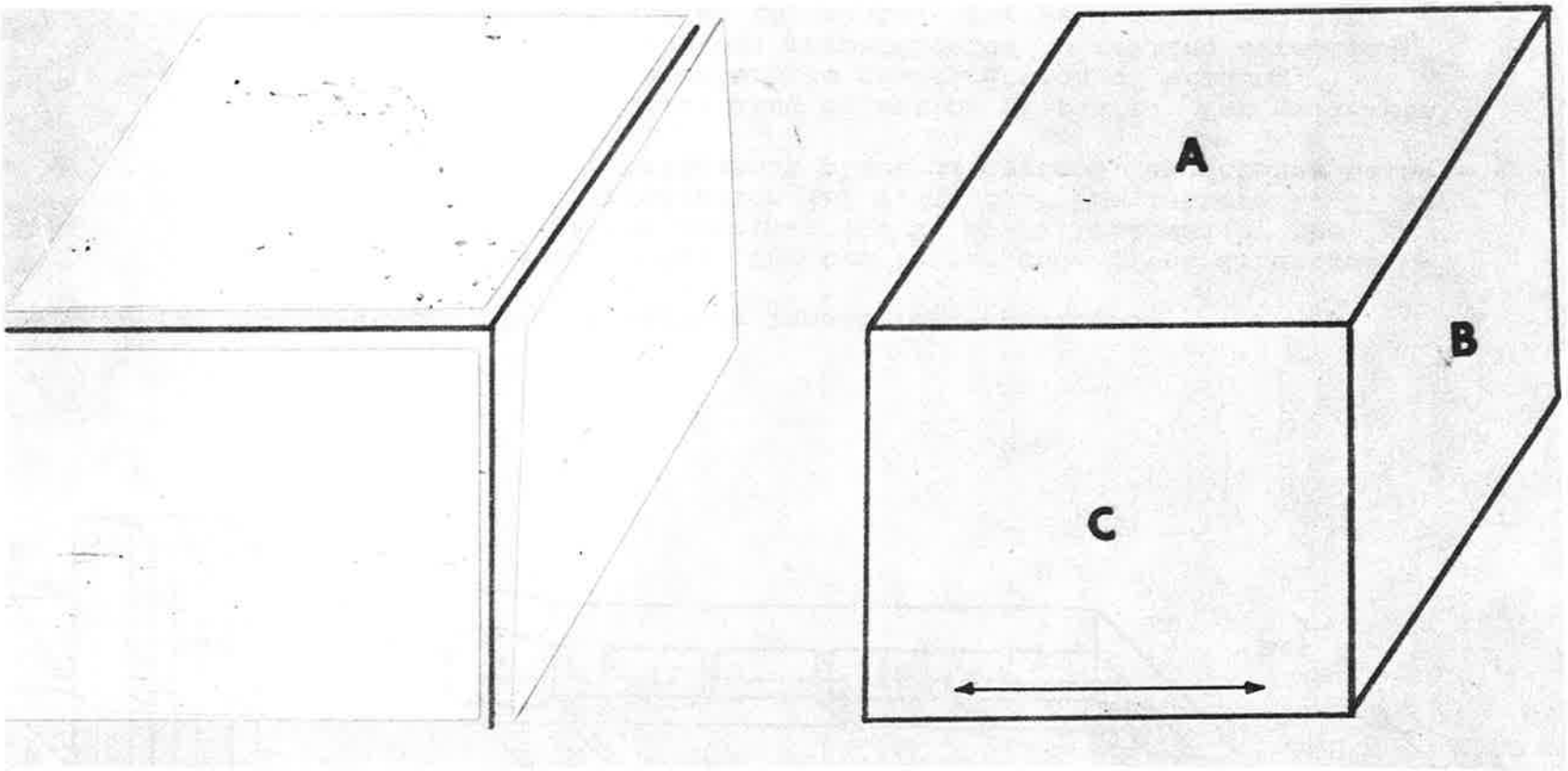

Figure 16. Inclusions on Three Mutually Perpendicular Planes of the Head Plate K-1.

The A plane is parallel to the plate surface. The B and C planes are approximately perpendicular and parallel respectively to the direction determined to be the principal rolling direction which is represented by the arrow contained in the C plane. Unetched. X 100

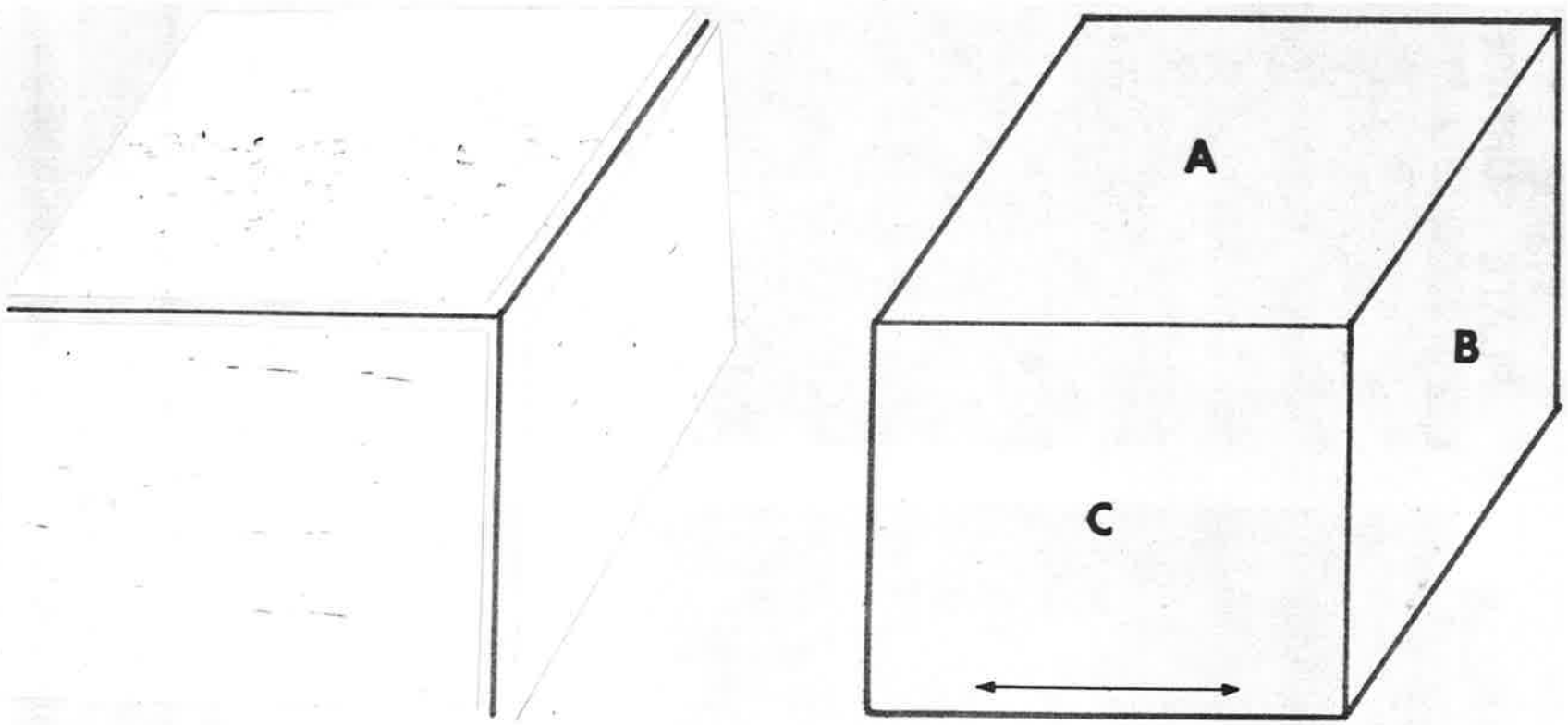

Figure 17. Inclusions on Three Mutually Perpendicular Planes of the Shell Plate K-5.

The A plane is parallel to the plate surface. The B and C planes are approximately perpendicular and parallel respectively to the direction determined to be the principal rolling direction of the plate, which itself is represented by the arrow contained in the C plane. Unetched. X 100

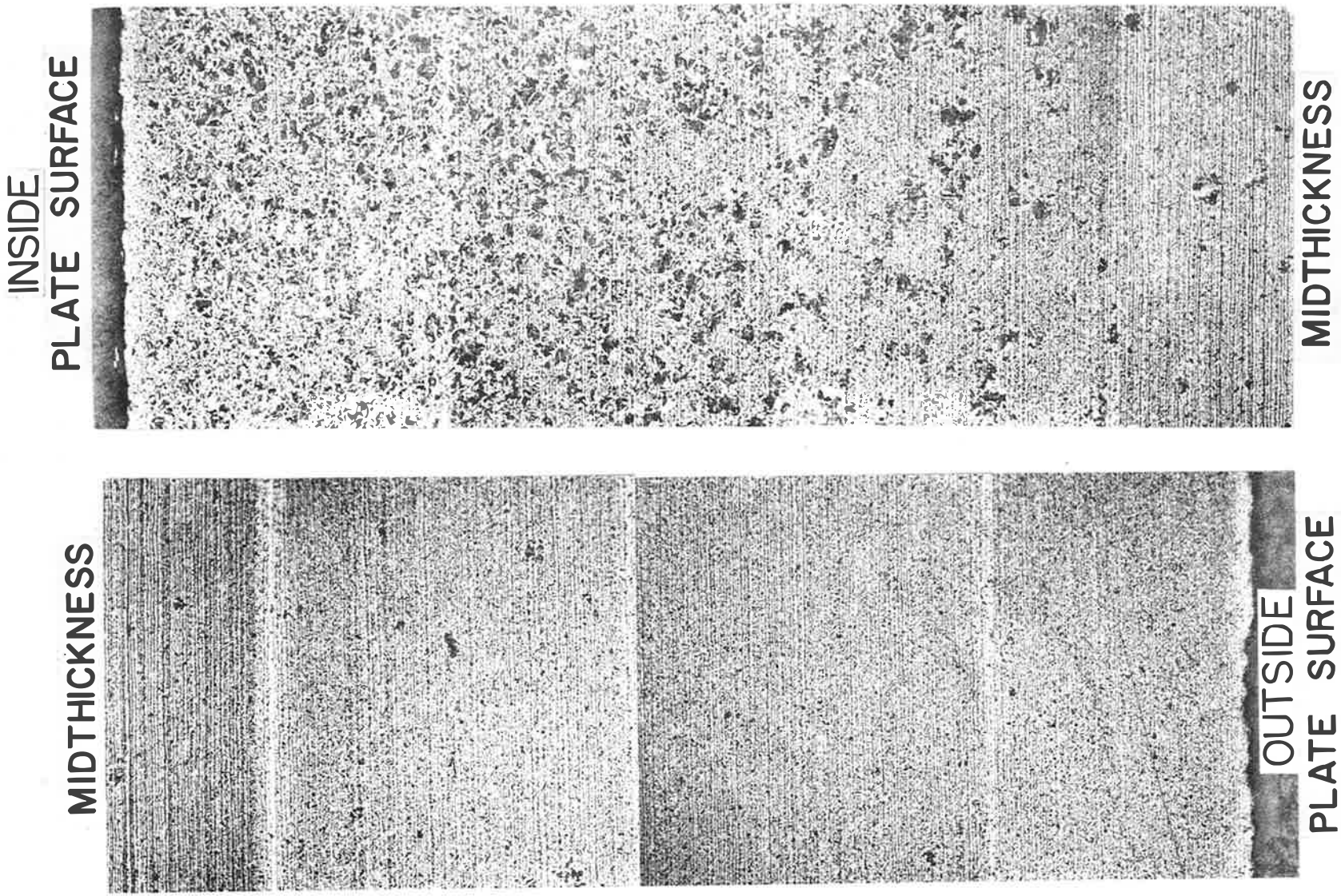

Figure 18. Montage of Microstructures Throughout the Thickness of Head Plate K-1 as Observed at Selected Locations, Including the Longitudinal Dynamic-Tear-Test Specimen K1-60, and Two Etched Specimens from the Region (near M in Figure 4) Used for the Determination of Plate Rolling Direction.

Etched: 1% Nital. Mag. X 30.

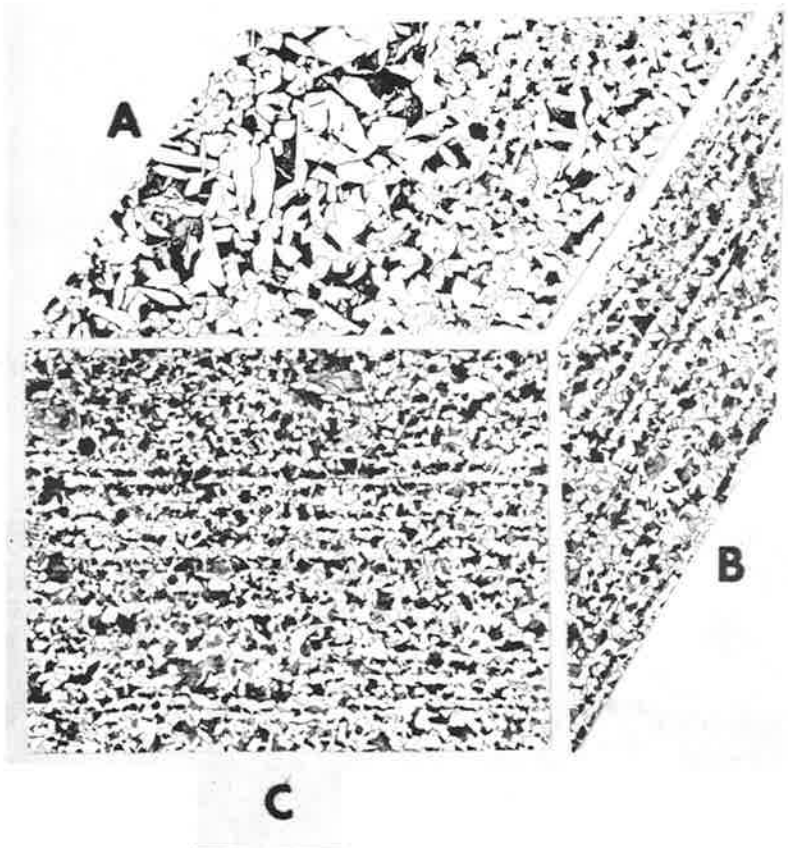

X 100

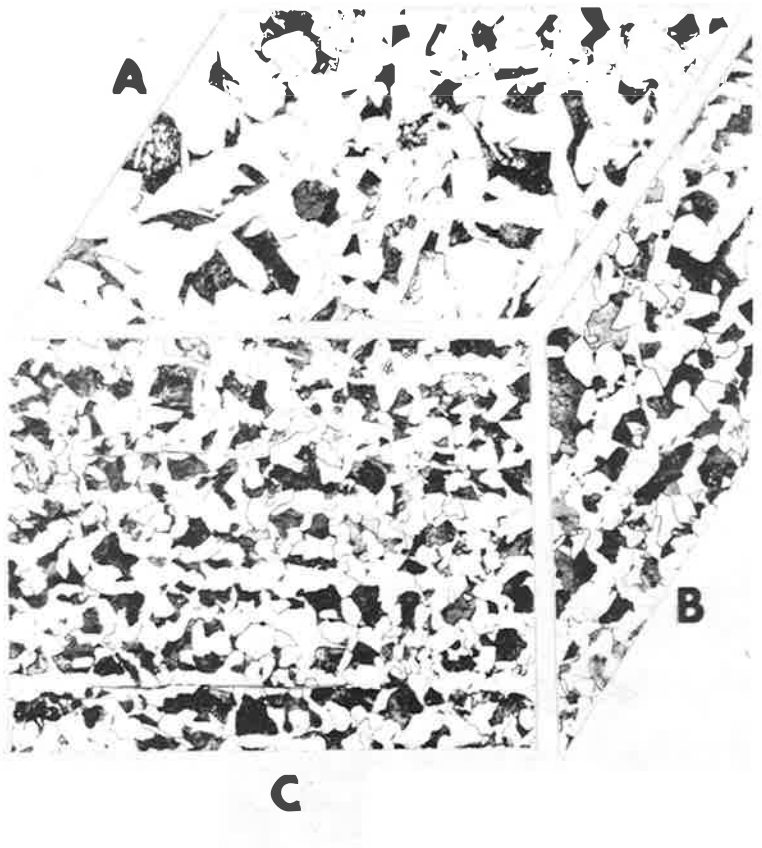

X 240

Figure 19. Microstructure of Head Plate K-1, as Observed in Three Mutually Perpendicular Planes at the Plate Quarterthickness Located at the Outside of the Tank Car.

The orientations of the A, B, and C planes are oriented as in Figure 17. Ferrite grain size number 9. Etched: 1% Nital.

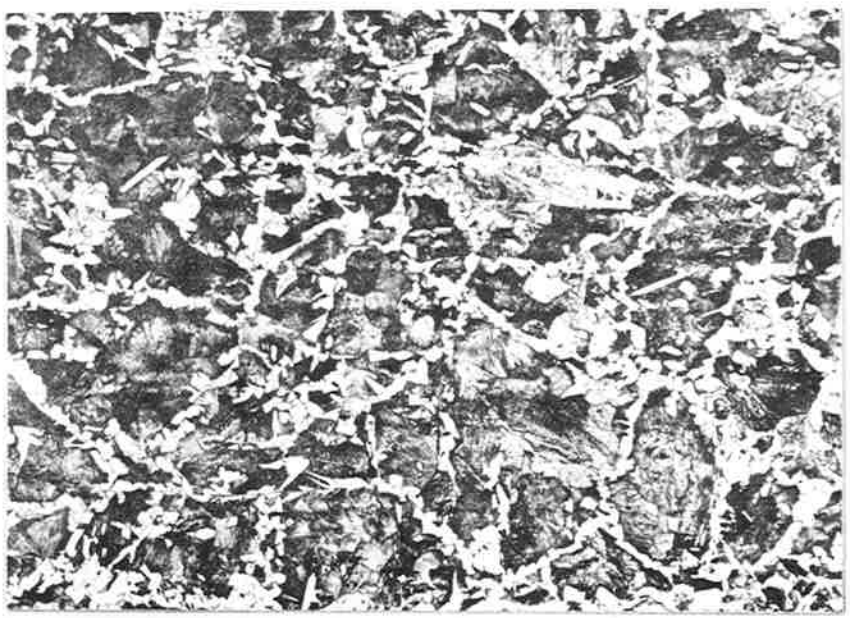

X 100

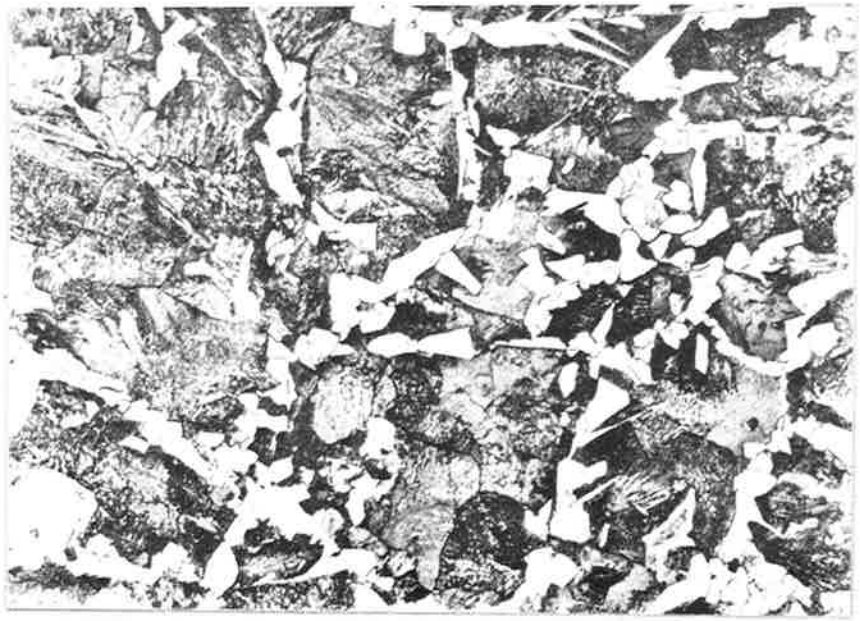

X 240

Figure 20. Microstructure of a Longitudinal Section of Head-Plate K-1 Taken at an Inside Plate-Quarterthickness Location of Specimen HDTT-38.

This microstructure is also typical of the microstructures observed on Charpy V-notch specimens HLI-24, HLH-10, HTG-46 and HFT-63.

Ferrite grain size number 7. Etched: 1% Nital.

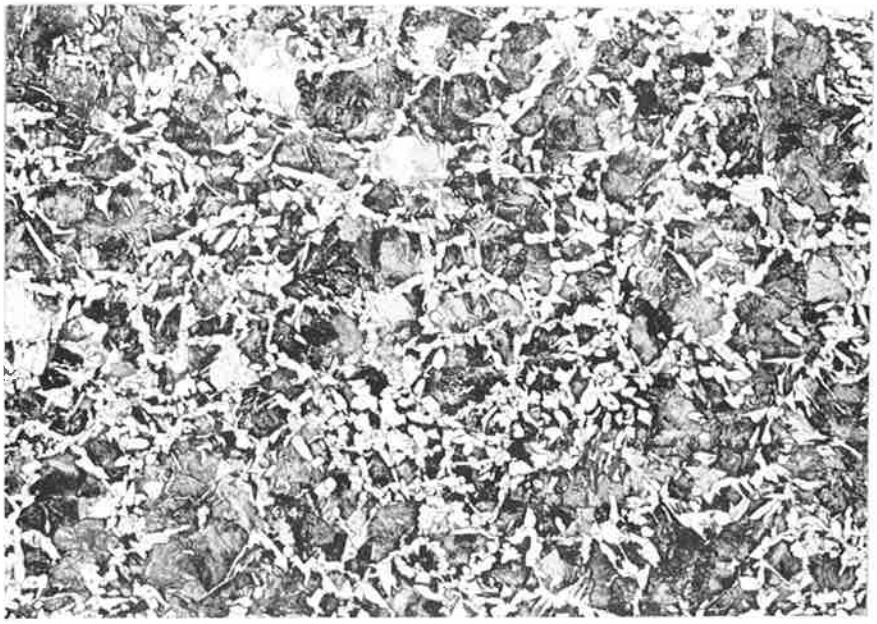

X 100

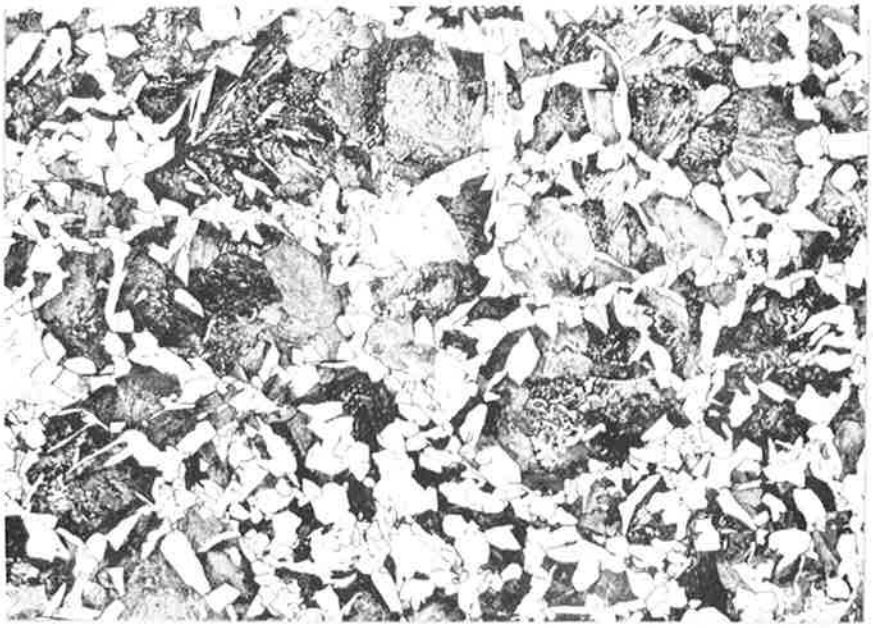

X 240

Figure 21. Microstructure of a Longitudinal Section of Head-Plate Sample K-2.

Ferrite grain size number 8.
Etched: 1% Nital.

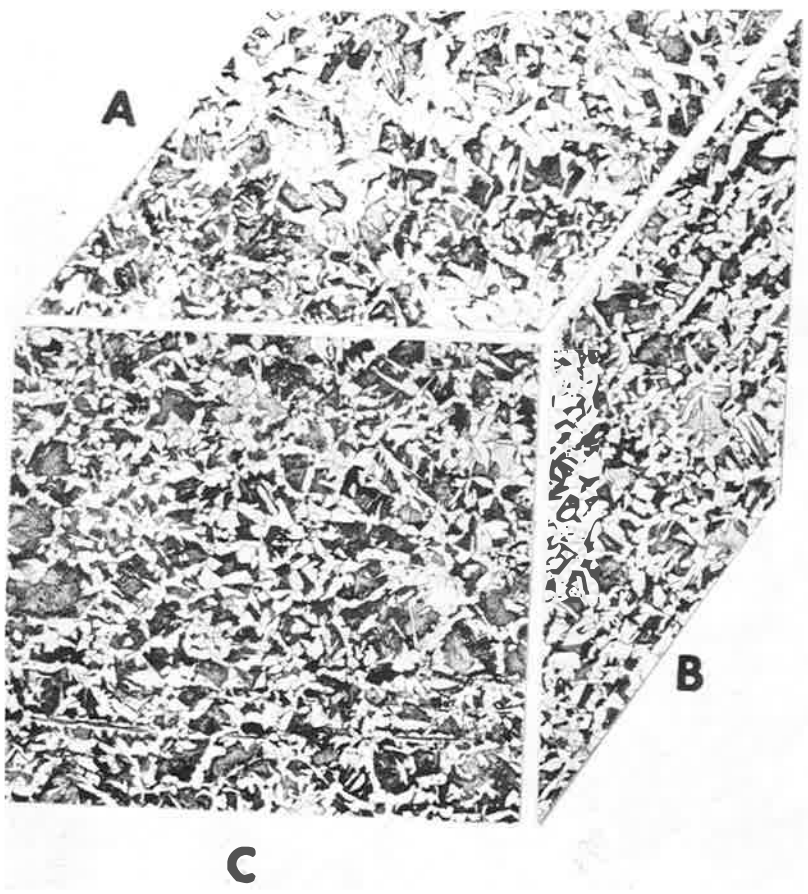

X 100

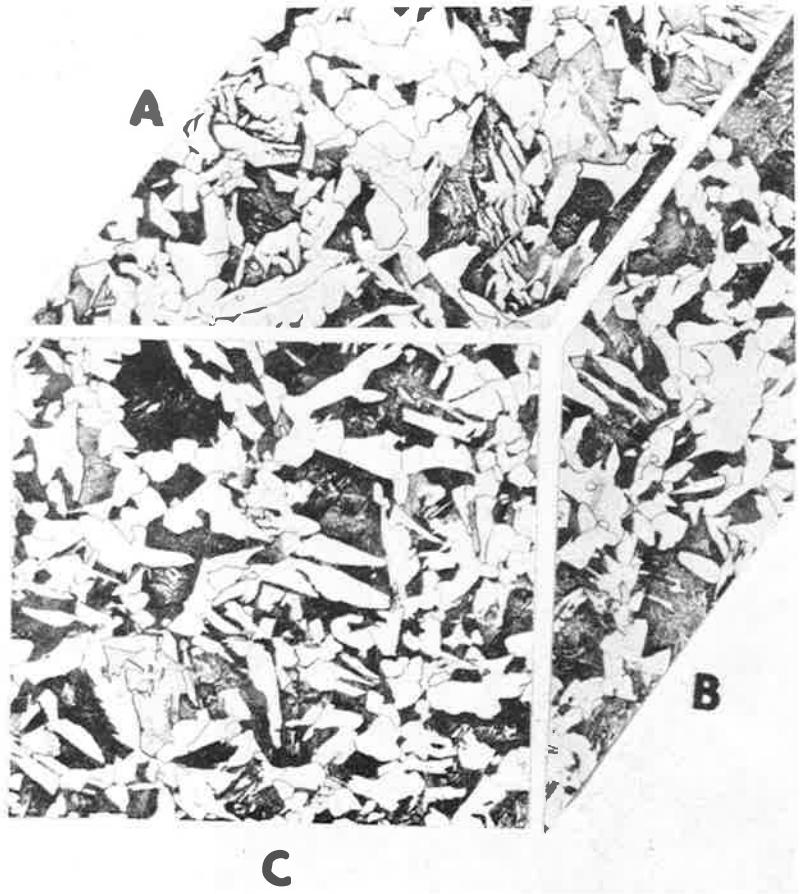

X .240

Figure 22. Microstructure of the Shell Plate K-5, as Observed in Three Mutually Perpendicular Planes.

The orientations of the A, B, and C planes are oriented as in Figure 17. Ferrite grain size number 7. Etched: 1% Nital.

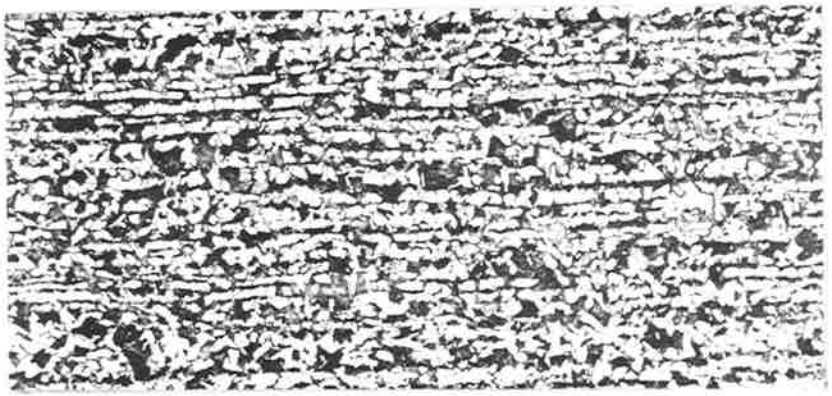

Shell Course No. 2 — Sample K-7
Ferrite Grain Size No. 8

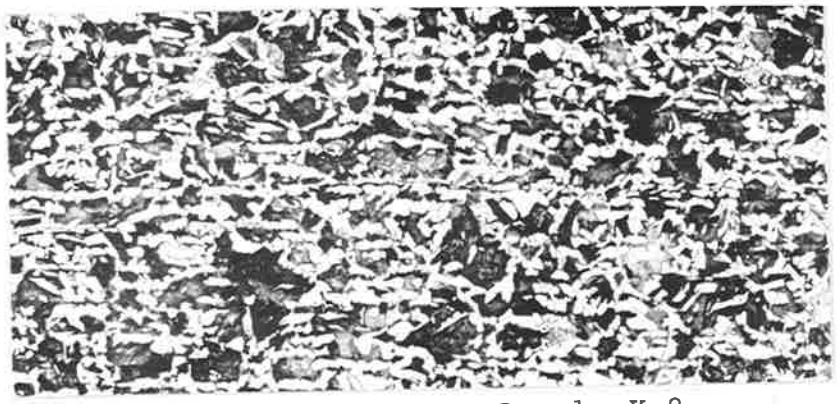

Shell Course No. 2 — Sample K-8
Ferrite Grain Size No. 7

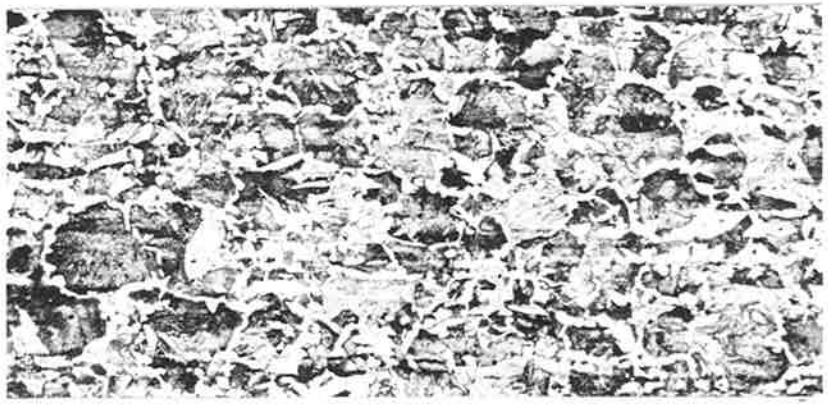

Shell Course No. 4 — Sample K-12
Ferrite Grain Size No. 7

Figure 23. Typical Microstructures of Longitudinal Sections from Shell-Course Numbers 2 and 4.

Etched: 1% Nital. X 100

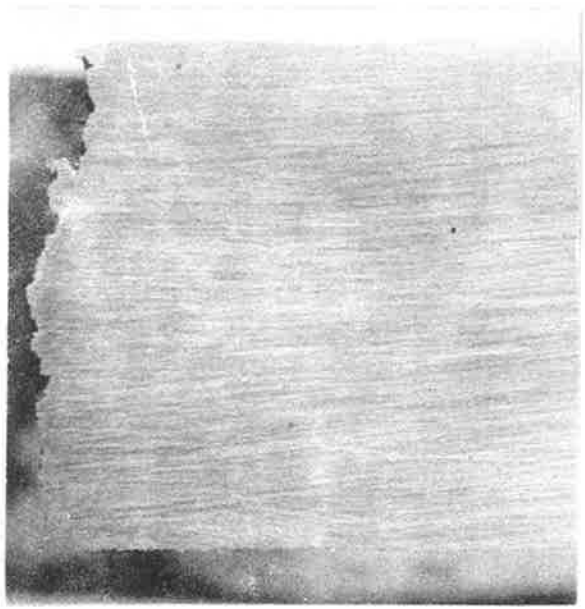

Plate K-1, (Area A, of Fig. 4)

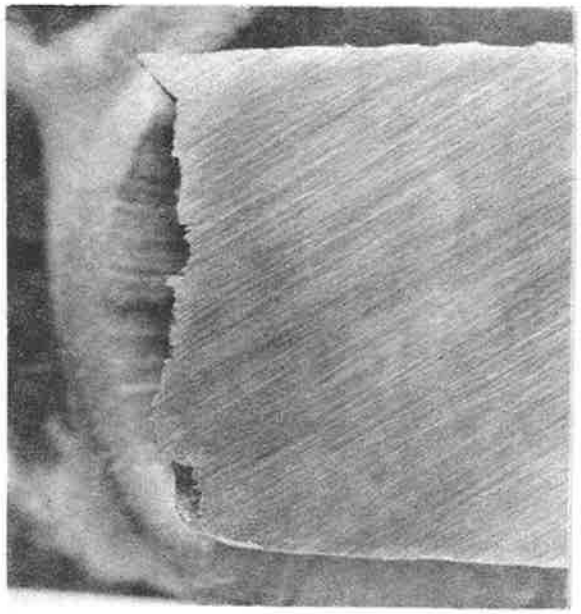

Plate K-1, (Area B, of Fig. 4)

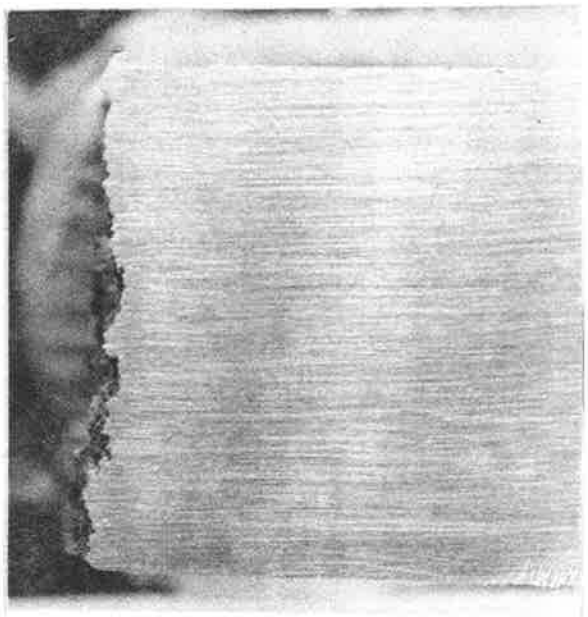

Plate K-1, (Area C, of Fig. 4)

Figure 24. Profile Views of Fracture Samples From the "A" Head Plate. Unetched: Mag. X 4.

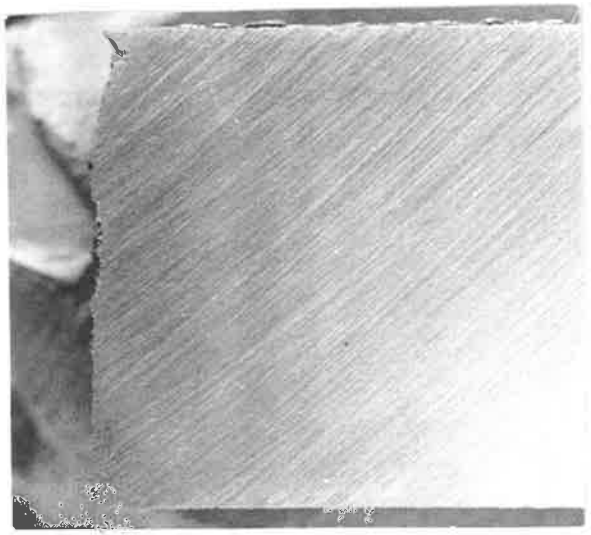

Plate K-3, (Area D, of Fig. 6)

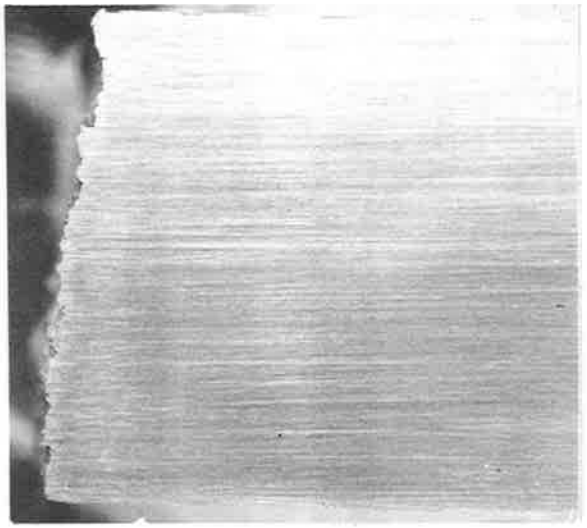

Plate K-3, (Area E, of Fig. 6)

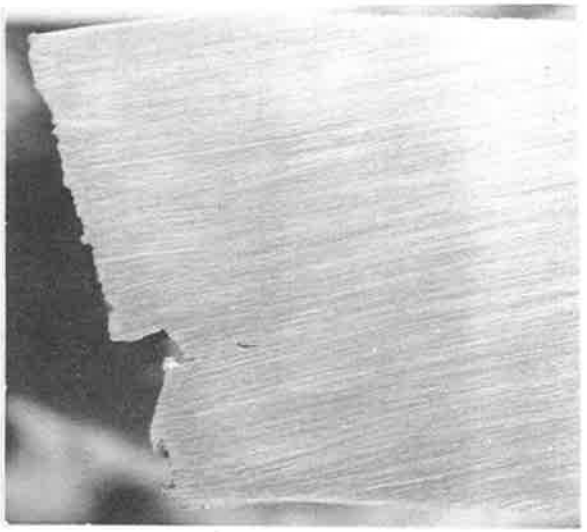

Plate K-3, (Area F, of Fig. 6)

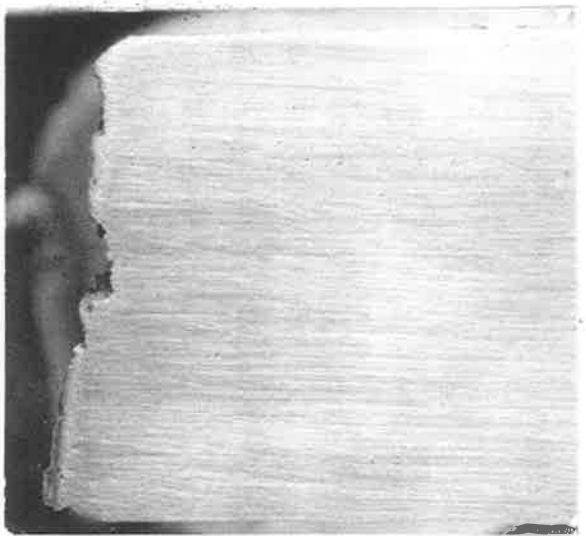

Plate K-5, (Area I, of Fig. 7)

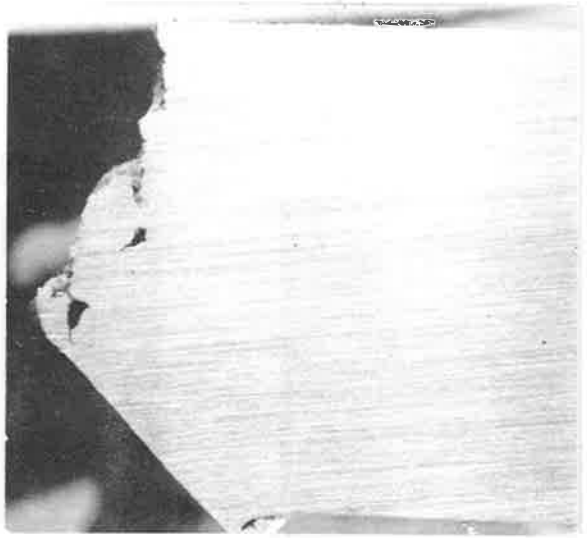

Plate K-5, (Area J. of Fig. 7)

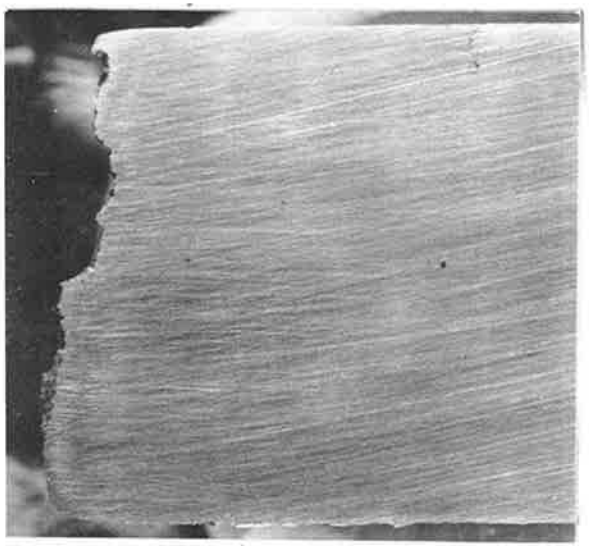

Plate K-6, (Area K, of Fig. 8)

Figure 25. Profile Views of Fractures on Plate Samples Taken From Shell Course Number 1. Unetched: Mag. X 4.

late K-7, (Area M, of Fig. 9)

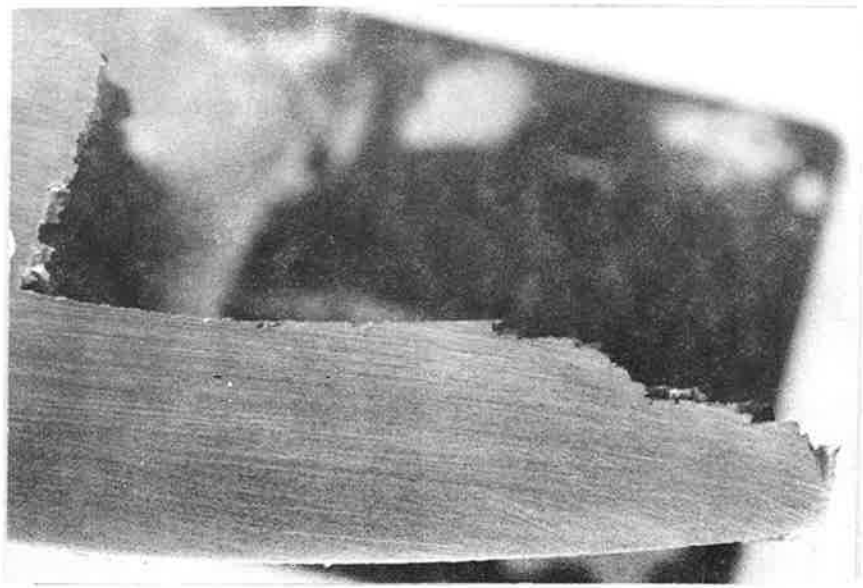

Plate K-7, (Area N, of Fig. 9)

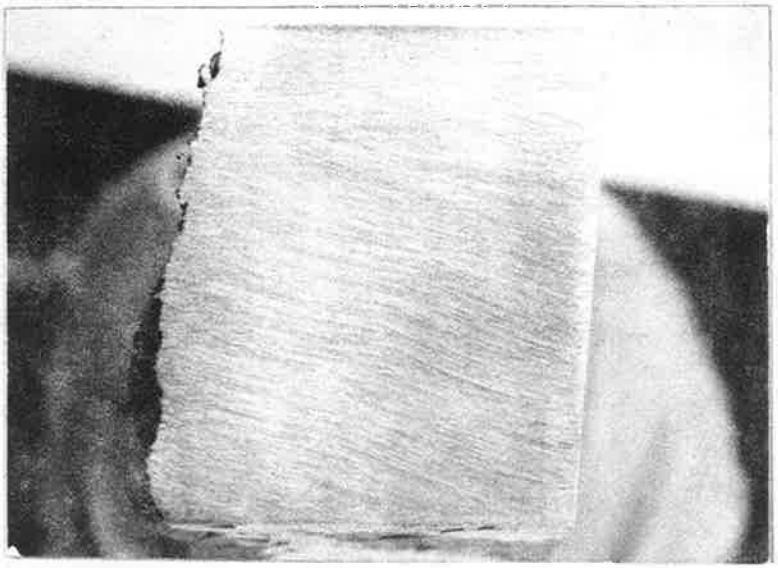

Plate K-9, (Area Q, of Fig. 11)

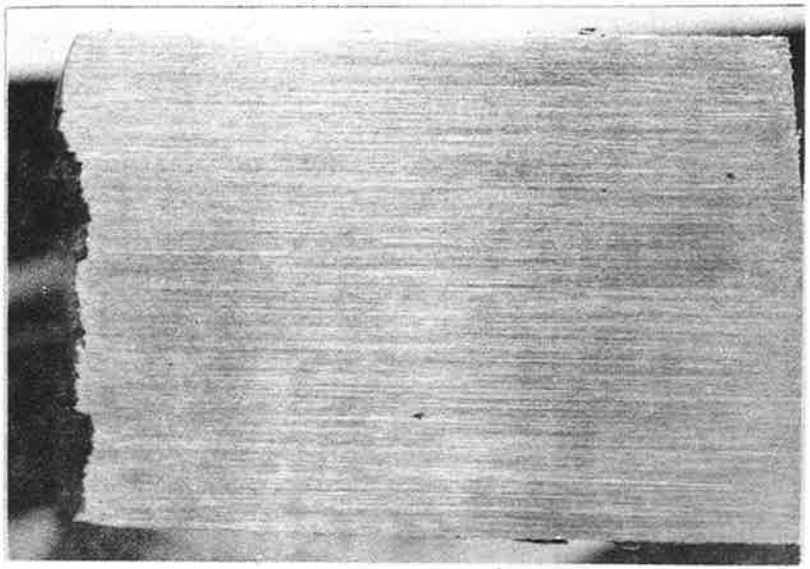

Plate K-9, (Area R, of Fig. 11)

Figure 26. Profile Views of Fractures on Plate Samples Taken From Shell Course Number 2. Unetched: Mag. X 4.

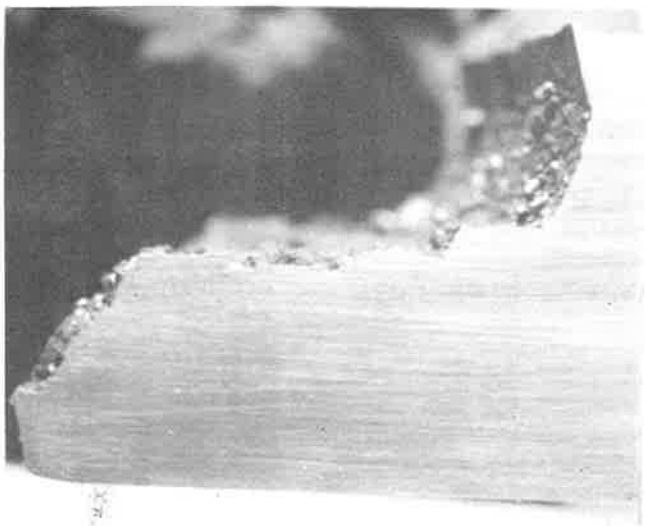

Plate K-9, (Area S, of Fig. 11)

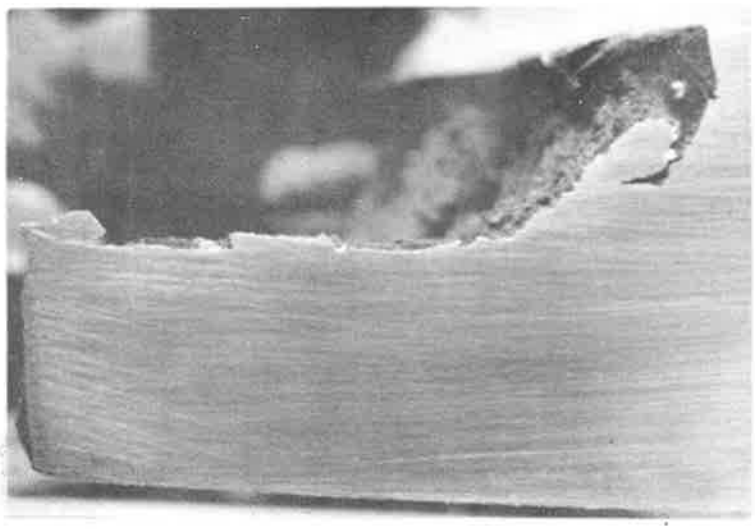

Plate K-9, (Area T, of Fig. 11)

Plate K-10, (Area W, of Fig. 12)

Plate K-10, (Area V, of Fig. 12)

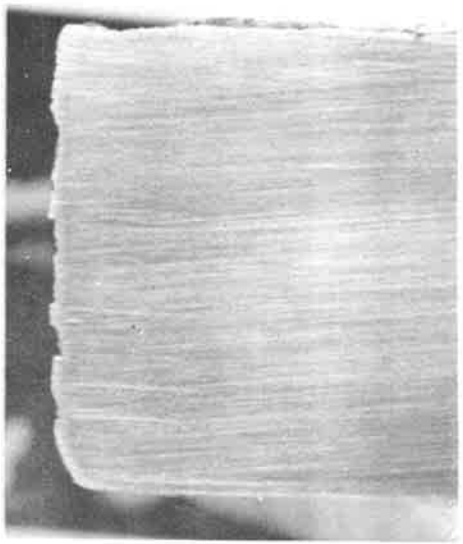

Plate K-12, (Area X, of Fig. 14)

Figure 27. Profile Views of Fractures on Plate Samples Taken From Shell Courses Numbered 2 and 4. Unetched: Mag. X 4.

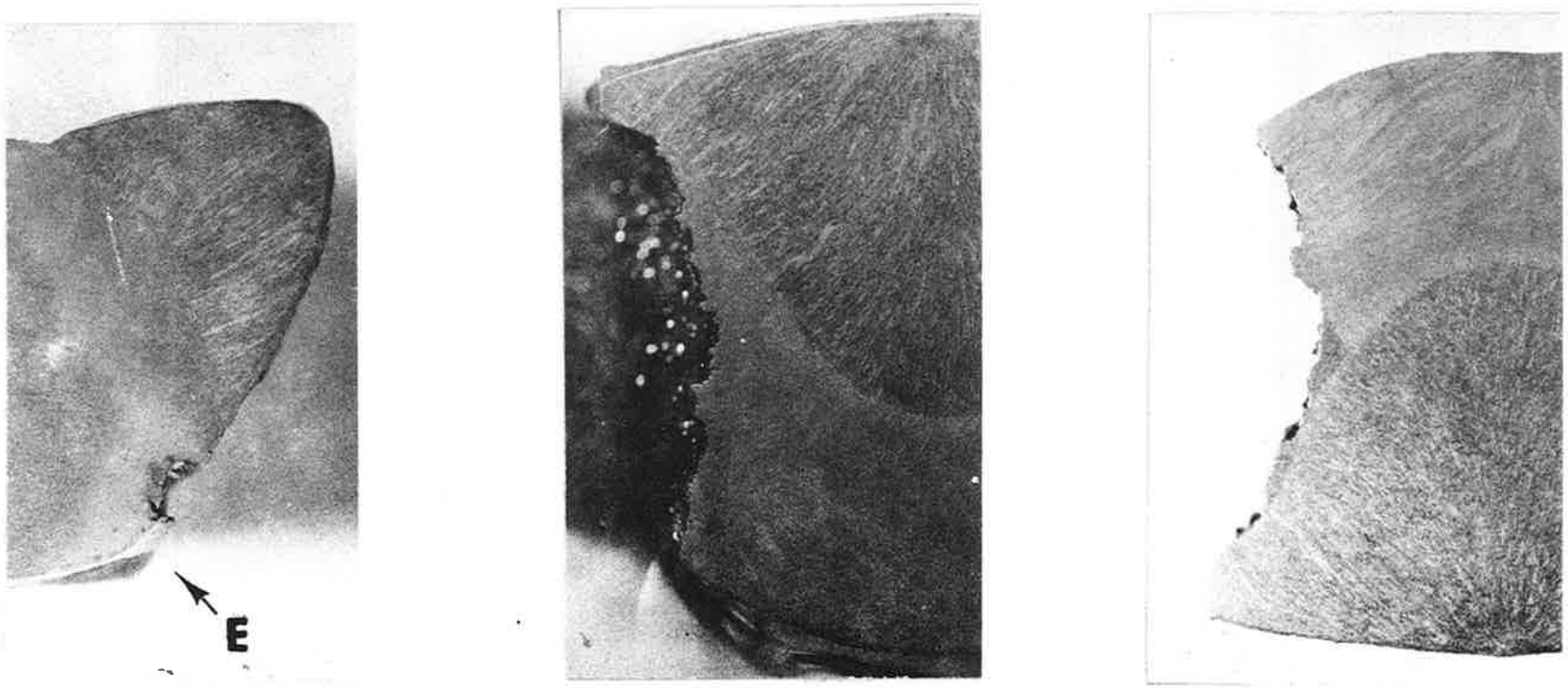

(a) (b) (c)

Figure 28. Photographs Showing Weld Fractures In Tank Car GATX 94451.

The top of photograph (a) shows a shear failure through the weld-metal and the bottom shows failure through the heat-affected zone. Region at E was mechanically deformed after fracture. Photographs (b) and (c) show brittle fractures of the weld heat-affected zone. Etched: 1% Nital. Mag. X 4.

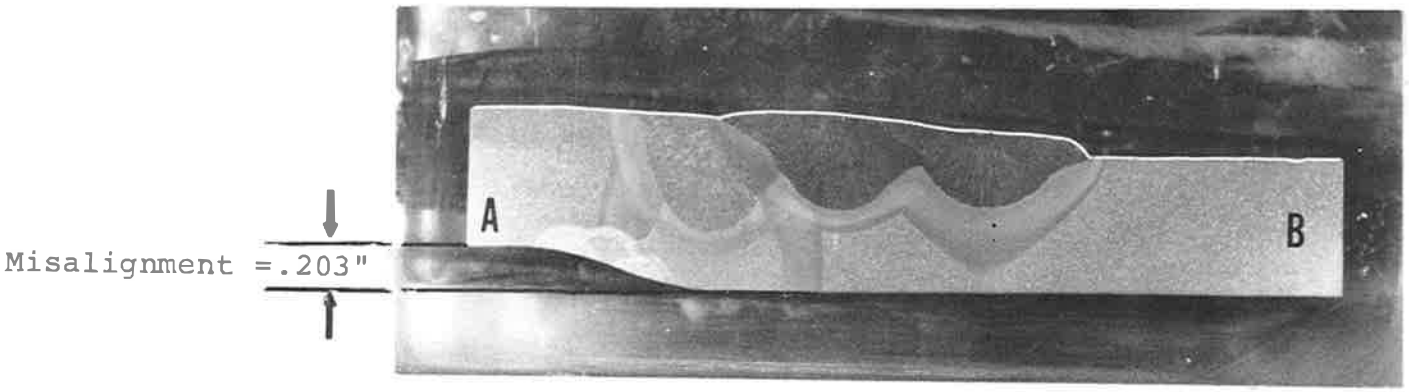

Figure 29. Weld Cross-Section 11A, Taken from Sample K-11 at the Weld Between Shell Courses Numbered 4 and 5.

A is shell course 5, and B is shell course 4. Etched: 1% Nital. Mag. X 1.1

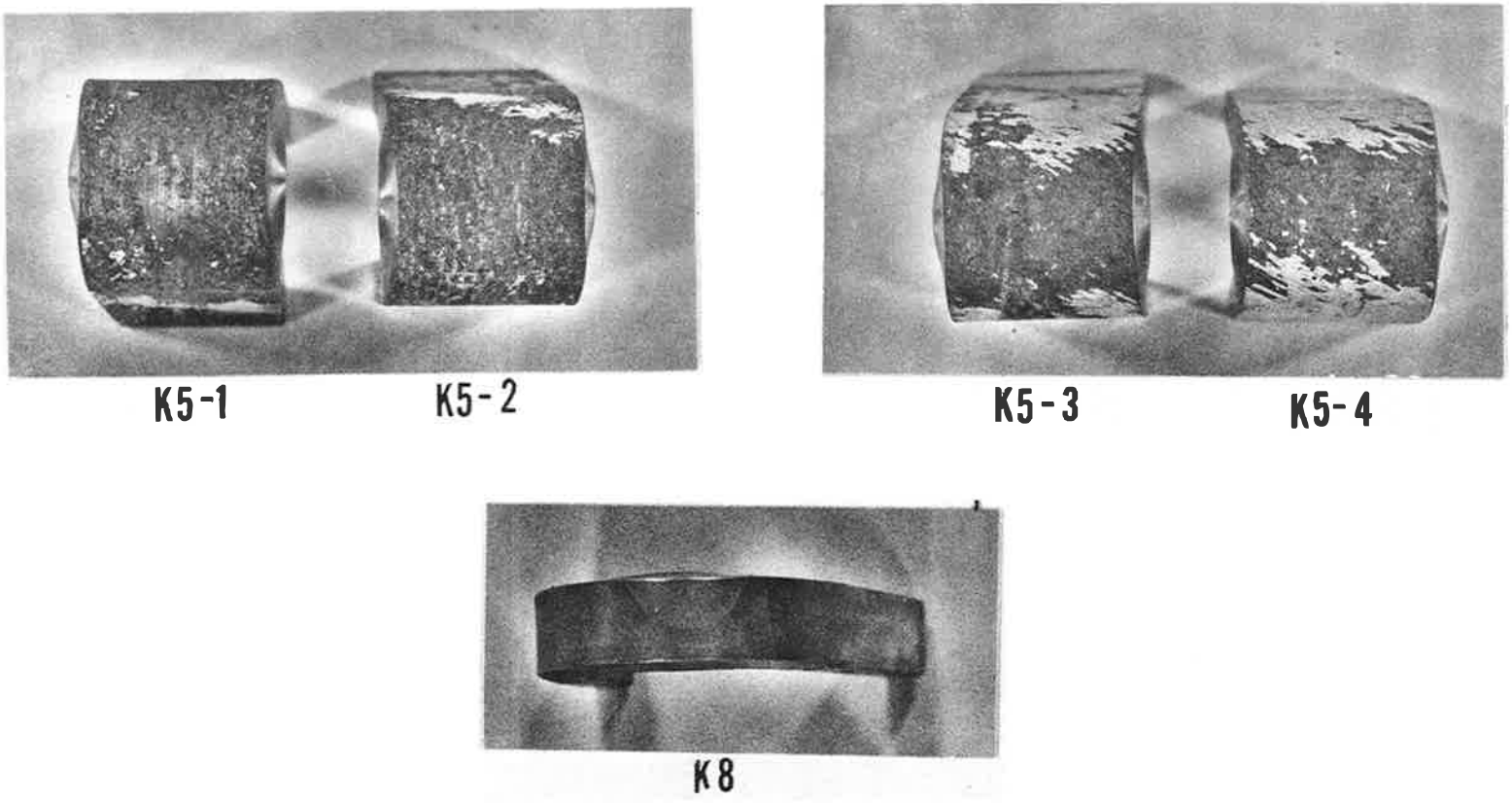

Figure 30. Bend Test Specimens of Shell-Plate K-5 and of the Weldment of K-8.

K5-1 and -2 are transverse shell-plate specimens.
K5-3 and -4 are longitudinal shell-plate specimens.
K8 is a side-bend specimen of a weld between shell courses 1 and 2.
Mag. X 3/4.

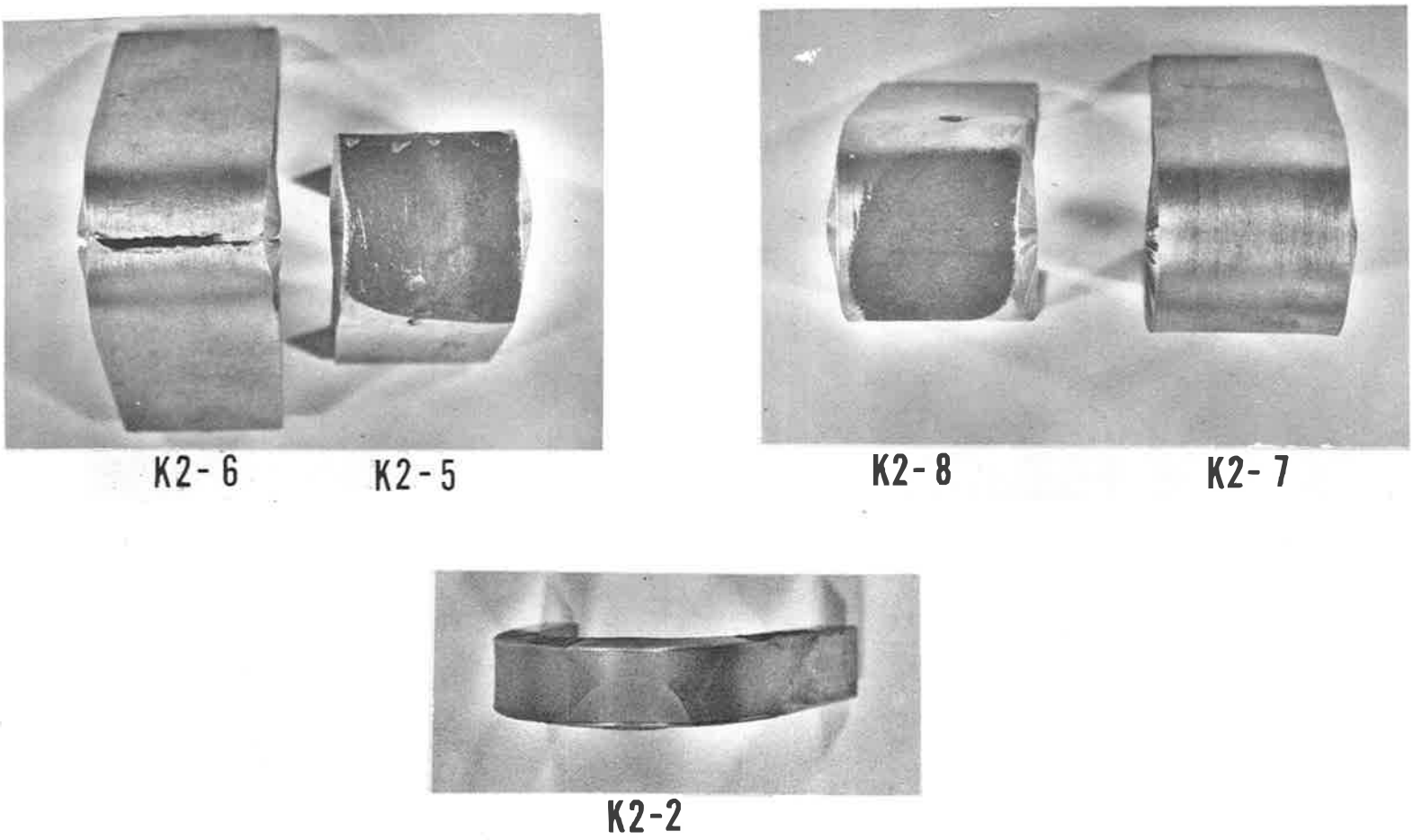

Figure 31. Bend Test Specimens of Head-Plate and of a Weldment in Sample K-2.

K2-6 and -5 are transverse head-plate specimens.
K2-8 and -7 are longitudinal head plate specimens.
K2-2 is a side-bend specimen of the weldment between the A head plate and shell course 1. Mag.X 3/4

Transverse

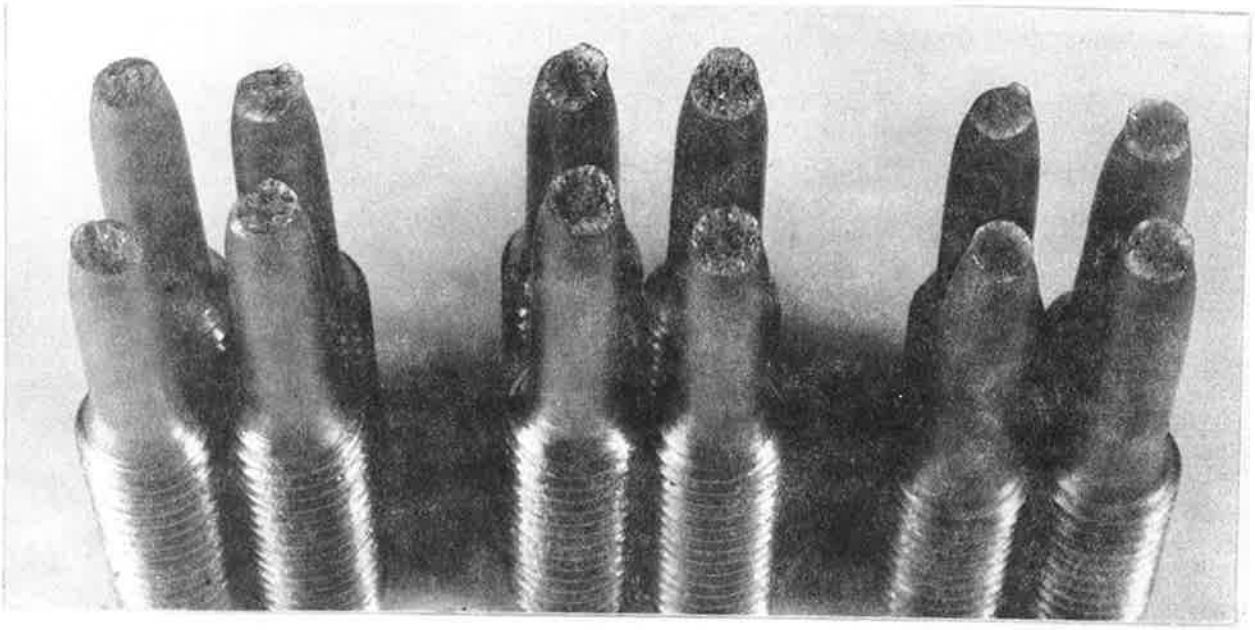

(a)

K5-1 K5-2 K1-5 K1-6 K2-11 K8-12

Shell Head Weld

Longitudinal

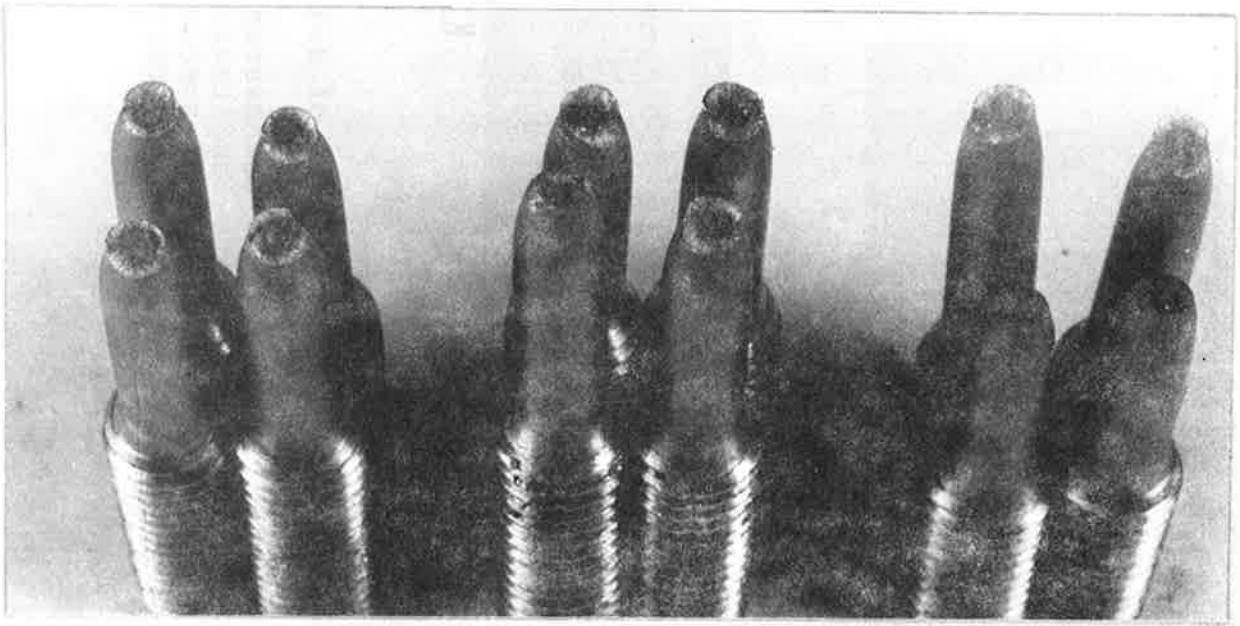

(b)

K5-3 K5-4 K1-7 K1-8 K8-9 K2-10

Shell Head Weld

Figure 32. Fracture Appearance of Tension Test Specimens. Mag. X 3

Figure 33A

IMPACT TEST RESULTS FOR LONGITUDINAL HEAD-PLATE SPECIMENS TAKEN FROM CALLAO PLATE K-1.

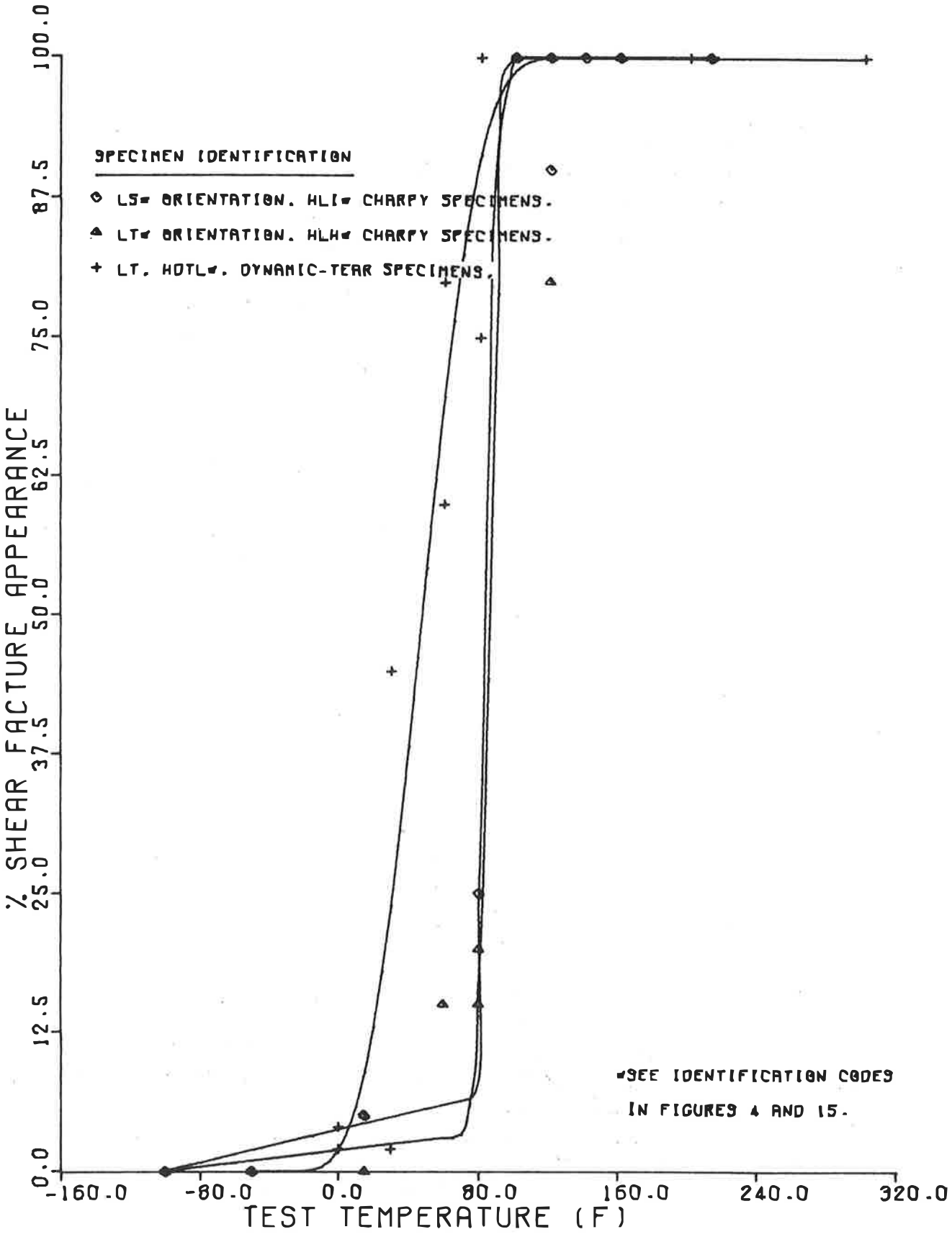

Figure 33B

IMPACT TEST RESULTS FOR LONGITUDINAL HEAD-PLATE SPECIMENS TAKEN FROM CALLAO PLATE K-1.

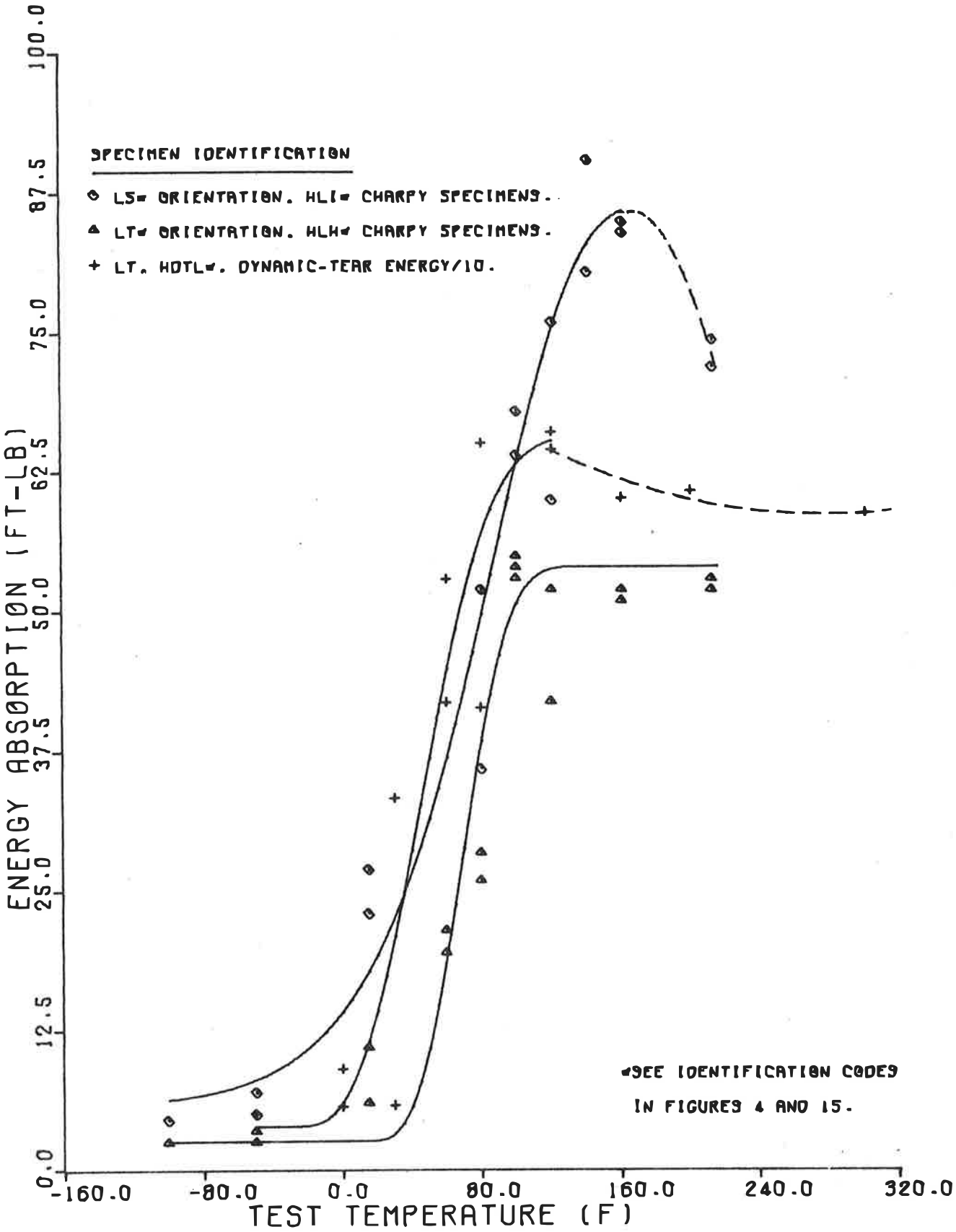

Figure 33C

IMPACT TEST RESULTS FOR LONGITUDINAL HEAD-PLATE SPECIMENS TAKEN FROM CALLAO PLATE K-1.

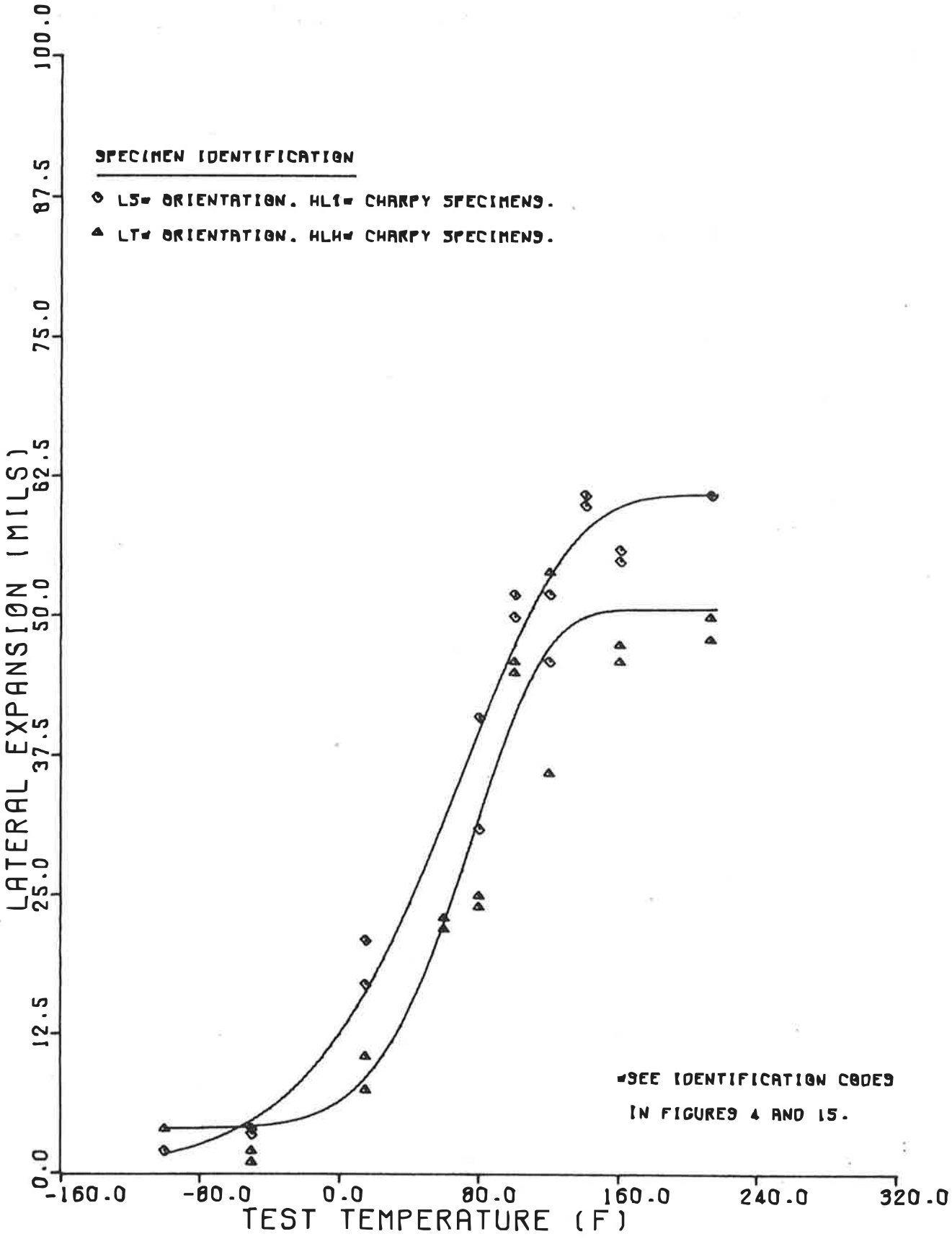

Figure 34A

IMPACT TEST RESULTS FOR TRANSVERSE AND SHORT-TRANSVERSE HEAD-PLATE SPECIMENS TAKEN FROM CALLAO PLATE K-1.

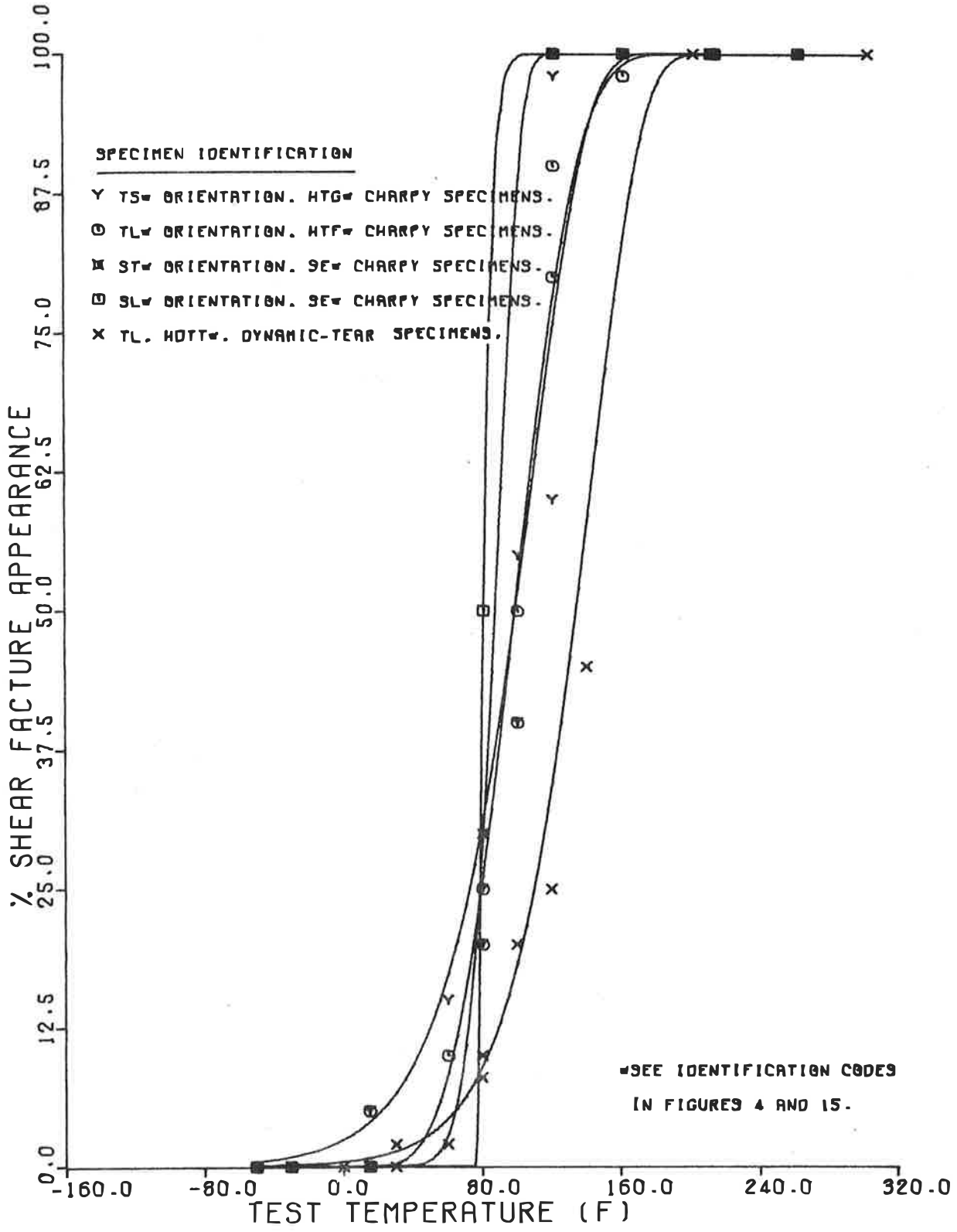

Figure 34B

IMPACT TEST RESULTS FOR TRANSVERSE AND SHORT-TRANSVERSE HEAD-PLATE SPECIMENS TAKEN FROM CALLAO PLATE K-1.

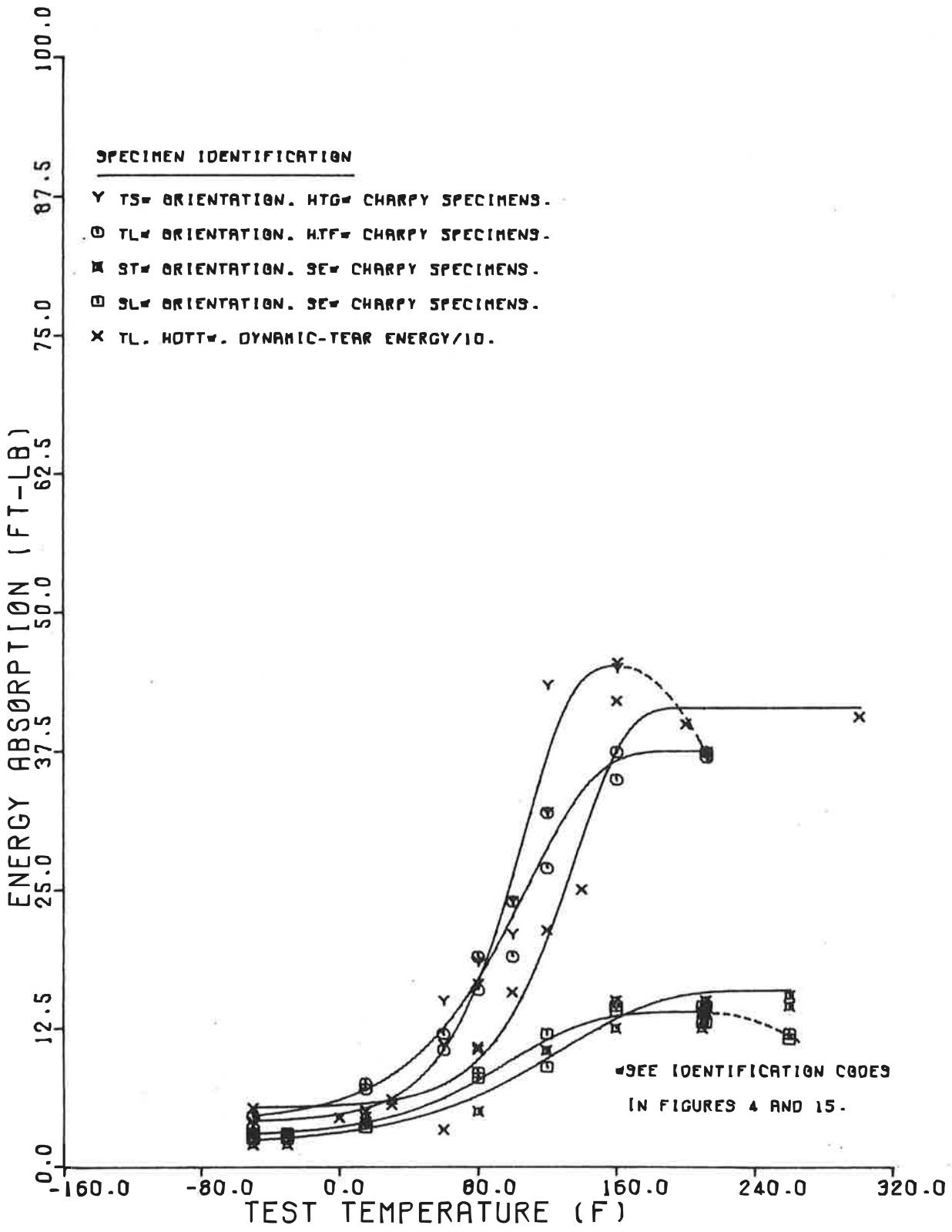

Figure 34C

IMPACT TEST RESULTS FOR TRANSVERSE AND SHORT-TRANSVERSE HEAD-PLATE SPECIMENS TAKEN FROM CALLAO PLATE K-1.

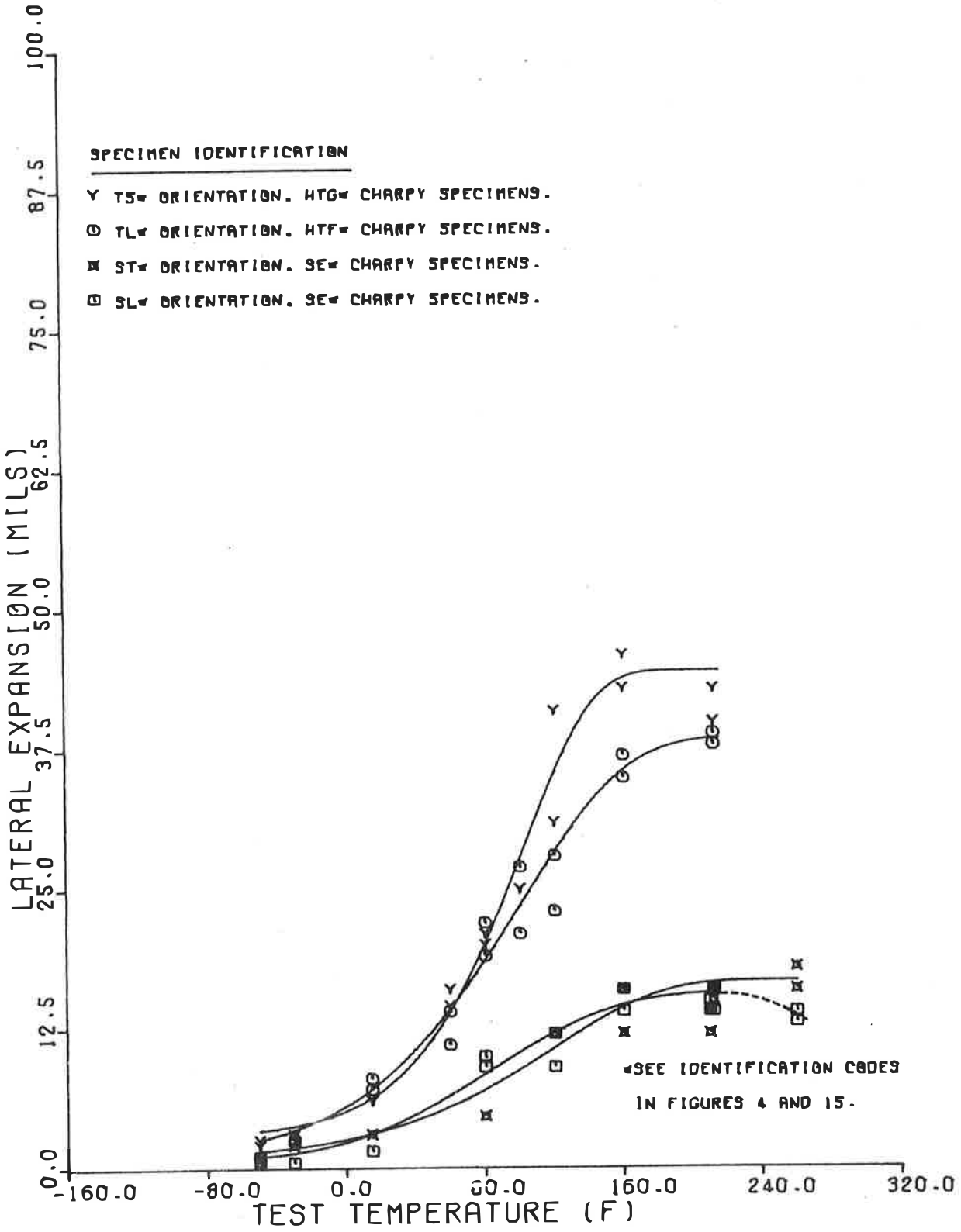

Figure 35A

IMPACT TEST RESULTS FOR LONGITUDINAL SHELL-PLATE SPECIMENS TAKEN FROM CALLAO PLATE K-5.

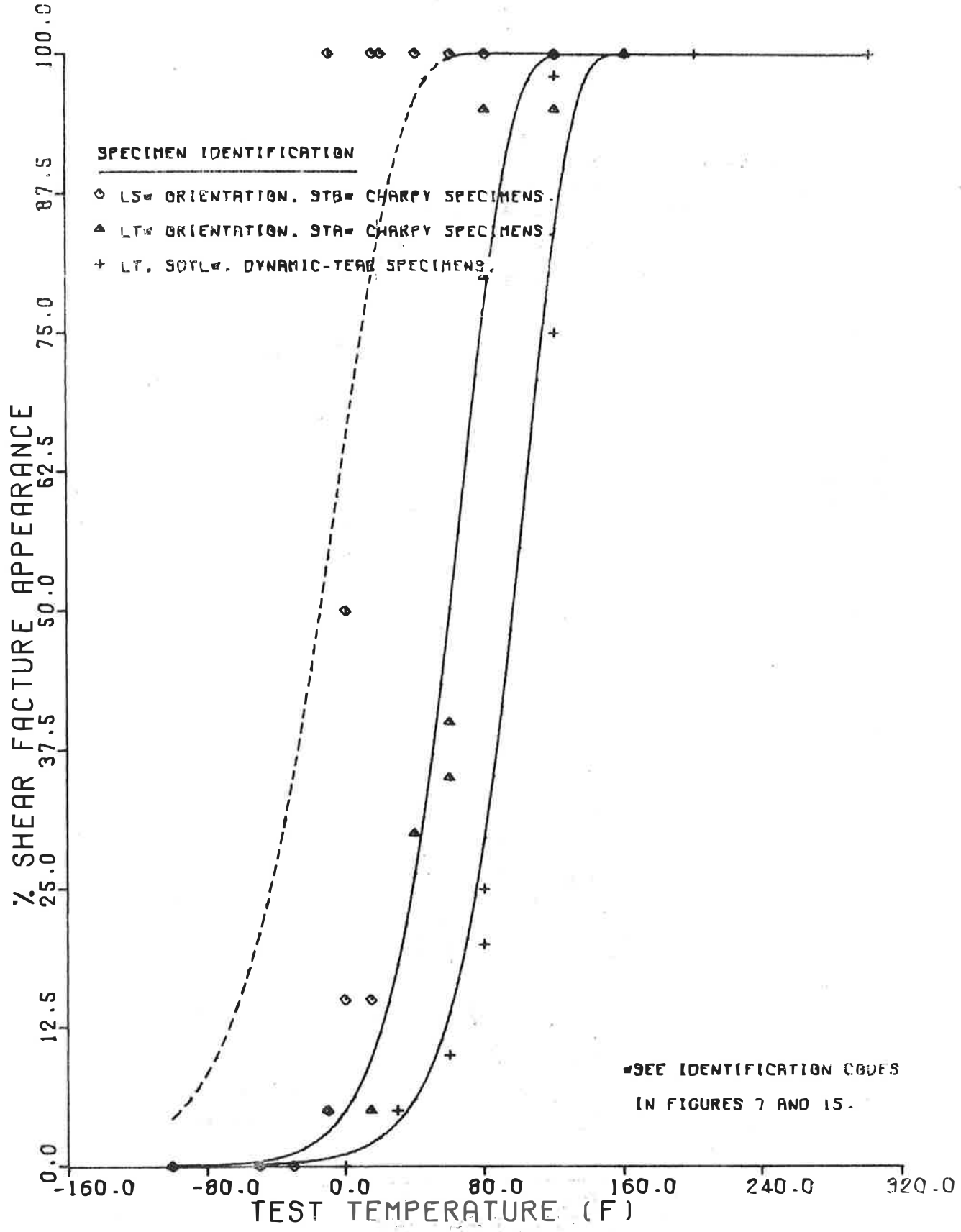

Figure 35B

IMPACT TEST RESULTS FOR LONGITUDINAL SHELL-PLATE SPECIMENS TAKEN FROM CALLAO PLATE K-5.

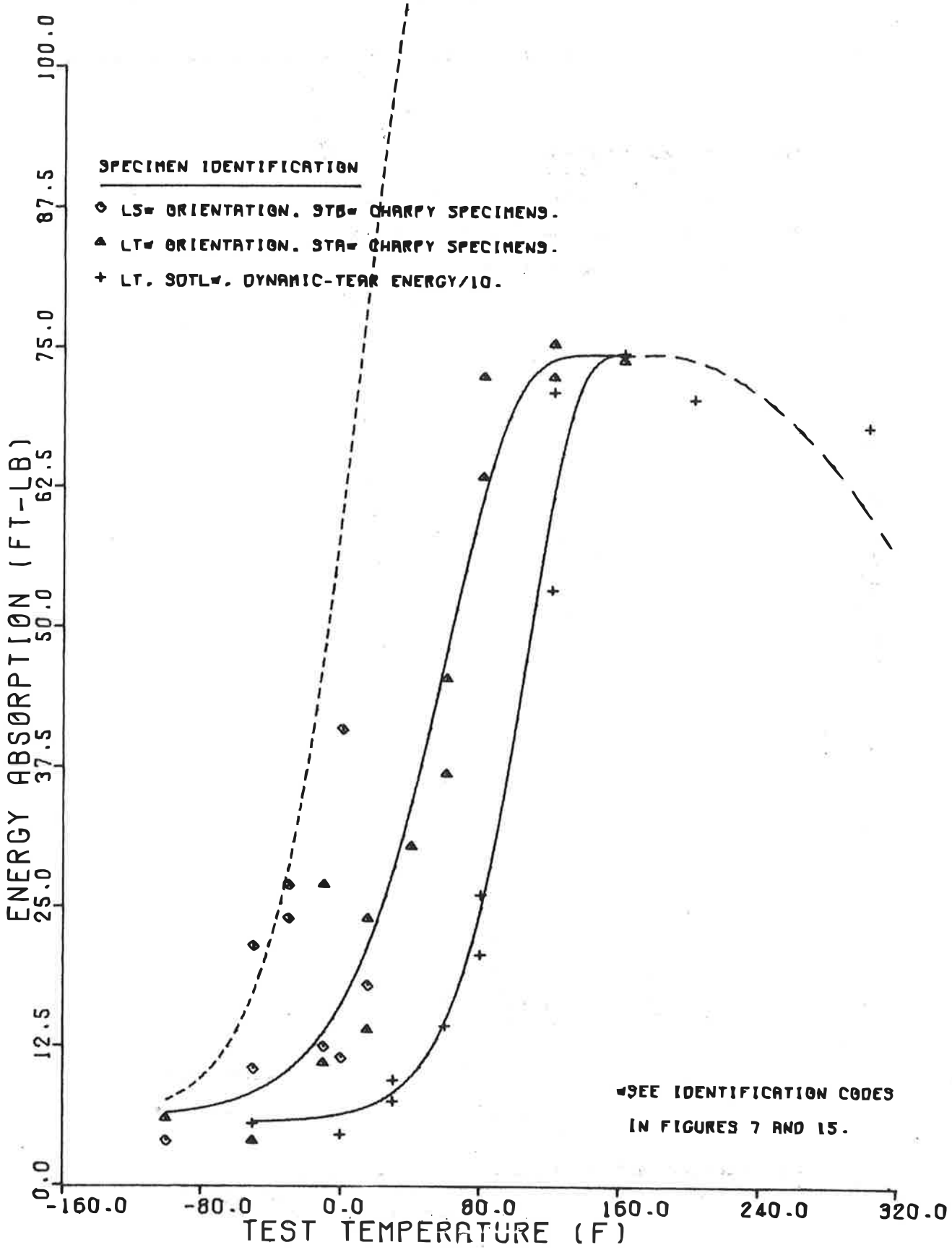

Figure 35C

IMPACT TEST RESULTS FOR LONGITUDINAL SHELL-PLATE SPECIMENS TAKEN FROM CALLAO PLATE K-5.

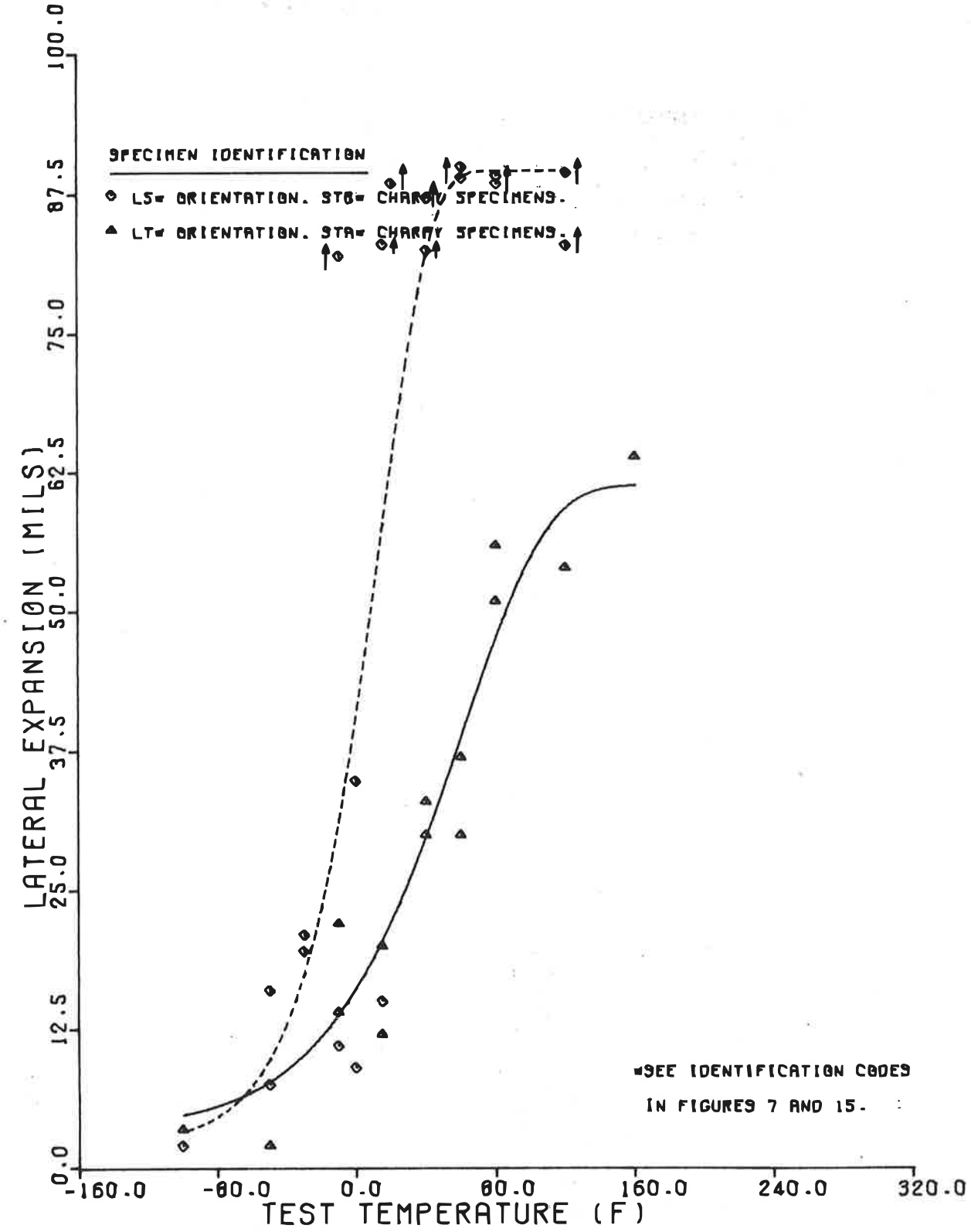

Figure 36A

IMPACT TEST RESULTS FOR TRANSVERSE SHELL-PLATE SPECIMENS TAKEN FROM CALLAO PLATE K-5.

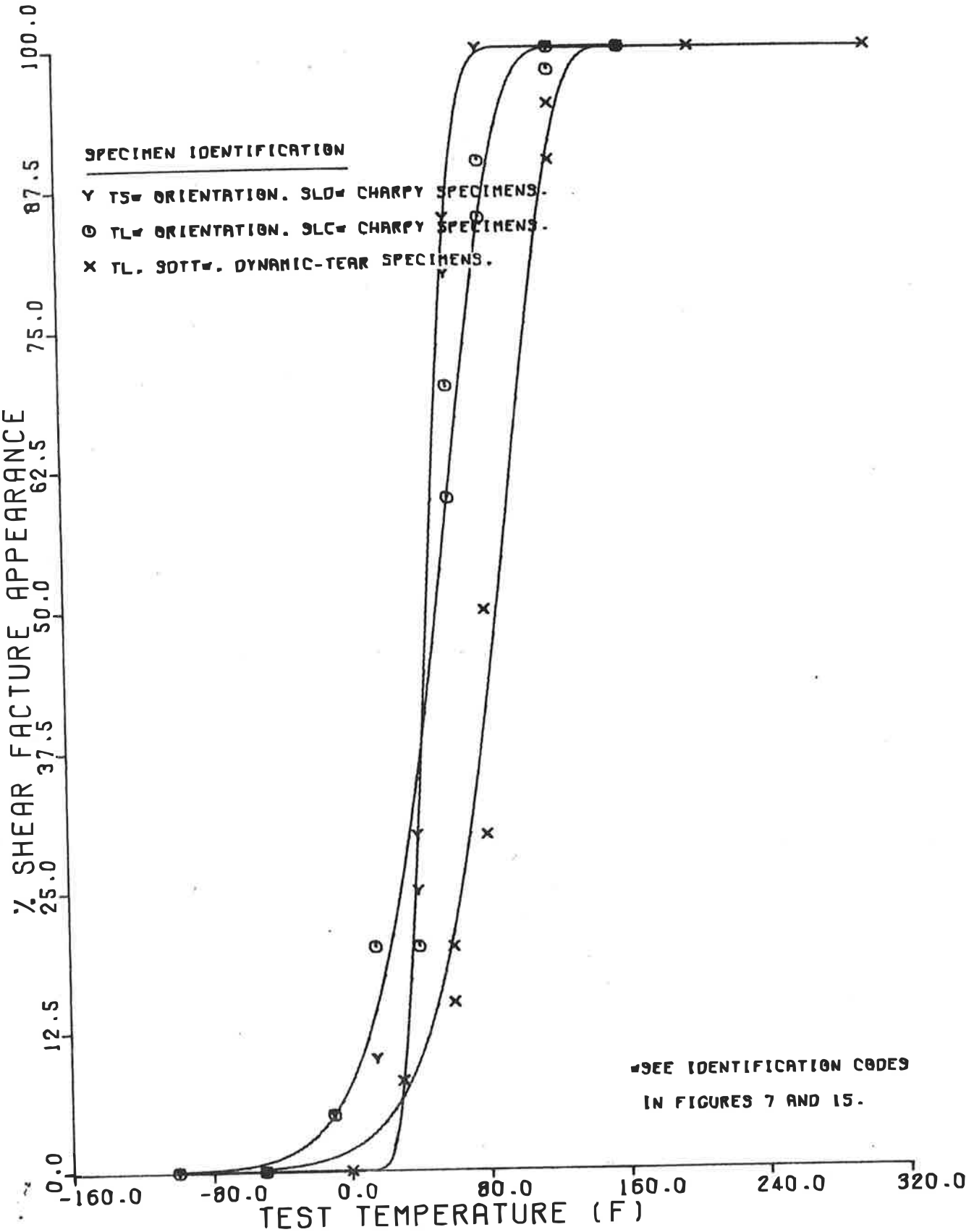

Figure 36B

IMPACT TEST RESULTS FOR TRANSVERSE SHELL-PLATE SPECIMENS TAKEN FROM CALLAO PLATE K-5.

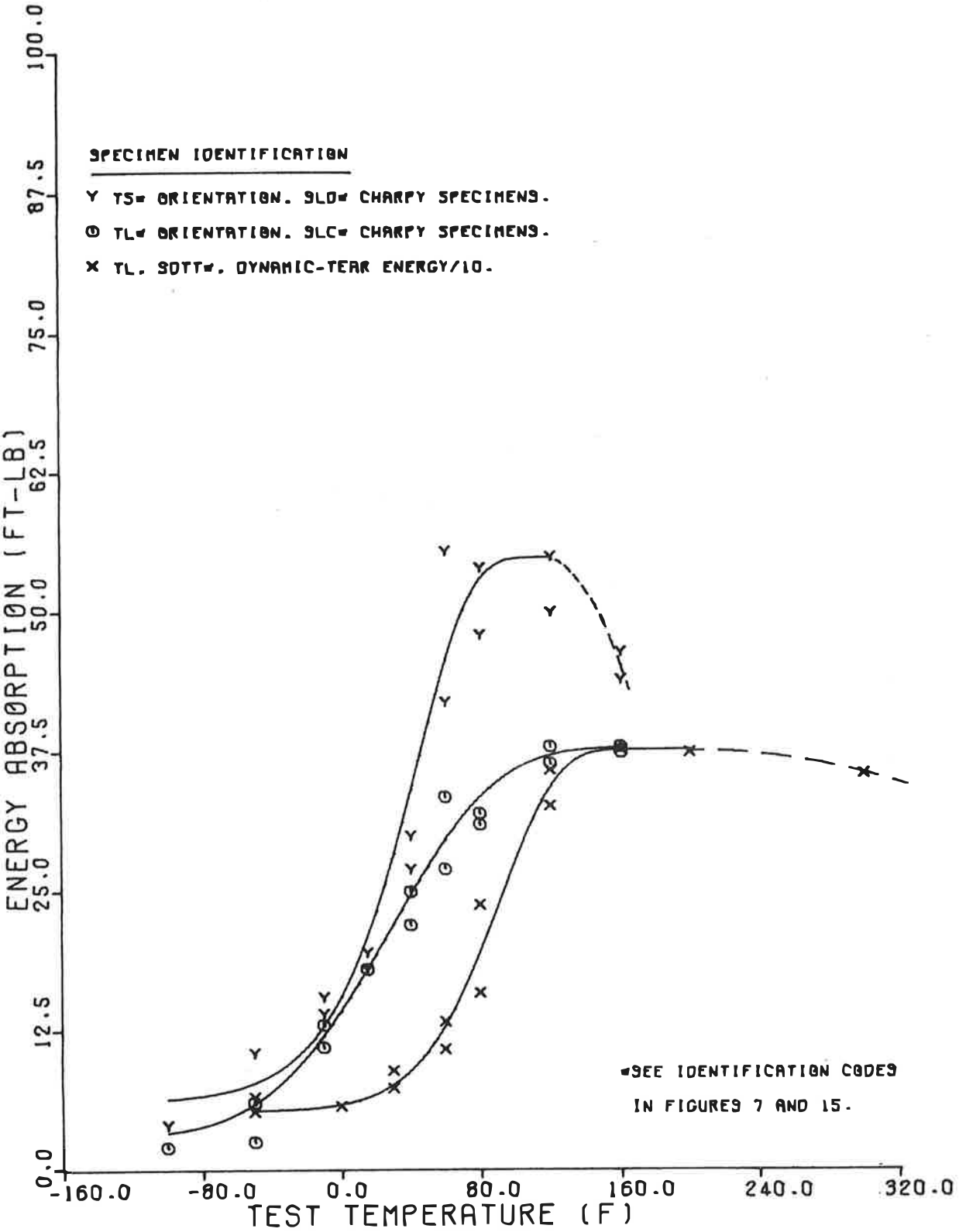

Figure 36C

IMPACT TEST RESULTS FOR TRANSVERSE SHELL-PLATE SPECIMENS TAKEN FROM CALLAO PLATE K-5.

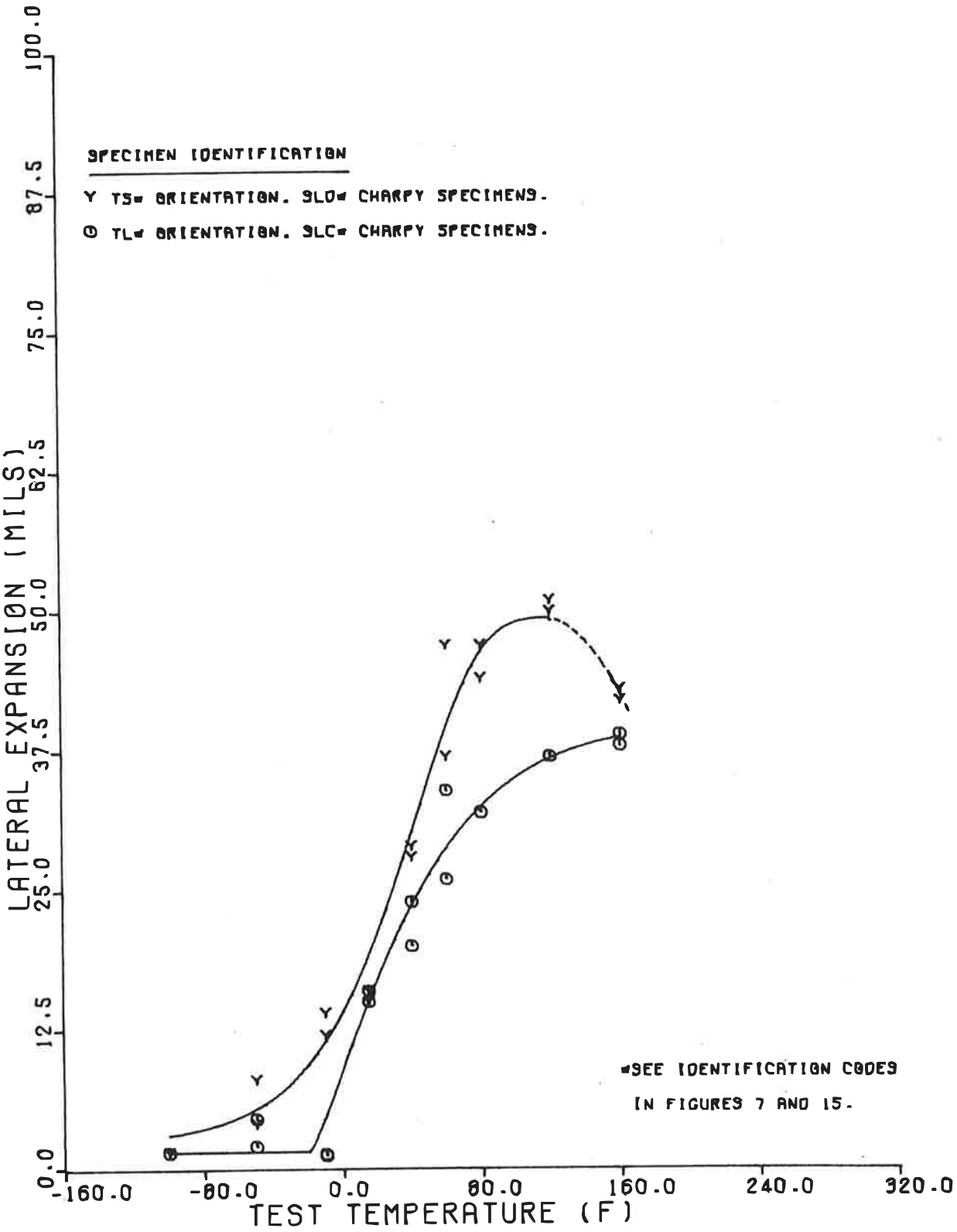

Figure 37A

CHARPY V-NOTCH TEST RESULTS FOR HEAT-AFFECTED ZONE SPECIMENS TAKEN FROM WELDMENTS FROM THE CALLAO ACCIDENT.

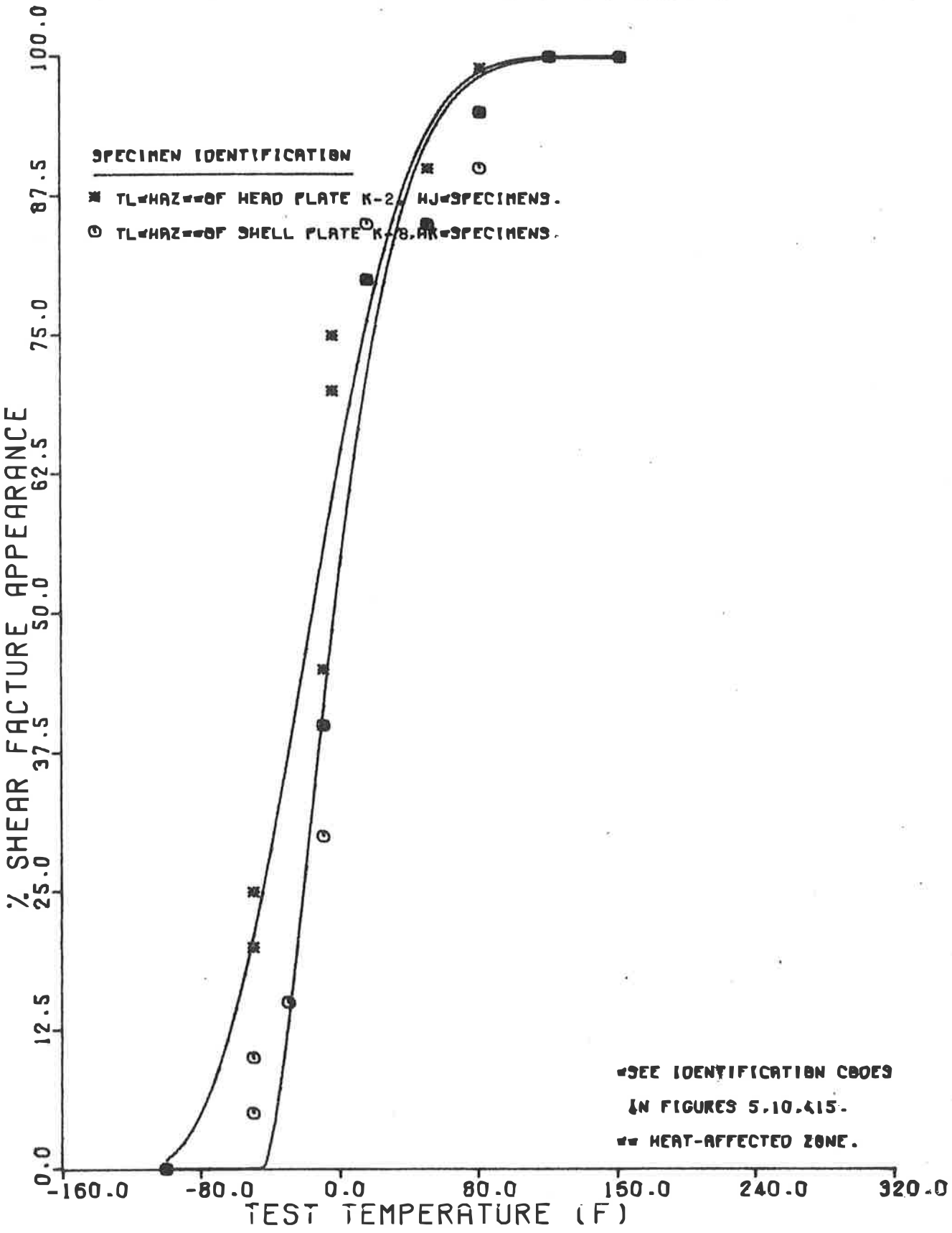

Figure 37B

CHARPY V-NOTCH TEST RESULTS FOR HEAT-AFFECTED ZONE SPECIMENS TAKEN FROM WELDMENTS FROM THE CALLAO ACCIDENT.

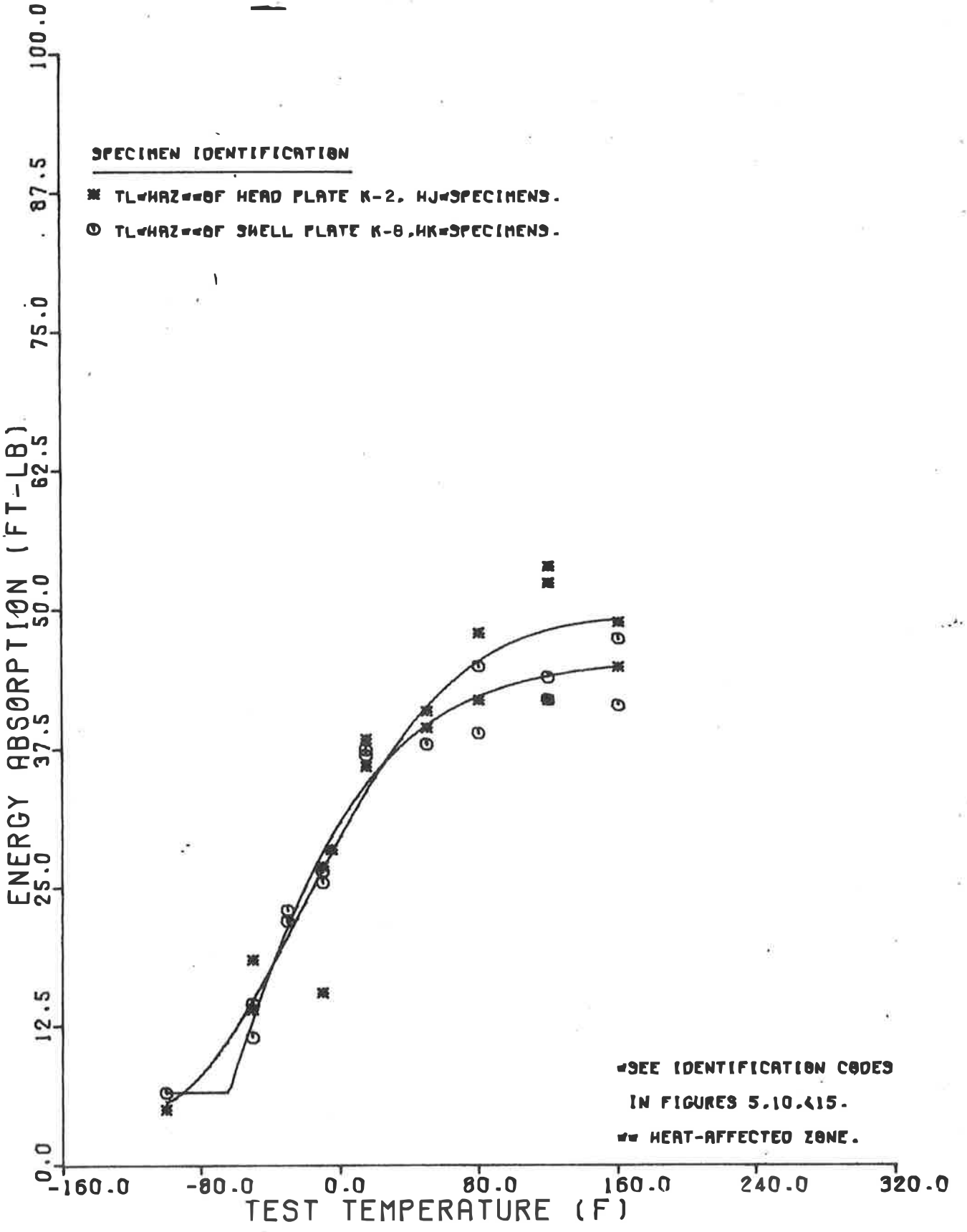

Figure 37C

CHARPY V-NOTCH TEST RESULTS FOR HEAT-AFFECTED ZONE SPECIMENS TAKEN FROM WELDMENTS FROM THE CALLAO ACCIDENT.

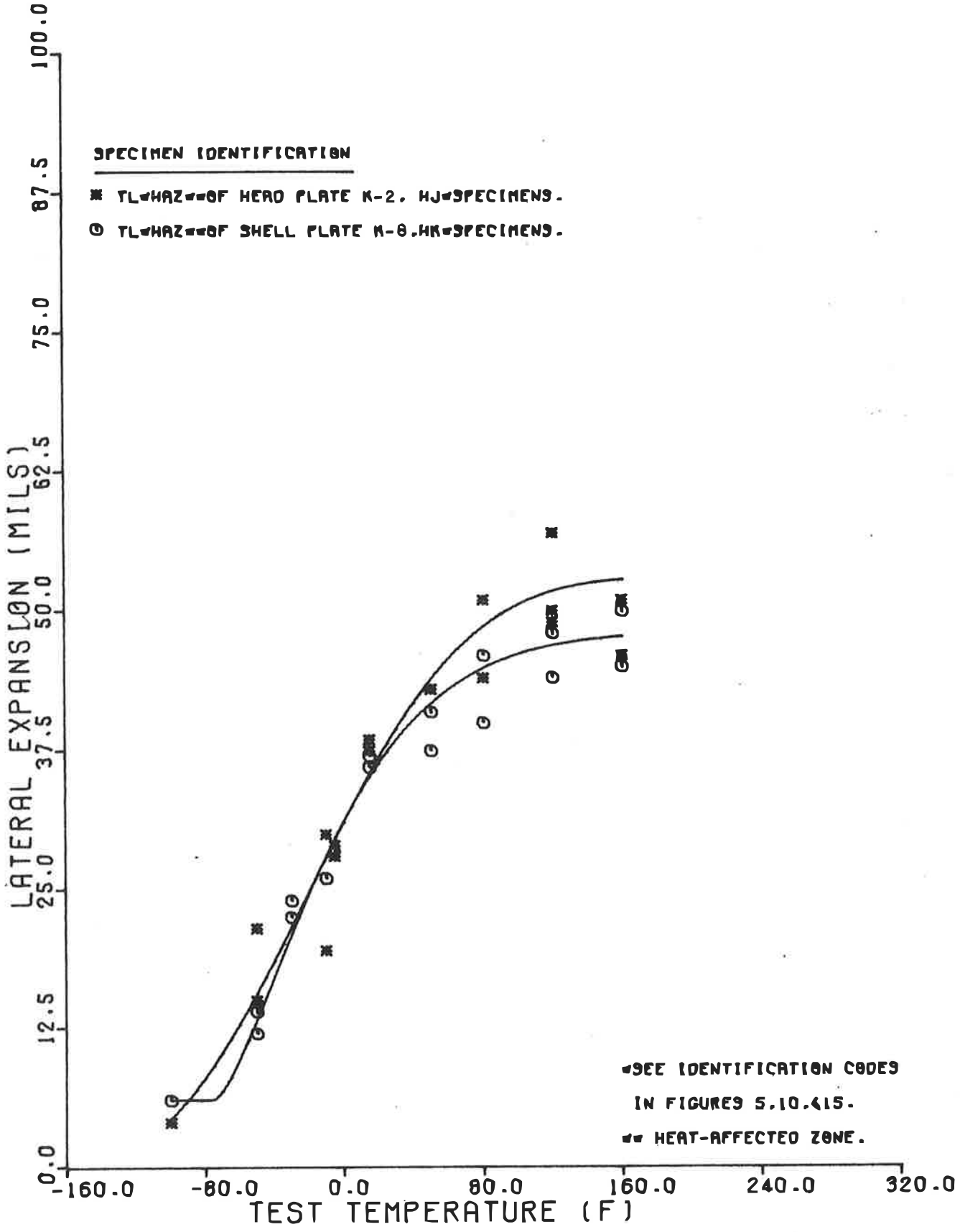

Figure 38A

CHARPY V-NOTCH TEST RESULTS FOR WELD-METAL SPECIMENS TAKEN FROM THE CALLAO ACCIDENT.

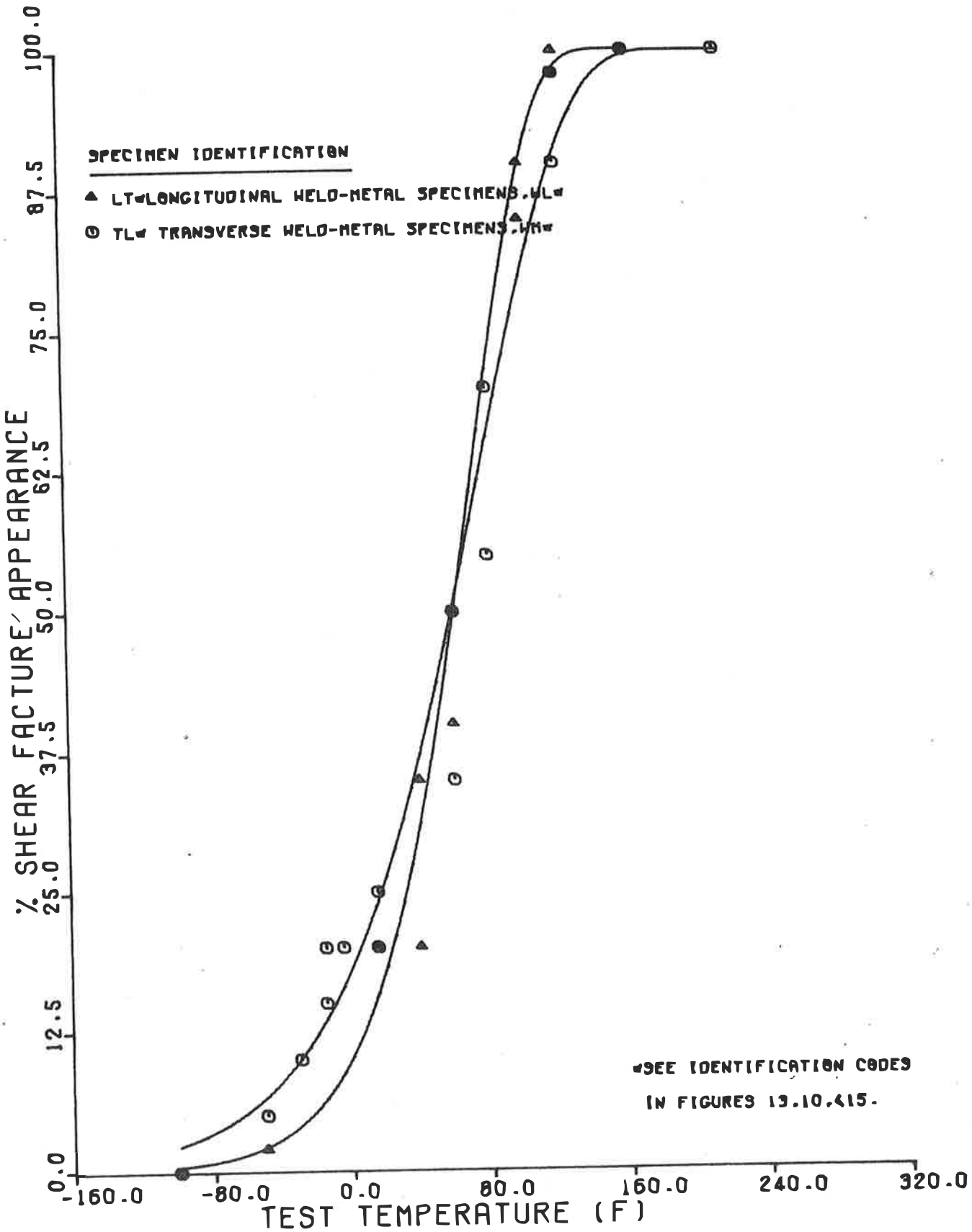

Figure 38B

CHARPY V-NOTCH TEST RESULTS FOR WELD-METAL SPECIMENS TAKEN FROM THE CALLAO ACCIDENT.

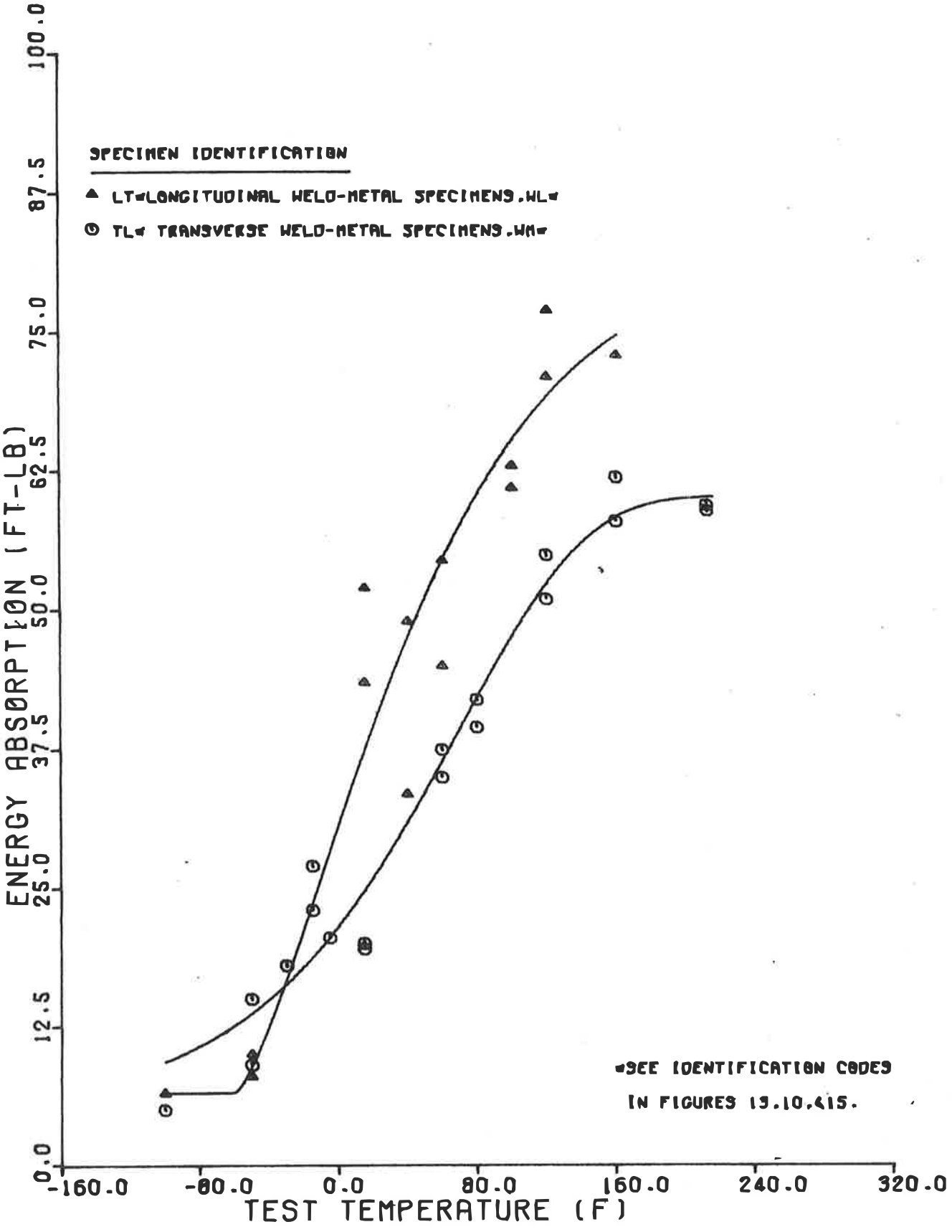

Figure 38C

CHARPY V-NOTCH TEST RESULTS FOR WELD-METAL SPECIMENS TAKEN FROM THE CALLAO ACCIDENT.

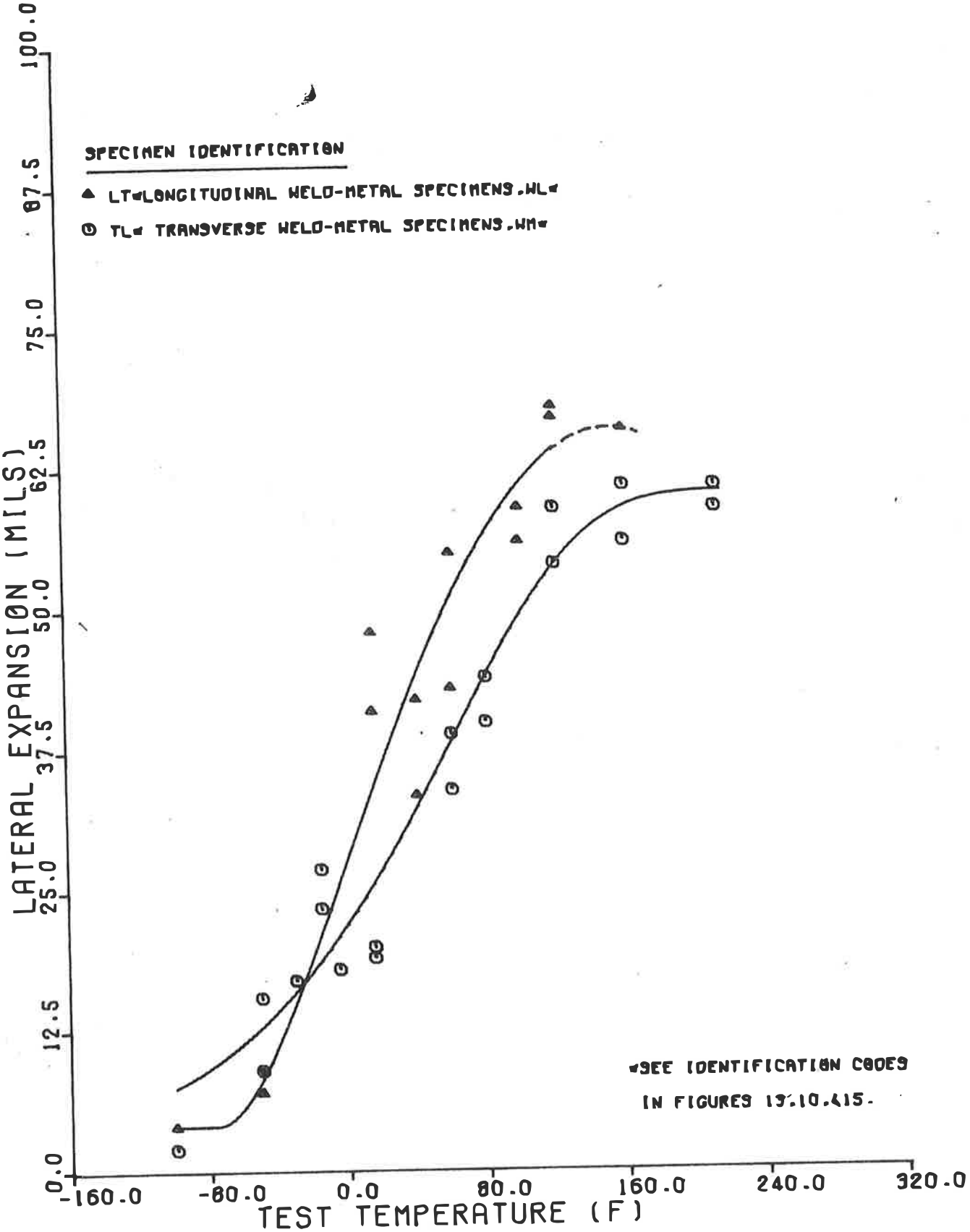

Figure 39

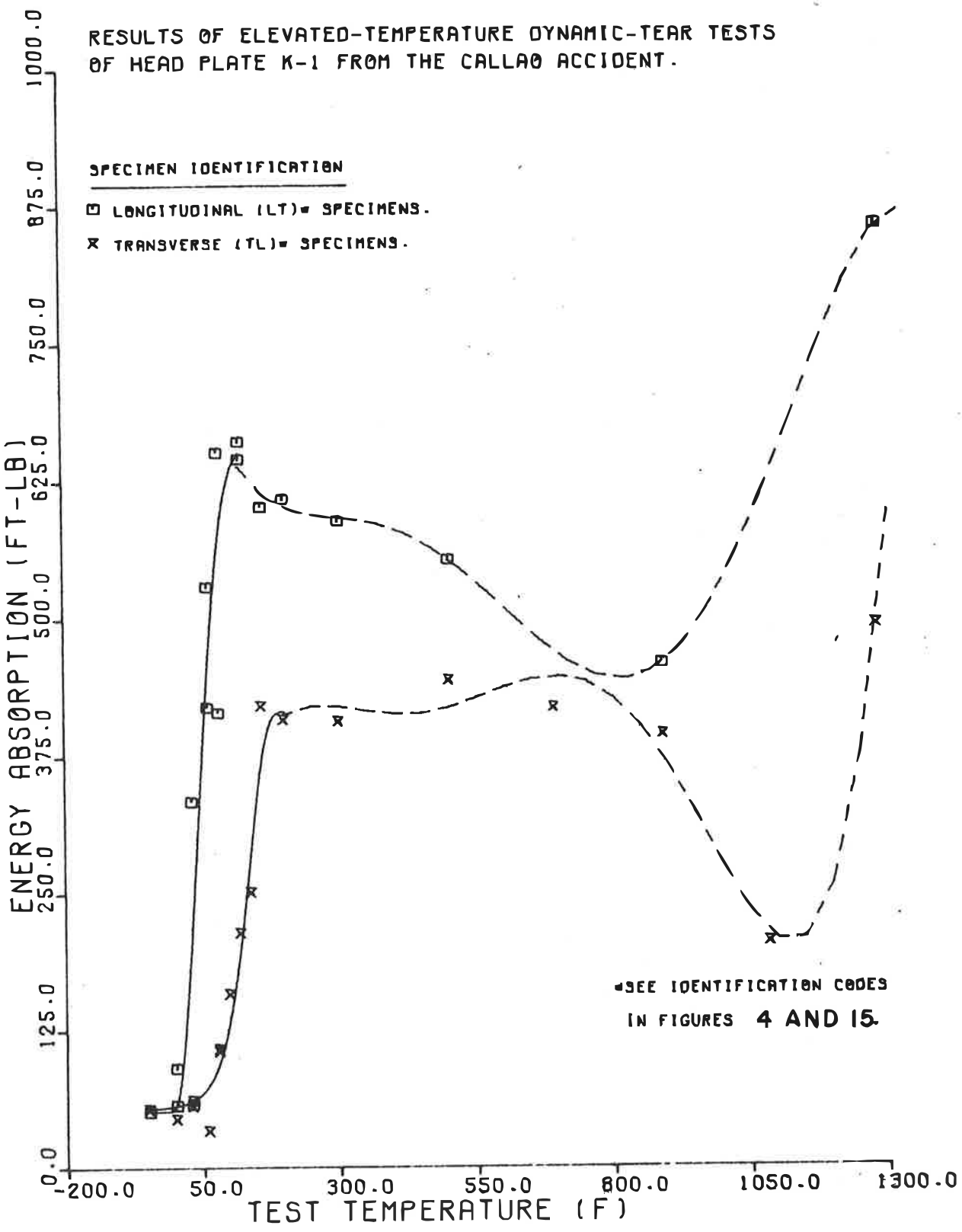
RESULTS OF ELEVATED-TEMPERATURE DYNAMIC-TEAR TESTS OF HEAD PLATE K-1 FROM THE CALLAO ACCIDENT.
SPECIMEN IDENTIFICATION
LONGITUDINAL (LT)* SPECIMENS.
TRANSVERSE (TL)* SPECIMENS.
*SEE IDENTIFICATION CODES IN FIGURES 4 AND 15.
ENERGY ABSORPTION (FT-LB)
0.0
125.0
250.0
375.0
500.0
625.0
750.0
875.0
1000.0
-200.0
50.0
300.0
550.0
800.0
1050.0
1300.0
TEST TEMPERATURE (F)

Figure 40

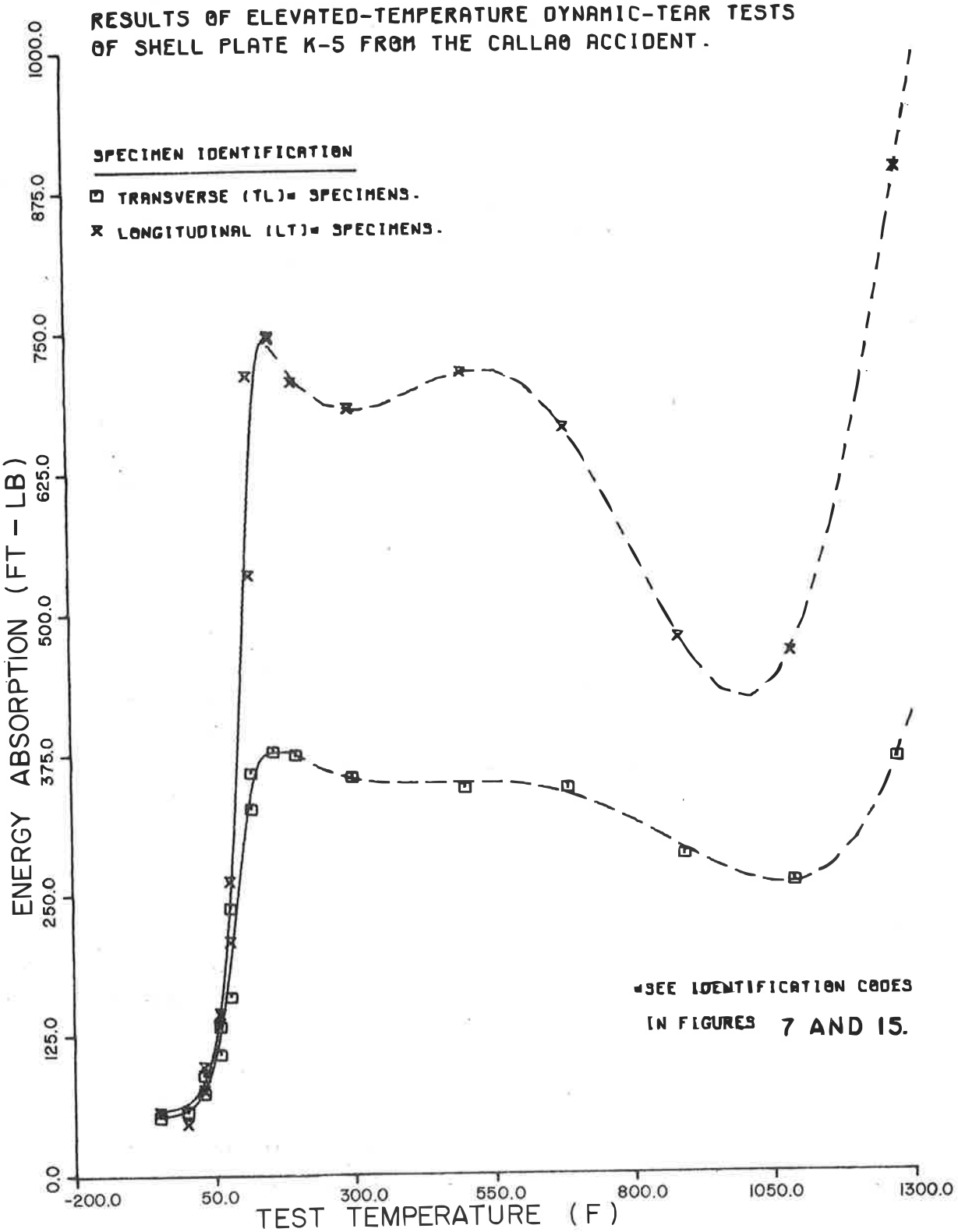
RESULTS OF ELEVATED-TEMPERATURE DYNAMIC-TEAR TESTS OF SHELL PLATE K-5 FROM THE CALLAO ACCIDENT.
SPECIMEN IDENTIFICATION
TRANSVERSE (TL)* SPECIMENS.
LONGITUDINAL (LT)* SPECIMENS.
ENERGY ABSORPTION (FT - LB)
0.0
125.0
250.0
375.0
500.0
625.0
750.0
875.0
1000.0
-200.0
50.0
300.0
550.0
800.0
1050.0
1300.0
TEST TEMPERATURE (F)
*SEE IDENTIFICATION CODES IN FIGURES 7 AND 15.

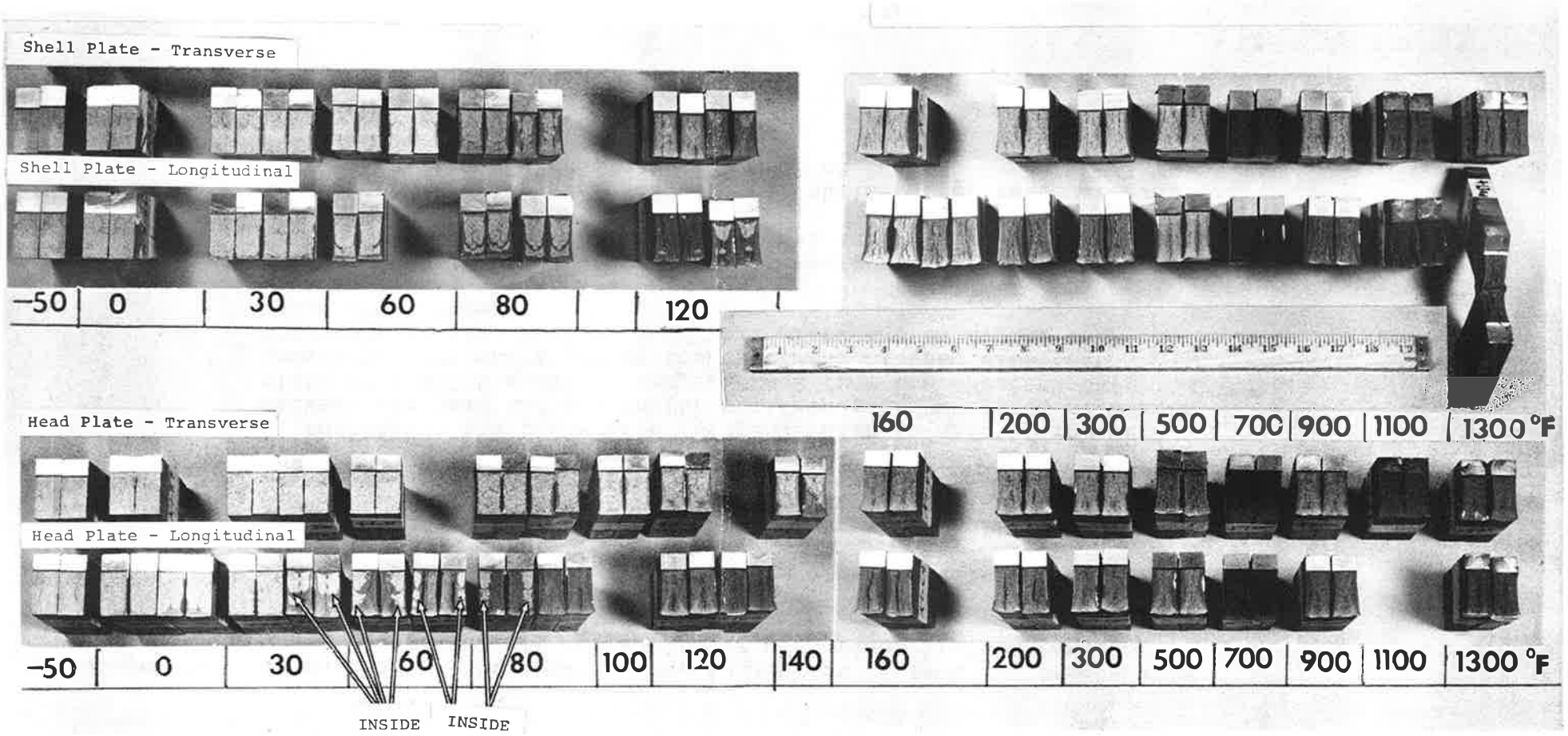

Figure 41. Fracture Appearances of Dynamic-Tear Specimens.

The arrows point to the half-thickness of the plate corresponding with the inside of the head plate of the tank car. Mag. X 5/16.

Figure 42. Comparison of the Shelf Energy Absorption of Tank Car Steels with Other Conventionally Melted Steels of Various Yield Strength Levels.

o Represents data for various steels given in Reference 14.

+ Represents the longitudinal shelf energy of shell plates of the M128 steel of the South Byron sample (ref. 10) and of the A 212-B steel of sample FRA-2 taken at Crescent City,

x Represents the transverse (perpendicular to axis of the weld between the head and the shell) shelf-energy absorption of a head plate of A 212-B steel of sample FRA-2 from the Crescent City accident. The shelf energy for specimens aligned with the principal rolling direction of this plate may be higher than the value shown here.

□ Represents the longitudinal shelf energy of shell and head plates of the M128 steel of Callao samples K-5 and K-1, respectively.

Δ Represents weld-metal longitudinal shelf-energy value as measured on samples from a circumferential weld of "Callao Tank-Car" GATX 94451.

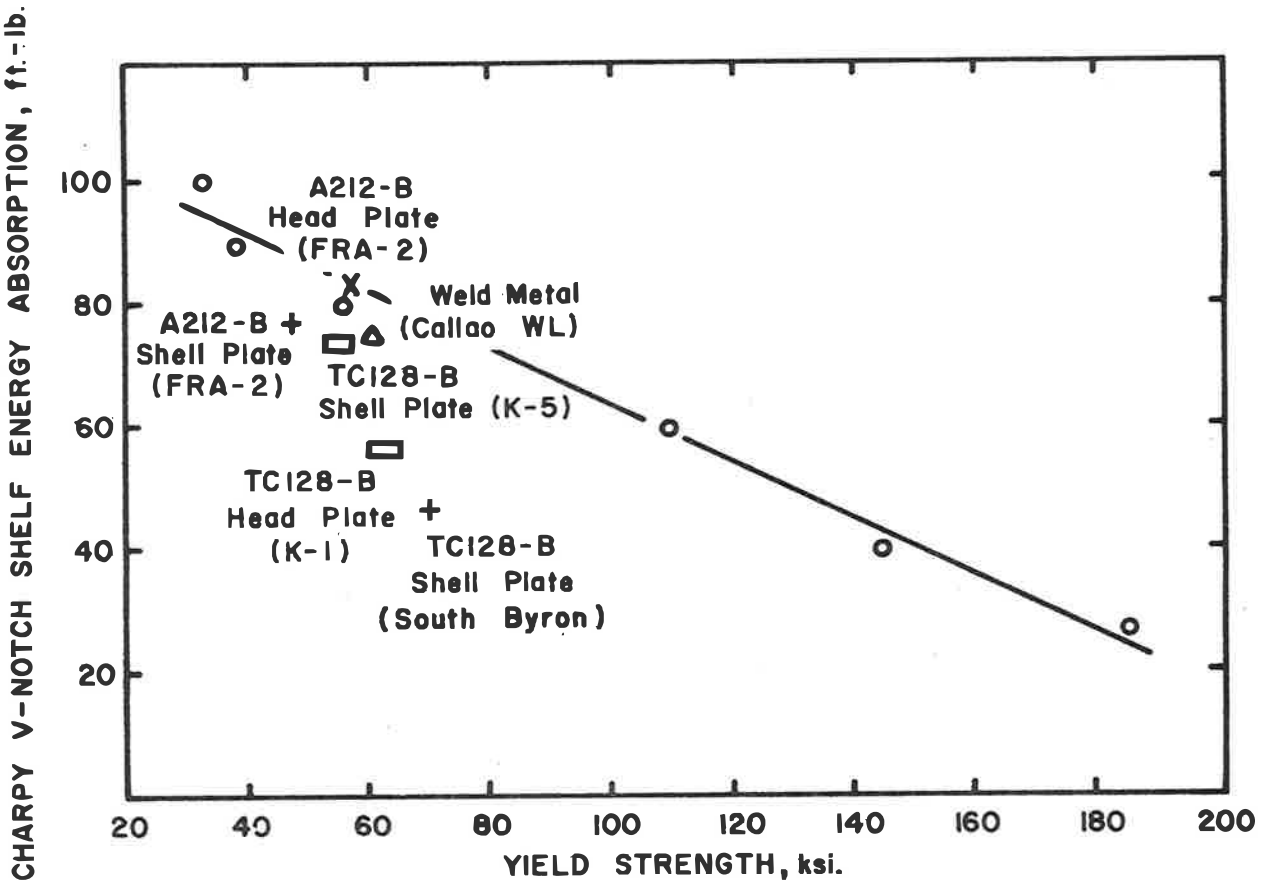
CHARPY V-NOTCH SHELF ENERGY ABSORPTION, ft.-lb.
100
80
60
40
20
A212-B
Head Plate
(FRA-2)
Weld Metal
(Callao WL)
A212-B +
Shell Plate
(FRA-2)
TC128-B
Shell Plate (K-5)
TC128-B
Head Plate
(K-1)
+
TC128-B
Shell Plate
(South Byron)
20
40
60
80
100
120
140
160
180
200
YIELD STRENGTH, ksi.

Appendix A

Specifications

AAR-TC128-65 and -70

ASSOCIATION OF AMERICAN RAILROADS
OPERATIONS AND MAINTENANCE DEPARTMENT
MECHANICAL DIVISION

SPECIFICATIONS
M-128-65
HIGH TENSILE STRENGTH CARBON-MANGANESE STEEL PLATES FOR TANK CAR TANKS AND OTHER PRESSURE VESSELS

ADOPTED, 1964; REVISED, 1965

1. **Scope.**—This specification covers two grades of high strength carbon-manganese steel plate of flange quality. The maximum thickness shall be 1 inch. Moderately high manganese content, together with small amounts of other elements, provide for high tensile strength with limited carbon content. The steel shall be made to fine grain practice.

Welding technique is of fundamental importance, and it is pre-supposed that welding procedures will be in accordance with good practice.

2. **General Conditions for Delivery.**—Material furnished under these specifications shall conform to the applicable requirements of the current edition of the Specification for General Requirements for Delivery of Rolled Steel Plates of Flange and Firebox Qualities (A.S.T.M. Designation: A-20).

3. **Process.**—The steel shall be made by one or more of the following processes: Open hearth, electric furnace or basic oxygen.

4. **Chemical Composition.**—The steel shall conform to the requirements as to chemical composition prescribed in Table I.

TABLE I. CHEMICAL REQUIREMENTS
(LADLE ANALYSIS)

	Grade A	Grade B
Carbon, max. per cent	0.25	0.25
Manganese, max. per cent		
For plates ½" and under in thickness	1.35	1.35
For plates over ½" to 1" incl. in thickness	1.50	1.50
Phosphorus, max. per cent	0.040	0.040
Sulphur, max. per cent	0.050	0.050
Silicon, max. per cent		
For plates ½" and under in thickness	0.30	0.30
For plates over ½" to 1" incl. in thickness	0.50	0.50
Vanadium, min. per cent	0.02	—

Grade B will contain small amounts of other elements not exceeding the following percentages:

Copper	0.35%
Nickel	0.25
Chromium	0.25
Molybdenum	0.08

These elements will be reported when requested by the purchaser.

TABLE II. TENSILE REQUIREMENTS

	Grade A	Grade B
Tensile strength, psi	81,000 to 101,000	
Yieldpoint, min. psi	50,000	
Elongation in 8 inches, min. per cent	18.0 (b, c)	

5. **Tensile Properties.**—(a) The material as represented by the test specimens shall conform to the requirements as to tensile properties prescribed in Table II.

(b) For material under ½ inch in thickness, a deduction from the percentage of elongation in 8 inches specified in Table II of 1.25 per cent shall be made for each decrease of 1/32 inch of the specified thickness below ½ inch.

(c) For material over ¾ inch in thickness a deduction from the percentage of elongation in 8 in. specified in Table II of 0.5 per cent shall be made for each increase of 1/32 in. of the specified thickness above ¾ inch. This deduction shall not exceed 3 per cent.

6. **Bending Properties.**—The bend test specimen shall stand being bent cold through 180° without cracking on the outside of the bent portion through an inside diameter which shall have the relation to the thickness of the specimen prescribed in Table III. When the test is made on a specimen reduced in thickness, the rolled surface shall be on the outer curve of the bend.

TABLE III. BEND DIAMETERS

Thickness of Material, in.	Ratio of Bend Diameter to Thickness of Specimen
1 and under	2

7. **Test Specimens.**—Test specimens shall be prepared from the material in the as-rolled condition.

8. **Number of Tests.**—One tension test and one bend test shall be made from each plate as-rolled.

9. **Inspection.**—(a) The inspector representing the purchaser shall have free entry, at all times while the work on the contract of the purchaser is being performed, to all parts of the manufacturer's works which concern the manufacture of the material ordered. The manufacturer shall afford the inspector, free of charge, all reasonable facilities and necessary assistance to satisfy him that the material is being furnished in accordance with these specifications. Tests and inspection shall be made at the place of manufacture prior to shipment, unless otherwise specified.

(b) The purchaser may make tests to cover the acceptance or rejection of the material in his own laboratory or elsewhere. Such tests shall be made at the expense of the purchaser.

10. **Rejection.**—(a) Material represented by samples which fail to conform to the requirements of these specifications will be rejected.

(b) Material which shows injurious defects subsequent to its original inspection and acceptance at the manufacturer's works, or elsewhere, will be rejected, and the manufacturer shall be notified.

11. **Rehearing.**—Samples tested in accordance with these specifications which represent rejected material, shall be held for a period of fourteen, (14) days from date of the test report. In case of dissatisfaction with the results of the tests, the manufacturer may make claim for a rehearing within that time.

M128.00 SPECIFICATION FOR HIGH STRENGTH CARBON MANGANESE STEEL PLATES FOR TANK CARS — AAR TC128-70.

M128.01 SCOPE

(a) This specification covers two grades of high strength carbon-manganese steel plate of flange quality. The maximum thickness shall be 1 inch. Moderately high manganese content, together with small amounts of other elements provide for high strength with limited carbon content. The steel shall be made to fine grain practice. Welding technique is of fundamental importance, and it is presupposed that welding procedure will be in accordance with good practice.

(b) The material shall be furnished in the as-rolled condition. When specified for low temperature service the material shall be furnished normalized to meet requirements of ASTM Specification A300-68, Class 1, except that impact specimens shall be Type A Charpy V-Notch as shown in ASTM Specification A370-68 and meet impact requirements at the temperature specified in the tank car specification.

M128.02 GENERAL CONDITIONS FOR DELIVERY

(a) Material furnished under this specification shall conform to the applicable requirements of ASTM Specification A20-69a titled, "General Requirements for Delivery of Steel Plates for Pressure Vessels."

(b) See M128.01(b).

M128.03 PROCESS

(a) The steel shall be made by one or more of the following processes:

(1) Open-hearth,
(2) Electric furnace, or
(3) Basic oxygen.

M128.04 CHEMICAL COMPOSITION

(a) The steel shall conform to the requirements as to chemical composition prescribed in Table M128.04(a).

TABLE M128.04(a) CHEMICAL REQUIREMENTS

Element		Ladle Analysis, Percent	
		Grade A	Grade B
Carbon	Max.	0.25	0.25
Manganese,	Max.		
For plates 3/4" and under in thickness		1.35	1.35
For plates over 3/4" to 1" incl. in thickness		1.50	1.50
Phosphorus	Max.	0.040	0.040
Sulfur	Max.	0.050	0.050
Silicon	Max.		
For plates 3/4" and under in thickness		0.30	0.30
For plates over 3/4" to 1" incl. in thickness		0.50	0.50
Vanadium a/		0.02 Min.	0.08 Max.
Copper a/	Max.	---	0.35
Nickel a/	Max.	---	0.25
Chromium a/	Max.	---	0.25
Molybdenum a/	Max.	---	0.08

a/ These elements will be reported when requested by the purchaser.

M128.05 TENSILE PROPERTIES

(a) The material as represented by the test specimens shall conform to the requirements as to tensile properties prescribed in Table M128.05(a).

TABLE M128.05(a) TENSILE REQUIREMENTS

Property		Grade A and Grade B
Tensile strength, psi		81,000 to 101,000
Yield point, psi	Min.	50,000
Elongation in 8 inches percent	Min.	16.0 a/
Elongation in 2 inches percent	Min.	19.0

a/ For material under 5/16 inch thick a reduction from the specified percent of elongation of 1.25 percent shall be made for each decrease of 1/32 inch of thickness below 5/16 inch. For material over 3/4 inch thick a reduction from the specified percent elongation of 0.5 percent shall be made for each increase of 1/8 inch of the thickness above 3/4 inch; this deduction shall not exceed 3 percent.

M128.06 BENDING PROPERTIES

(a) The bend test specimens shall stand being bent cold through 180° without cracking on the outside of the bent portion through an inside diameter which shall have the relation to the thickness of the specimen prescribed in Table M128.06(a). When the test is made on a specimen reduced in thickness, the rolled surface shall be on the outer curve of the bend.

TABLE M128.06(a) BEND DIAMETERS

Thickness of Material, Inches	Ratio of Bend Diameter to Thickness of Specimen
1 and under	2

M128.07 TEST SPECIMENS

(a) Test specimens shall be prepared from the material in the as-rolled condition.

M128.08 NUMBER OF TESTS

(a) One tension test and one bend test shall be made from each plate as rolled.

Note: The term "plate as rolled" used here refers to the unit plate rolled from a slab or directly from an ingot in its relation to the location and number of specimens, not to its condition.

M128.09 INSPECTION

(a) The inspector representing the purchaser shall have free entry, at all times while the work on the contract of the purchaser is being performed, to all parts of the manufacturer's works which concern the manufacture of the material ordered. The manufacturer shall afford the inspector, free of charge, all reasonable facilities and necessary assistance to satisfy him that the material is being furnished in accordance with these specifications. Tests and inspection shall be made at the place of manufacture prior to shipment, unless otherwise specified.

(b) The purchaser may make tests to cover the acceptance or rejection of the material in his own laboratory or elsewhere. Such tests shall be made at the expense of the purchaser.

M128.10 REJECTION

(a) Material represented by samples which fail to conform to the requirements of these specifications will be rejected.

(b) Material which shows injurious defects subsequent to its original inspection and acceptance at the manufacturer's works, or elsewhere, will be rejected, and the manufacturer shall be notified.

M128.11 REHEARING

(a) Samples tested in accordance with these specifications which represent rejected material, shall be held for a period of fourteen days from date of the test report. In case of dissatisfaction with the results of the tests, the manufacturer may make claim for a rehearing within that time.

Appendix B

Impact Test Results for Lontitudinal Head-Plate Specimens Taken from Callao Plate K-1

Appendix B, Table 1A

CHARPY V-NOTCH TEST RESULTS FOR LONGITUDINAL HEAD-PLATE SPECIMENS TAKEN FROM CALLAO PLATE K-1.
CALCULATIONS FOR SHEAR FRACTURE APPEARANCE DATA OF LS* ORIENTATION, HLI* CHARPY SPECIMENS.
*SEE IDENTIFICATION CODES IN FIGURES 4 AND 15.

SPECIMEN	TEMPERATURE(F)	OBSERVED SHEAR FRACTURE (%)	CALCULATED SHEAR FRACTURE (%)
HLI-37*	-100.0	.0	.0
HLI-22	-50.0	.0	1.8
HLI-21	-50.0	.0	1.8
HLI-28	15.0	5.0	4.2
HLI-27	15.0	5.0	4.2
HLI-24	80.0	25.0	25.0
HLI-23	80.0	25.0	25.0
HLI-38	100.0	100.0	100.0
HLI-39	100.0	100.0	100.0
HLI-26	120.0	90.0	100.0
HLI-40	120.0	100.0	100.0
HLI-35	140.0	100.0	100.0
HLI-36	140.0	100.0	100.0
HLI-29	160.0	100.0	100.0
HLI-30	160.0	100.0	100.0
HLI-33	212.0	100.0	100.0
HLI-34	212.0	100.0	100.0

% SHEAR FRACTURE	CALCULATED TEMPERATURE(F)	/	TEMPERATURE (F)	CALCULATED SHEAR FRACTURE(%)
2.0	-45.3	/	-40.0	2.2
5.0	36.7	/	-30.0	2.6
10.0	77.3	/	-20.0	2.9
15.0	78.4	/	-10.0	3.3
50.0	83.0	/	.0	3.7
85.0	87.9	/	10.0	4.0
90.0	89.1	/	20.0	4.4
95.0	91.0	/	30.0	4.8
98.0	93.0	/	40.0	5.1
		/	50.0	5.5
		/	60.0	5.9
		/	70.0	6.2
		/	80.0	25.0
		/	90.0	92.7

Appendix B, Table 1B

CHARPY V-NOTCH TEST RESULTS FOR LONGITUDINAL HEAD-PLATE SPECIMENS TAKEN FROM CALLAO PLATE K-1.
CALCULATIONS FOR ENERGY ABSORPTION DATA OF LS. ORIENTATION, HLI. CHARPY SPECIMENS.
*SEE IDENTIFICATION CODES IN FIGURES 4 AND 15.

SPECIMEN	TEMPERATURE(F)	OBSERVED ENERGY ABSORPTION(FT-LB)	CALCULATED ENERGY ABSORPTION(FT-LB)
HLI-37*	-100.0	4.5	6.2
HLI-22	-50.0	7.0	8.0
HLI-21	-50.0	5.0	8.0
HLI-28	15.0	27.0	17.8
HLI-27	15.0	23.0	17.8
HLI-24	80.0	52.0	49.8
HLI-23	80.0	36.0	49.8
HLI-38	100.0	64.0	63.5
HLI-39	100.0	68.0	63.5
HLI-26	120.0	60.0	75.4
HLI-40	120.0	76.0	75.4
HLI-35	140.0	90.5	82.9
HLI-36	140.0	80.5	82.9
HLI-29	160.0	85.0	85.9
HLI-30	160.0	84.0	85.9
HLI-33	212.0	72.0	73.3
HLI-34	212.0	74.5	73.3

ENERGY ABSORPTION	CALCULATED TEMPERATURE(F)	/	TEMPERATURE (F)	CALCULATED ENERGY ABSORPTION(FT-LB)
10.0	-26.8	/	-20.0	10.8
15.0	4.0	/	-10.0	12.3
20.0	22.4	/	.0	14.1
25.0	36.0	/	10.0	16.4
30.0	47.0	/	20.0	19.2
35.0	56.5	/	30.0	22.6
40.0	65.0	/	40.0	26.7
45.0	72.9	/	50.0	31.5
50.0	80.3	/	60.0	37.0
55.0	87.6	/	70.0	43.1
60.0	94.8	/	80.0	49.8
65.0	102.2	/	90.0	56.7
70.0	110.1	/	100.0	63.5
75.0	119.1	/	110.0	69.9
80.0	130.5	/	120.0	75.4
85.0	151.0	/	130.0	79.8
		/	140.0	82.9
		/	150.0	84.9
		/	160.0	85.9

Appendix B, Table 1C

CHARPY V-NOTCH TEST RESULTS FOR LONGITUDINAL HEAD-PLATE SPECIMENS TAKEN FROM CALLAO PLATE K-1.
CALCULATIONS FOR LATERAL EXPANSION DATA OF LS* ORIENTATION, HLI* CHARPY SPECIMENS.
*SEE IDENTIFICATION CODES IN FIGURES 4 AND 15.

SPECIMEN	TEMPERATURE(F)	OBSERVED LATERAL EXPANSION (MILS)	CALCULATED LATERAL EXPANSION (MILS)
HLI-37*	-100.0	2.0	1.7
HLI-22	-50.0	3.5	4.7
HLI-21	-50.0	4.0	4.7
HLI-28	15.0	21.0	16.3
HLI-27	15.0	17.0	16.3
HLI-24	80.0	41.0	39.9
HLI-23	80.0	31.0	39.9
HLI-38	100.0	50.0	47.5
HLI-39	100.0	52.0	47.5
HLI-26	120.0	46.0	53.6
HLI-40	120.0	52.0	53.6
HLI-35	140.0	60.0	57.7
HLI-36	140.0	61.0	57.7
HLI-29	160.0	55.0	59.9
HLI-30	160.0	56.0	59.9
HLI-33	212.0	61.0	61.0
HLI-34	212.0	61.0	61.0

LATERAL EXPANSION(MILS)	CALCULATED TEMPERATURE(F)	/	TEMPERATURE (F)	CALCULATED LATERAL EXPANSION(MILS)
5.0	-47.0	/	-40.0	5.8
10.0	-12.2	/	-30.0	7.1
15.0	10.1	/	-20.0	8.6
20.0	27.3	/	-10.0	10.4
25.0	42.0	/	.0	12.5
30.0	55.2	/	10.0	15.0
35.0	67.8	/	20.0	17.8
40.0	80.3	/	30.0	20.9
45.0	93.2	/	40.0	24.3
50.0	107.6	/	50.0	28.0
55.0	125.8	/	60.0	31.9
60.0	161.8	/	70.0	35.9
		/	80.0	39.9
		/	90.0	43.8
		/	100.0	[illegible]
		/	110.0	[illegible]
		/	120.0	53.6
		/	130.0	55.9
		/	140.0	57.7
		/	150.0	59.0

Appendix B, Table 2A

CHARPY V-NOTCH TEST RESULTS FOR LONGITUDINAL HEAD-PLATE SPECIMENS TAKEN FROM CALLAO PLATE K-1.
CALCULATIONS FOR SHEAR FRACTURE APPEARANCE DATA OF LT. ORIENTATION, HLH. CHARPY SPECIMENS.
*SEE IDENTIFICATION CODES IN FIGURES 4 AND 15.

SPECIMEN	TEMPERATURE(F)	OBSERVED SHEAR FRACTURE (%)	CALCULATED SHEAR FRACTURE (%)
HLH-15*	-100.0	.0	.0
HLH-2	-50.0	.0	.9
HLH-1	-50.0	.0	.9
HLH-8	15.0	5.0	2.1
HLH-7	15.0	.0	2.1
HLH-10	60.0	15.0	2.9
HLH-9	60.0	15.0	2.9
HLH-4	80.0	20.0	17.3
HLH-3	80.0	15.0	17.3
HLH-16	100.0	100.0	99.9
HLH-17	100.0	100.0	99.9
HLH-18	100.0	100.0	99.9
HLH-6	120.0	80.0	100.0
HLH-19	120.0	100.0	100.0
HLH-12	160.0	100.0	100.0
HLH-11	160.0	100.0	100.0
HLH-14	212.0	100.0	100.0
HLH-13	212.0	100.0	100.0

% SHEAR FRACTURE	CALCULATED TEMPERATURE(F)	/	TEMPERATURE (F)	CALCULATED SHEAR FRACTURE(%)
2.0	9.4	/	10.0	2.0
5.0	73.9	/	20.0	2.2
10.0	77.5	/	30.0	2.4
15.0	79.3	/	40.0	2.6
50.0	85.8	/	50.0	2.7
85.0	91.1	/	60.0	2.9
90.0	92.2	/	70.0	3.3
95.0	93.8	/	80.0	17.3
98.0	95.5	/	90.0	78.9

Appendix B, Table 2B

CHARPY V-NOTCH TEST RESULTS FOR LONGITUDINAL HEAD-PLATE SPECIMENS TAKEN FROM CALLAO PLATE K-1.
CALCULATIONS FOR ENERGY ABSORPTION DATA OF LT. ORIENTATION, HLH. CHARPY SPECIMENS.
.SEE IDENTIFICATION CODES IN FIGURES 4 AND 15.

SPECIMEN	TEMPERATURE(F)	OBSERVED ENERGY ABSORPTION(FT-LB)	CALCULATED ENERGY ABSORPTION(FT-LB)
HLH-15.	-100.0	2.5	2.5
HLH-2	-50.0	2.5	2.5
HLH-1	-50.0	3.5	2.5
HLH-8	15.0	6.0	2.5
HLH-7	15.0	11.0	2.5
HLH-10	60.0	19.5	18.9
HLH-9	60.0	21.5	18.9
HLH-4	80.0	26.0	38.5
HLH-3	80.0	28.5	38.5
HLH-16	100.0	55.0	50.7
HLH-17	100.0	53.0	50.7
HLH-18	100.0	54.0	50.7
HLH-6	120.0	42.0	53.7
HLH-19	120.0	52.0	53.7
HLH-12	160.0	51.0	54.0
HLH-11	160.0	52.0	54.0
HLH-14	212.0	52.0	54.0
HLH-13	212.0	53.0	54.0

ENERGY ABSORPTION	CALCULATED TEMPERATURE(F)	/	TEMPERATURE (F)	CALCULATED ENERGY ABSORPTION(FT-LB)
5.0	38.3	/	40.0	5.6
10.0	48.7	/	50.0	10.8
15.0	55.6	/	60.0	18.9
20.0	61.2	/	70.0	28.8
25.0	66.2	/	80.0	38.5
30.0	71.2	/	90.0	46.0
35.0	76.2	/	100.0	50.7
40.0	81.8	/	110.0	52.9
45.0	88.4	/		
50.0	98.0	/		

Appendix B, Table 2C

CHARPY V-NOTCH TEST RESULTS FOR LONGITUDINAL HEAD-PLATE SPECIMENS TAKEN FROM CALLAO PLATE K-1.
CALCULATIONS FOR LATERAL EXPANSION DATA OF LT. ORIENTATION, HLH. CHARPY SPECIMENS.
*SEE IDENTIFICATION CODES IN FIGURES 4 AND 15.

SPECIMEN	TEMPERATURE(F)	OBSERVED LATERAL EXPANSION (MILS)	CALCULATED LATERAL EXPANSION (MILS)
HLH-15*	-100.0	4.0	4.0
HLH-2	-50.0	1.0	4.1
HLH-1	-50.0	2.0	4.1
HLH-8	15.0	7.5	8.6
HLH-7	15.0	10.5	8.6
HLH-10	60.0	23.0	22.6
HLH-9	60.0	22.0	22.6
HLH-4	80.0	25.0	32.1
HLH-3	80.0	24.0	32.1
HLH-16	100.0	46.0	41.1
HLH-17	100.0	45.0	41.1
HLH-18	100.0	46.0	41.1
HLH-6	120.0	36.0	47.2
HLH-19	120.0	54.0	47.2
HLH-12	160.0	47.5	50.6
HLH-11	160.0	46.0	50.6
HLH-14	212.0	50.0	50.7
HLH-13	212.0	48.0	50.7

LATERAL EXPANSION(MILS)	CALCULATED TEMPERATURE(F)
5.0	-18.8
10.0	22.4
15.0	40.7
20.0	54.0
25.0	65.3
30.0	75.7
35.0	86.0
40.0	97.2
45.0	111.2
50.0	141.2

TEMPERATURE (F)	CALCULATED LATERAL EXPANSION(MILS)
-10.0	5.5
.0	6.5
10.0	7.7
20.0	9.5
30.0	11.8
40.0	14.8
50.0	18.4
60.0	22.6
70.0	27.3
80.0	32.1
90.0	36.8
100.0	41.1
110.0	44.6
120.0	47.2
130.0	48.9
140.0	49.9

Appendix B, Table 3A

DYNAMIC-TEAR TEST RESULTS FOR LONGITUDINAL HEAD-PLATE SPECIMENS TAKEN FROM CALLAO PLATE K-1.
CALCULATIONS FOR SHEAR FRACTURE APPEARANCE DATA OF LT, HDTL*, DYNAMIC-TEAR SPECIMENS.
*SEE IDENTIFICATION CODES IN FIGURES 4 AND 15.

SPECIMEN	TEMPERATURE(F)	OBSERVED SHEAR FRACTURE (%)	CALCULATED SHEAR FRACTURE (%)
HDTL-69*	-50.0	.0	.0
HDTL-58	.0	4.0	1.9
HDTL-56	.0	2.0	1.9
HDTL-55	30.0	2.0	23.9
HDTL-71	30.0	45.0	23.9
HDTL-60	60.0	60.0	69.6
HDTL-72	60.0	80.0	69.6
HDTL-57	80.0	75.0	91.3
HDTL-70	80.0	100.0	91.3
HDTL-59	120.0	100.0	99.9
HDTL-61	120.0	100.0	99.9
HDTL-64	160.0	100.0	100.0
HDTL-65	200.0	100.0	100.0
HDTL-62	300.0 **	100.0	100.0

% SHEAR FRACTURE	CALCULATED TEMPERATURE(F)	/	TEMPERATURE (F)	CALCULATED SHEAR FRACTURE(%)
2.0	.5	/	10.0	5.7
5.0	8.6	/	20.0	12.9
10.0	16.5	/	30.0	23.9
15.0	22.2	/	40.0	38.2
50.0	47.4	/	50.0	54.2
85.0	72.5	/	60.0	69.6
90.0	78.2	/	70.0	82.4
95.0	86.6	/	80.0	91.3
98.0	95.7	/	90.0	96.4

** Specimens tested at temperatures between 300 and 1300 F had 100 percent shear fracture appearances.

Appendix B, Table 3B

DYNAMIC-TEAR TEST RESULTS FOR LONGITUDINAL HEAD-PLATE SPECIMENS TAKEN FROM CALLAO PLATE K-1.
CALCULATIONS FOR ENERGY ABSORPTION DATA OF LT, HDTL*, DYNAMIC-TEAR ENERGY/10.
*SEE IDENTIFICATION CODES IN FIGURES 4 AND 15.

SPECIMEN	TEMPERATURE(F)	OBSERVED ENERGY ABSORPTION(FT-LB)	CALCULATED ENERGY ABSORPTION(FT-LB)
HDTL-69*	-50.0	5.1	3.8
HDTL-58	.0	9.1	6.0
HDTL-56	.0	5.7	6.0
HDTL-55	30.0	5.8	20.9
HDTL-71	30.0	33.4	20.9
HDTL-60	60.0	42.0	44.8
HDTL-72	60.0	53.0	44.8
HDTL-57	80.0	41.5	57.0
HDTL-70	80.0	65.2	57.0
HDTL-59	120.0	66.2	65.2
HDTL-61	120.0	64.6	65.2
HDTL-64	160.0	60.2	61.7
HDTL-65	200.0	60.9	59.9
HDTL-62	300.0	58.9	58.9

ENERGY ABSORPTION	CALCULATED TEMPERATURE(F)	/	TEMPERATURE (F)	CALCULATED ENERGY ABSORPTION(FT-LB)
5.0	-5.0	/	.0	6.0
10.0	11.8	/	10.0	9.2
15.0	21.3	/	20.0	14.2
20.0	28.8	/	30.0	20.9
25.0	35.4	/	40.0	28.7
30.0	41.6	/	50.0	36.9
35.0	47.6	/	60.0	44.8
40.0	53.8	/	70.0	51.7
45.0	60.2	/	80.0	57.0
50.0	67.4	/	90.0	60.8
55.0	75.9	/	100.0	63.2
60.0	87.6	/	110.0	64.5
65.0	116.1	/		

Appendix C

Impact Test Results for Transverse and Short-Transverse Head-Plate Specimens Taken from Callao Plate K-1

Appendix C, Table 1A

CHARPY V-NOTCH TEST RESULTS FOR TRANSVERSE HEAD-PLATE SPECIMENS TAKEN FROM CALLAO PLATE K-1.
CALCULATIONS FOR SHEAR FRACTURE APPEARANCE DATA OF TS. ORIENTATION, HTG. CHARPY SPECIMENS.
.SEE IDENTIFICATION CODES IN FIGURES 4 AND 15.

SPECIMEN	TEMPERATURE(F)	OBSERVED SHEAR FRACTURE (%)	CALCULATED SHEAR FRACTURE (%)
HTG-41.	-50.0	.0	.4
HTG-44	-50.0	.0	.4
HTG-49	15.0	5.0	4.0
HTG-50	15.0	5.0	4.0
HTG-51	60.0	15.0	17.4
HTG-52	60.0	15.0	17.4
HTG-45	80.0	20.0	31.3
HTG-46	80.0	25.0	31.3
HTG-57	100.0	55.0	51.9
HTG-58	100.0	40.0	51.9
HTG-47	120.0	98.0	75.8
HTG-48	120.0	60.0	75.8
HTG-53	160.0	100.0	99.5
HTG-54	160.0	100.0	99.5
HTG-55	212.0	100.0	100.0
HTG-56	212.0	100.0	100.0

% SHEAR FRACTURE	CALCULATED TEMPERATURE(F)	/	TEMPERATURE (F)	CALCULATED SHEAR FRACTURE(%)
2.0	-5.1	/	.0	2.4
5.0	21.6	/	10.0	3.4
10.0	42.5	/	20.0	4.7
15.0	55.2	/	30.0	6.6
50.0	98.3	/	40.0	9.2
85.0	128.8	/	50.0	12.7
90.0	134.8	/	60.0	17.4
95.0	142.8	/	70.0	23.5
98.0	151.1	/	80.0	31.3
		/	90.0	40.8

Appendix C, Table 1B

CHARPY V-NOTCH TEST RESULTS FOR TRANSVERSE HEAD-PLATE SPECIMENS TAKEN FROM CALLAO PLATE K-1.
CALCULATIONS FOR ENERGY ABSORPTION DATA OF TS. ORIENTATION, HTG. CHARPY SPECIMENS.
*SEE IDENTIFICATION CODES IN FIGURES 4 AND 15.

SPECIMEN	TEMPERATURE(F)	OBSERVED ENERGY ABSORPTION(FT-LB)	CALCULATED ENERGY ABSORPTION(FT-LB)
HTG-41*	-50.0	4.0	4.1
HTG-44	-50.0	4.0	4.1
HTG-49	15.0	5.0	5.2
HTG-50	15.0	5.0	5.2
HTG-51	60.0	15.0	10.5
HTG-52	60.0	11.0	10.5
HTG-45	80.0	16.5	16.7
HTG-46	80.0	18.5	16.7
HTG-57	100.0	24.0	26.4
HTG-58	100.0	21.0	26.4
HTG-47	120.0	43.5	37.2
HTG-48	120.0	32.0	37.2
HTG-53	160.0	45.5	45.2
HTG-54	160.0	45.0	45.2
HTG-55	212.0	37.0	37.2
HTG-56	212.0	37.5	37.2

ENERGY ABSORPTION	CALCULATED TEMPERATURE(F)	/	TEMPERATURE (F)	CALCULATED ENERGY ABSORPTION(FT-LB)
5.0	10.0	/	10.0	5.0
10.0	57.6	/	20.0	5.5
15.0	75.4	/	30.0	6.2
20.0	87.6	/	40.0	7.2
25.0	97.5	/	50.0	8.6
30.0	106.5	/	60.0	10.5
35.0	115.6	/	70.0	13.2
40.0	126.3	/	80.0	16.7
45.0	151.2	/	90.0	21.1
		/	100.0	26.4
		/	110.0	32.0
		/	120.0	37.2
		/	130.0	41.4
		/	140.0	43.9

Appendix C, Table 1C

CHARPY V-NOTCH TEST RESULTS FOR TRANSVERSE HEAD-PLATE SPECIMENS TAKEN FROM CALLAO PLATE K-1.
CALCULATIONS FOR LATERAL EXPANSION DATA OF TS• ORIENTATION, HTG• CHARPY SPECIMENS.
•SEE IDENTIFICATION CODES IN FIGURES 4 AND 15.

SPECIMEN	TEMPERATURE(F)	OBSERVED LATERAL EXPANSION (MILS)	CALCULATED LATERAL EXPANSION (MILS)
HTG-41•	-50.0	2.0	3.3
HTG-44	-50.0	2.5	3.3
HTG-49	15.0	6.0	6.2
HTG-50	15.0	6.0	6.2
HTG-51	60.0	16.0	13.9
HTG-52	60.0	14.5	13.9
HTG-45	80.0	21.0	20.1
HTG-46	80.0	20.0	20.1
HTG-57	100.0	25.0	27.8
HTG-58	100.0	25.0	27.8
HTG-47	120.0	41.0	35.5
HTG-48	120.0	31.0	35.5
HTG-53	160.0	46.0	43.8
HTG-54	160.0	43.0	43.8
HTG-55	212.0	40.0	44.5
HTG-56	212.0	43.0	44.5

LATERAL EXPANSION(MILS)	CALCULATED TEMPERATURE(F)	/	TEMPERATURE (F)	CALCULATED LATERAL EXPANSION(MILS)
5.0	-.2	/	.0	5.0
10.0	42.4	/	10.0	5.8
15.0	63.9	/	20.0	6.7
20.0	79.7	/	30.0	8.0
25.0	93.0	/	40.0	9.6
30.0	105.6	/	50.0	11.5
35.0	118.6	/	60.0	13.9
40.0	134.7	/	70.0	16.8
		/	80.0	20.1
		/	90.0	23.8
		/	100.0	27.8
		/	110.0	31.8
		/	120.0	35.5
		/	130.0	38.7
		/	140.0	41.2
		/	150.0	42.9
		/	160.0	43.8

Appendix C, Table 2A

CHARPY V-NOTCH TEST RESULTS FOR TRANSVERSE HEAD-PLATE SPECIMENS TAKEN FROM CALLAO PLATE K-1.
CALCULATIONS FOR SHEAR FRACTURE APPEARANCE DATA OF TL. ORIENTATION, HTF. CHARPY SPECIMENS.
*SEE IDENTIFICATION CODES IN FIGURES 4 AND 15.

SPECIMEN	TEMPERATURE(F)	OBSERVED SHEAR FRACTURE (%)	CALCULATED SHEAR FRACTURE (%)
HTF-61*	-50.0	.0	.0
HTF-62	-50.0	.0	.0
HTF-67	15.0	5.0	.0
HTF-68	15.0	5.0	.0
HTF-69	60.0	10.0	8.4
HTF-70	60.0	10.0	8.4
HTF-63	80.0	25.0	26.2
HTF-64	80.0	20.0	26.2
HTF-75	100.0	50.0	52.7
HTF-76	100.0	40.0	52.7
HTF-65	120.0	90.0	78.2
HTF-66	120.0	80.0	78.2
HTF-71	160.0	98.0	98.9
HTF-72	160.0	98.0	98.9
HTF-73	212.0	100.0	100.0
HTF-74	212.0	100.0	100.0

% SHEAR FRACTURE	CALCULATED TEMPERATURE(F)	/	TEMPERATURE (F)	CALCULATED SHEAR FRACTURE(%)
2.0	44.1	/	50.0	3.7
5.0	53.3	/	60.0	8.4
10.0	62.5	/	70.0	15.9
15.0	69.0	/	80.0	26.2
50.0	98.1	/	90.0	38.8
85.0	127.1	/		
90.0	133.7	/		
95.0	143.4	/		
98.0	154.0	/		

Appendix C, Table B

CHARPY V-NOTCH TEST RESULTS FOR TRANSVERSE HEAD-PLATE SPECIMENS TAKEN FROM CALLAO PLATE K-1.
CALCULATIONS FOR ENERGY ABSORPTION DATA OF TL. ORIENTATION, HTF. CHARPY SPECIMENS. .
*SEE IDENTIFICATION CODES IN FIGURES 4 AND 15.

SPECIMEN	TEMPERATURE(F)	OBSERVED ENERGY ABSORPTION(FT-LB)	CALCULATED ENERGY ABSORPTION(FT-LB)
HTF-61*	-50.0	3.5	4.5
HTF-62	-50.0	4.5	4.5
HTF-67	15.0	7.0	6.9
HTF-68	15.0	7.5	6.9
HTF-69	60.0	12.0	12.5
HTF-70	60.0	10.5	12.5
HTF-63	80.0	19.0	16.9
HTF-64	80.0	16.0	16.9
HTF-75	100.0	24.0	22.6
HTF-76	100.0	19.0	22.6
HTF-65	120.0	32.0	28.8
HTF-66	120.0	27.0	28.8
HTF-71	160.0	35.0	36.6
HTF-72	160.0	37.5	36.6
HTF-73	212.0	37.0	37.5
HTF-74	212.0	37.5	37.5

ENERGY ABSORPTION	CALCULATED TEMPERATURE(F)	/	TEMPERATURE (F)	CALCULATED ENERGY ABSORPTION(FT-LB)
5.0	-26.1	/	-20.0	5.2
10.0	44.8	/	-10.0	5.5
15.0	72.0	/	.0	6.0
20.0	91.2	/	10.0	6.6
25.0	107.7	/	20.0	7.3
30.0	124.3	/	30.0	8.2
35.0	146.4	/	40.0	9.4
		/	50.0	10.8
		/	60.0	12.5
		/	70.0	14.6
		/	80.0	16.9
		/	90.0	19.7
		/	100.0	22.6
		/	110.0	25.7
		/	120.0	28.8
		/	130.0	31.5
		/	140.0	33.8
		/	150.0	35.5
		/	160.0	36.6

Appendix C, Table 2C

CHARPY V-NOTCH TEST RESULTS FOR TRANSVERSE HEAD-PLATE SPECIMENS TAKEN FROM CALLAO PLATE K-1.
CALCULATIONS FOR LATERAL EXPANSION DATA OF TL. ORIENTATION, HTF. CHARPY SPECIMENS.
*SEE IDENTIFICATION CODES IN FIGURES 4 AND 15.

SPECIMEN	TEMPERATURE(F)	OBSERVED LATERAL EXPANSION (MILS)	CALCULATED LATERAL EXPANSION (MILS)
HTF-61*	-50.0	1.0	2.5
HTF-62	-50.0	1.0	2.5
HTF-67	15.0	7.0	7.0
HTF-68	15.0	8.0	7.0
HTF-69	60.0	14.0	14.2
HTF-70	60.0	11.0	14.2
HTF-63	80.0	22.0	18.6
HTF-64	80.0	19.0	18.6
HTF-75	100.0	27.0	23.5
HTF-76	100.0	21.0	23.5
HTF-65	120.0	23.0	28.3
HTF-66	120.0	28.0	28.3
HTF-71	160.0	35.0	35.6
HTF-72	160.0	37.0	35.6
HTF-73	212.0	39.0	38.4
HTF-74	212.0	38.0	38.4

LATERAL EXPANSION(MILS)	CALCULATED TEMPERATURE(F)
5.0	-5.0
10.0	37.0
15.0	63.9
20.0	85.9
25.0	106.2
30.0	127.5
35.0	155.4

TEMPERATURE (F)	CALCULATED LATERAL EXPANSION(MILS)
.0	5.4
10.0	6.4
20.0	7.6
30.0	8.9
40.0	10.5
50.0	12.2
60.0	14.2
70.0	16.3
80.0	18.6
90.0	21.0
100.0	23.5
110.0	25.9
120.0	28.3
130.0	30.5
140.0	32.5
150.0	34.2
160.0	35.6
170.0	36.6
180.0	37.4
190.0	37.9

Appendix C, Table 3A

CHARPY V-NOTCH TEST RESULTS FOR SHORT-TRANSVERSE HEAD-PLATE SPECIMENS TAKEN FROM CALLAO PLATE K-1.
CALCULATIONS FOR SHEAR FRACTURE APPEARANCE DATA OF SL. ORIENTATION, SE. CHARPY SPECIMENS.
*SEE IDENTIFICATION CODES IN FIGURES 4 AND 15.

SPECIMEN	TEMPERATURE(F)	OBSERVED SHEAR FRACTURE (%)	CALCULATED SHEAR FRACTURE (%)
SE-1*	-50.0	.0	.0
SE-3	-50.0	.0	.0
SE-29	-30.0	.0	.0
SE-31	-30.0	.0	.0
SE-21	15.0	.0	.0
SE-23	15.0	.0	.0
SE-5	80.0	50.0	50.0
SE-7	80.0	50.0	50.0
SE-9	120.0	100.0	100.0
SE-11	120.0	100.0	100.0
SE-17	160.0	100.0	100.0
SE-19	160.0	100.0	100.0
SE-33	210.0	100.0	100.0
SE-35	210.0	100.0	100.0
SE-13	212.0	100.0	100.0
SE-15	212.0	100.0	100.0
SE-25	260.0	100.0	100.0
SE-27	260.0	100.0	100.0

% SHEAR FRACTURE	CALCULATED TEMPERATURE(F)	/	TEMPERATURE (F)	CALCULATED SHEAR FRACTURE(%)
2.0	75.3	/	80.0	50.0
5.0	75.7	/	90.0	95.0
10.0	76.2	/		
15.0	76.7	/		
50.0	80.0	/		
85.0	85.7	/		
90.0	87.3	/		
95.0	90.0	/		
98.0	93.4	/		

Appendix C, Table 3B

CHARPY V-NOTCH TEST RESULTS FOR SHORT-TRANSVERSE HEAD-PLATE SPECIMENS TAKEN FROM CALLAO PLATE K-1.
CALCULATIONS FOR ENERGY ABSORPTION DATA OF SL. ORIENTATION, SE. CHARPY SPECIMENS.
.SEE IDENTIFICATION CODES IN FIGURES 4 AND 15.

SPECIMEN	TEMPERATURE(F)	OBSERVED ENERGY ABSORPTION(FT-LB)	CALCULATED ENERGY ABSORPTION(FT-LB)
SE-1.	-50.0	3.0	2.9
SE-3	-50.0	2.5	2.9
SE-29	-30.0	3.0	3.0
SE-31	-30.0	2.5	3.0
SE-21	15.0	3.5	3.9
SE-23	15.0	3.5	3.9
SE-5	80.0	8.0	7.8
SE-7	80.0	8.5	7.8
SE-9	120.0	9.0	11.4
SE-11	120.0	12.0	11.4
SE-17	160.0	14.5	13.5
SE-19	160.0	14.0	13.5
SE-33	210.0	14.5	13.9
SE-35	210.0	13.0	13.9
SE-13	212.0	13.0	13.9
SE-15	212.0	14.5	13.9
SE-25	260.0	11.5	11.8
SE-27	260.0	12.0	11.8

ENERGY ABSORPTION	CALCULATED TEMPERATURE(F)
5.0	41.5
10.0	104.4

TEMPERATURE (F)	CALCULATED ENERGY ABSORPTION(FT-LB)
50.0	5.5
60.0	6.2
70.0	6.9
80.0	7.8
90.0	8.7
100.0	9.6
110.0	10.5
120.0	11.4
130.0	12.1
140.0	12.7
150.0	13.2

Appendix C, Table 3C

CHARPY V-NOTCH TEST RESULTS FOR SHORT-TRANSVERSE HEAD-PLATE SPECIMENS TAKEN FROM CALLAO PLATE K-1.
CALCULATIONS FOR LATERAL EXPANSION DATA OF SL• ORIENTATION, SE• CHARPY SPECIMENS.
•SEE IDENTIFICATION CODES IN FIGURES 4 AND 15.

SPECIMEN	TEMPERATURE(F)	OBSERVED LATERAL EXPANSION (MILS)	CALCULATED LATERAL EXPANSION (MILS)
SE-1•	-50.0	.5	1.0
SE-3	-50.0	1.0	1.0
SE-29	-30.0	.5	1.3
SE-31	-30.0	2.5	1.3
SE-21	15.0	1.5	3.0
SE-23	15.0	1.5	3.0
SE-5	80.0	9.0	8.3
SE-7	80.0	10.0	8.3
SE-9	120.0	9.0	12.1
SE-11	120.0	12.0	12.1
SE-17	160.0	16.0	14.5
SE-19	160.0	14.0	14.5
SE-33	210.0	15.0	15.5
SE-35	210.0	14.0	15.5
SE-13	212.0	14.0	15.6
SE-15	212.0	16.0	15.6
SE-25	260.0	13.0	13.5
SE-27	260.0	14.0	13.5

LATERAL EXPANSION(MILS)	CALCULATED TEMPERATURE(F)	/	TEMPERATURE (F)	CALCULATED LATERAL EXPANSION(MILS)
5.0	43.9	/	50.0	5.5
10.0	97.0	/	60.0	6.4
15.0	175.0	/	70.0	7.4
		/	80.0	8.3
		/	90.0	9.3
		/	100.0	10.3
		/	110.0	11.2
		/	120.0	12.1
		/	130.0	12.8
		/	140.0	13.5
		/	150.0	14.0
		/	160.0	14.5
		/	170.0	14.9
		/	180.0	15.1

Appendix C, Table 4A

CHARPY V-NOTCH TEST RESULTS FOR SHORT-TRANSVERSE HEAD-PLATE SPECIMENS TAKEN FROM CALLAO PLATE K-1.
CALCULATIONS FOR SHEAR FRACTURE APPEARANCE DATA OF ST. ORIENTATION, SE. CHARPY SPECIMENS.
*SEE IDENTIFICATION CODES IN FIGURES 4 AND 15.

SPECIMEN	TEMPERATURE(F)	OBSERVED SHEAR FRACTURE (%)	CALCULATED SHEAR FRACTURE (%)
SE-2*	-50.0	.0	.0
SE-4	-50.0	.0	.0
SE-32	-30.0	.0	.0
SE-34	-30.0	.0	.0
SE-40	-30.0	.0	.0
SE-24	15.0	.0	.0
SE-22	15.0	.0	.0
SE-6	80.0	30.0	30.0
SE-12	120.0	100.0	100.0
SE-20	160.0	100.0	100.0
SE-18	160.0	100.0	100.0
SE-38	210.0	100.0	100.0
SE-36	210.0	100.0	100.0
SE-16	212.0	100.0	100.0
SE-14	212.0	100.0	100.0
SE-30	260.0	100.0	100.0
SE-28	260.0	100.0	100.0

% SHEAR FRACTURE	CALCULATED TEMPERATURE(F)	/	TEMPERATURE (F)	CALCULATED SHEAR FRACTURE(%)
2.0	57.6	/	60.0	2.9
5.0	63.8	/	70.0	10.9
10.0	69.3	/	80.0	30.0
15.0	72.9	/	90.0	61.0
50.0	86.7	/		
85.0	98.2	/		
90.0	100.6	/		
95.0	104.0	/		
98.0	107.5	/		

Appendix C, Table 4B

CHARPY V-NOTCH TEST RESULTS FOR SHORT-TRANSVERSE HEAD-PLATE SPECIMENS TAKEN FROM CALLAO PLATE K-1.
CALCULATIONS FOR ENERGY ABSORPTION DATA OF ST. ORIENTATION, SE. CHARPY SPECIMENS.
*SEE IDENTIFICATION CODES IN FIGURES 4 AND 15.

SPECIMEN	TEMPERATURE(F)	OBSERVED ENERGY ABSORPTION(FT-LB)	CALCULATED ENERGY ABSORPTION(FT-LB)
SE-2*	-50.0	2.0	2.3
SE-4	-50.0	3.0	2.3
SE-32	-30.0	2.0	2.5
SE-34	-30.0	3.0	2.5
SE-40	-30.0	3.0	2.5
SE-24	15.0	4.0	3.4
SE-22	15.0	4.5	3.4
SE-6	80.0	5.0	6.4
SE-12	120.0	10.5	9.7
SE-20	160.0	15.0	13.3
SE-18	160.0	12.5	13.3
SE-38	210.0	12.5	15.6
SE-36	210.0	14.0	15.6
SE-16	212.0	15.0	15.6
SE-14	212.0	14.0	15.6
SE-30	260.0	14.5	15.8
SE-28	260.0	15.5	15.8

ENERGY ABSORPTION	CALCULATED TEMPERATURE(F)
5.0	57.5
10.0	123.5
15.0	188.1

TEMPERATURE (F)	CALCULATED ENERGY ABSORPTION(FT-LB)
60.0	5.1
70.0	5.7
80.0	6.4
90.0	7.1
100.0	7.9
110.0	8.8
120.0	9.7
130.0	10.6
140.0	11.5
150.0	12.4
160.0	13.3
170.0	14.0
180.0	14.6
190.0	15.1

Appendix C, Table 4C

CHARPY V-NOTCH TEST RESULTS FOR SHORT-TRANSVERSE HEAD-PLATE SPECIMENS TAKEN FROM CALLAO PLATE K-1.
CALCULATIONS FOR LATERAL EXPANSION DATA OF ST. ORIENTATION, SE. CHARPY SPECIMENS.
*SEE IDENTIFICATION CODES IN FIGURES 4 AND 15.

SPECIMEN	TEMPERATURE(F)	OBSERVED LATERAL EXPANSION (MILS)	CALCULATED LATERAL EXPANSION (MILS)
SE-2*	-50.0	1.0	1.4
SE-4	-50.0	.5	1.4
SE-32	-30.0	3.0	1.8
SE-34	-30.0	2.0	1.8
SE-40	-30.0	2.0	1.8
SE-24	15.0	3.0	3.0
SE-22	15.0	3.0	3.0
SE-6	80.0	4.6	6.9
SE-12	120.0	12.0	10.7
SE-20	160.0	16.0	14.3
SE-18	160.0	12.0	14.3
SE-38	210.0	12.0	16.4
SE-36	210.0	14.0	16.4
SE-16	212.0	16.0	16.5
SE-14	212.0	15.0	16.5
SE-30	260.0	16.0	16.7
SE-28	260.0	18.0	16.7

LATERAL EXPANSION(MILS)	CALCULATED TEMPERATURE(F)	/	TEMPERATURE (F)	CALCULATED LATERAL EXPANSION(MILS)
5.0	54.3	/	60.0	5.4
10.0	113.3	/	70.0	6.1
15.0	170.3	/	80.0	6.9
		/	90.0	7.8
		/	100.0	8.7
		/	110.0	9.7
		/	120.0	10.7
		/	130.0	11.7
		/	140.0	12.6
		/	150.0	13.5
		/	160.0	14.3
		/	170.0	15.0
		/	180.0	15.5
		/	190.0	16.0

Appendix C, Table 5A

DYNAMIC-TEAR TEST RESULTS FOR TRANSVERSE HEAD-PLATE SPECIMENS TAKEN FROM CALLAO PLATE K-1.
CALCULATIONS FOR SHEAR FRACTURE APPEARANCE DATA OF TL, HDTT*, DYNAMIC-TEAR SPECIMENS.
*SEE IDENTIFICATION CODES IN FIGURES 4 AND 15.

SPECIMEN	TEMPERATURE(F)	OBSERVED SHEAR FRACTURE (%)	CALCULATED SHEAR FRACTURE (%)
HDTT-45*	-50.0	.0	.0
HDTT-53	.0	.0	.4
HDTT-52	30.0	2.0	1.3
HDTT-39	30.0	.0	1.3
HDTT-49	60.0	2.0	4.3
HDTT-38	80.0	8.0	9.0
HDTT-54	80.0	10.0	9.0
HDTT-47	100.0	20.0	18.3
HDTT-42	120.0	25.0	34.6
HDTT-37	140.0	45.0	58.5
HDTT-44	160.0	100.0	83.5
HDTT-40	200.0	100.0	99.9
HDTT-46	300.0 **	100.0	100.0

% SHEAR FRACTURE	CALCULATED TEMPERATURE(F)	/	TEMPERATURE (F)	CALCULATED SHEAR FRACTURE(%)
2.0	40.2	/	50.0	2.9
5.0	64.0	/	60.0	4.3
10.0	82.8	/	70.0	6.3
15.0	94.2	/	80.0	9.0
50.0	133.4	/	90.0	12.9
85.0	161.4	/		
90.0	166.9	/		
95.0	174.3	/		
98.0	182.0	/		

** Specimens tested at temperatures between 300 and 1300 F had 100 percent shear fracture appearances.

Appendix C, Table 5B

DYNAMIC-TEAR TEST RESULTS FOR TRANSVERSE HEAD-PLATE SPECIMENS TAKEN FROM CALLAO PLATE K-1.
CALCULATIONS FOR ENERGY ABSORPTION DATA OF TL, HDTT., DYNAMIC-TEAR ENERGY/10.
.SEE IDENTIFICATION CODES IN FIGURES 4 AND 15.

SPECIMEN	TEMPERATURE(F)	OBSERVED ENERGY ABSORPTION(FT-LB)	CALCULATED ENERGY ABSORPTION(FT-LB)
HDTT-45.	-50.0	5.3	5.3
HDTT-53	.0	4.4	5.5
HDTT-52	30.0	6.1	6.0
HDTT-39	30.0	5.6	6.0
HDTT-49	60.0	3.3	7.4
HDTT-38	80.0	10.6	9.6
HDTT-54	80.0	10.8	9.6
HDTT-47	100.0	15.8	13.8
HDTT-42	120.0	21.4	20.6
HDTT-37	140.0	25.1	29.7
HDTT-44	160.0	42.1	37.6
HDTT-40	200.0	40.0	41.4
HDTT-46	300.0	40.7	41.4

ENERGY ABSORPTION	CALCULATED TEMPERATURE(F)	/	TEMPERATURE (F)	CALCULATED ENERGY ABSORPTION(FT-LB)
10.0	82.5	/	90.0	11.4
15.0	104.3	/	100.0	13.8
20.0	118.5	/	110.0	16.8
25.0	130.0	/	120.0	20.6
30.0	140.7	/	130.0	25.0
35.0	152.2	/	140.0	29.7
40.0	170.5	/	150.0	34.1
		/	160.0	37.6
		/	170.0	39.9

Appendix D

Impact Test Results for Longitudinal Shell-Plate Specimens Taken from Callao Plate K-5

Appendix D, Table 1A

CHARPY V-NOTCH TEST RESULTS FOR LONGITUDINAL SHELL-PLATE SPECIMENS TAKEN FROM CALLAO PLATE K-5.
CALCULATIONS FOR SHEAR FRACTURE APPEARANCE DATA OF LS• ORIENTATION, STB• CHARPY SPECIMENS.
•SEE IDENTIFICATION CODES IN FIGURES 7 AND 15.

SPECIMEN	TEMPERATURE(F)	OBSERVED SHEAR FRACTURE (%)	CALCULATED SHEAR FRACTURE (%)
STB-7•	-100.0	.0	4.2
STB-2	-50.0	.0	20.8
STB-1	-50.0	.0	20.8
STB-10	-30.0	.0	35.3
STB-11	-30.0	.0	35.3
STB-8	-10.0	5.0	54.8
STB-9	-10.0	100.0	54.8
STB-16	.0	15.0	65.4
STB-17	.0	50.0	65.4
STB-6	15.0	15.0	80.3
STB-5	15.0	100.0	80.3
STB-20	20.0	100.0	84.6
STB-19	40.0	100.0	96.0
STB-18	40.0	100.0	96.0
STB-15	60.0	100.0	99.6
STB-14	60.0	100.0	99.6
STB-3	80.0	100.0	100.0
STB-4	80.0	100.0	100.0
STB-13	120.0	100.0	100.0
STB-12	120.0	100.0	100.0

% SHEAR FRACTURE	CALCULATED TEMPERATURE(F)	/	TEMPERATURE (F)	CALCULATED SHEAR FRACTURE(%)
5.0	-95.1	/	-90.0	5.9
10.0	-74.2	/	-80.0	8.3
15.0	-61.2	/	-70.0	11.4
50.0	-14.6	/	-60.0	15.5
85.0	20.6	/	-50.0	20.8
90.0	27.6	/	-40.0	27.4
95.0	37.4	/	-30.0	35.3
98.0	47.4	/	-20.0	44.6
		/	-10.0	54.8
		/	.0	65.4
		/	10.0	75.6
		/	20.0	84.6
		/	30.0	91.4
		/	40.0	96.0

Appendix D, Table 1B

CHARPY V-NOTCH TEST RESULTS FOR LONGITUDINAL SHELL-PLATE SPECIMENS TAKEN FROM CALLAO PLATE K-5.
CALCULATIONS FOR ENERGY ABSORPTION DATA OF LS- ORIENTATION, STB- CHARPY SPECIMENS.
*SEE IDENTIFICATION CODES IN FIGURES 7 AND 15.

SPECIMEN	TEMPERATURE(F)	OBSERVED ENERGY ABSORPTION(FT-LB)	CALCULATED ENERGY ABSORPTION(FT-LB)
STB-7*	-100.0	4.0	7.6
STB-2	-50.0	21.5	17.4
STB-1	-50.0	10.5	17.4
STB-10	-30.0	27.0	28.8
STB-11	-30.0	24.0	28.8
STB-8	-10.0	12.5	48.4
STB-9	-10.0	>120.0**	48.4
STB-16	.0	11.5	61.4
STB-17	.0	41.0	61.4
STB-6	15.0	18.0	83.0
STB-5	15.0	>120.0 **	83.0
STB-20	20.0	>120.0 **	90.0
STB-19	40.0	>120.0 **	111.8
STB-18	40.0	>120.0 **	111.8
STB-15	60.0	>120.0 **	119.3
STB-14	60.0	>120.0 **	119.3
STB-3	80.0	>120.0 **	120.0
STB-4	80.0	>120.0 **	120.0
STB-13	120.0	>120.0 **	120.0
STB-12	120.0	>120.0 **	120.0

ENERGY ABSORPTION	CALCULATED TEMPERATURE(F)	/	TEMPERATURE (F)	CALCULATED ENERGY ABSORPTION(FT-LB)
10.0	-77.4	/	-70.0	11.3
15.0	-56.3	/	-60.0	13.8
20.0	-44.2	/	-50.0	17.4
25.0	-35.5	/	-40.0	22.2
30.0	-28.5	/	-30.0	28.8
35.0	-22.6	/	-20.0	37.5
40.0	-17.5	/	-10.0	48.4
45.0	-12.9	/	.0	61.4
50.0	-8.7	/	10.0	75.7
55.0	-4.7	/	20.0	90.0
60.0	-1.0	/	30.0	102.6
65.0	2.6	/	40.0	111.8
70.0	6.1	/	50.0	117.1
75.0	9.5	/	60.0	119.3
80.0	13.0	/		
85.0	16.4	/		
90.0	20.0	/		
95.0	23.7	/		
100.0	27.7	/		
105.0	32.3	/		
110.0	37.7	/		
115.0	45.2	/		

** Specimen did not fracture completely, therefore true energy absorption exceeds the indicated machine capacity value of 120 ft-lb.

Appendix D, Table 1C

CHARPY V-NOTCH TEST RESULTS FOR LONGITUDINAL SHELL-PLATE SPECIMENS TAKEN FROM CALLAO PLATE K-5.
CALCULATIONS FOR LATERAL EXPANSION DATA OF LS* ORIENTATION, STB* CHARPY SPECIMENS.
*SEE IDENTIFICATION CODES IN FIGURES 7 AND 15.

SPECIMEN	TEMPERATURE(F)	OBSERVED LATERAL EXPANSION (MILS)	CALCULATED LATERAL EXPANSION (MILS)
STB-7*	-100.0	2.0	3.2
STB-2	-50.0	16.0	9.7
STB-1	-50.0	7.5	9.7
STB-10	-30.0	21.0	17.4
STB-11	-30.0	19.5	17.4
STB-8	-10.0	11.0	31.2
STB-9	-10.0	82.0**	31.2
STB-16	.0	9.0	40.9
STB-17	.0	34.8	40.9
STB-6	15.0	15.0	57.8
STB-5	15.0	83.0**	57.8
STB-20	20.0	88.5**	63.6
STB-19	40.0	82.5**	82.4
STB-18	40.0	87.2**	82.4
STB-15	60.0	89.0**	89.0
STB-14	60.0	90.0**	89.0
STB-3	80.0	88.5**	89.6
STB-4	80.0	89.2**	89.6
STB-13	120.0	89.5**	89.6
STB-12	120.0	83.0**	89.6

LATERAL EXPANSION(MILS)	CALCULATED TEMPERATURE(F)
5.0	-75.6
10.0	-48.9
15.0	-35.0
20.0	-25.4
25.0	-17.8
30.0	-11.4
35.0	-5.9
40.0	-.8
45.0	3.8
50.0	8.3
55.0	12.6
60.0	16.9
65.0	21.2
70.0	25.8
75.0	30.7
80.0	36.6
85.0	44.6

TEMPERATURE (F)	CALCULATED LATERAL EXPANSION(MILS)
-70.0	5.7
-60.0	7.3
-50.0	9.7
-40.0	12.9
-30.0	17.4
-20.0	23.4
-10.0	31.2
.0	40.9
10.0	52.0
20.0	63.6
30.0	74.3
40.0	82.4
50.0	87.1
60.0	89.0

** Specimen did not fracture completely, therefore true lateral expansion exceeds this measured value.

Appendix D, Table 2A

CHARPY V-NOTCH TEST RESULTS FOR LONGITUDINAL SHELL-PLATE SPECIMENS TAKEN FROM CALLAO PLATE K-5.
CALCULATIONS FOR SHEAR FRACTURE APPEARANCE DATA OF LT. ORIENTATION, STA. CHARPY SPECIMENS.
*SEE IDENTIFICATION CODES IN FIGURES 7 AND 15.

SPECIMEN	TEMPERATURE(F)	OBSERVED SHEAR FRACTURE (%)	CALCULATED SHEAR FRACTURE (%)
STA-34*	-100.0	.0	.0
STA-22	-50.0	.0	.4
STA-21	-50.0	.0	.4
STA-35	-10.0	5.0	3.0
STA-36	-10.0	5.0	3.0
STA-28	15.0	5.0	9.7
STA-37	15.0	5.0	9.7
STA-38	40.0	30.0	26.3
STA-39	40.0	30.0	26.3
STA-29	60.0	35.0	50.1
STA-30	60.0	40.0	50.1
STA-24	80.0	80.0	77.8
STA-23	80.0	95.0	77.8
STA-26	120.0	95.0	99.8
STA-25	120.0	100.0	99.8
STA-32	160.0	100.0	100.0
STA-33	160.0	100.0	100.0

% SHEAR FRACTURE	CALCULATED TEMPERATURE(F)	/	TEMPERATURE (F)	CALCULATED SHEAR FRACTURE(%)
2.0	-18.3	/	-10.0	3.0
5.0	.4	/	.0	4.9
10.0	15.8	/	10.0	7.8
15.0	25.4	/	20.0	12.0
50.0	60.0	/	30.0	18.0
85.0	86.2	/	40.0	26.3
90.0	91.5	/	50.0	37.1
95.0	98.7	/	60.0	50.1
98.0	106.3	/	70.0	64.2
		/	80.0	77.8
		/	90.0	88.7

Appendix D, Table 2B

CHARPY V-NOTCH TEST RESULTS FOR LONGITUDINAL SHELL-PLATE SPECIMENS TAKEN FROM CALLAO PLATE K-5.
CALCULATIONS FOR ENERGY ABSORPTION DATA OF LT* ORIENTATION, STA* CHARPY SPECIMENS.
*SEE IDENTIFICATION CODES IN FIGURES 7 AND 15.

SPECIMEN	TEMPERATURE(F)	OBSERVED ENERGY ABSORPTION(FT-LB)	CALCULATED ENERGY ABSORPTION(FT-LB)
STA-34*	-100.0	6.0	6.4
STA-22	-50.0	4.0	8.3
STA-21	-50.0	4.0	8.3
STA-35	-10.0	27.0	13.7
STA-36	-10.0	11.0	13.7
STA-28	15.0	14.0	21.5
STA-37	15.0	24.0	21.5
STA-38	40.0	30.5	34.4
STA-39	40.0	30.5	34.4
STA-29	60.0	37.0	48.1
STA-30	60.0	45.5	48.1
STA-24	80.0	63.5	61.6
STA-23	80.0	72.5	61.6
STA-26	120.0	72.5	74.0
STA-25	120.0	75.5	74.0
STA-32	160.0	74.0	74.5
STA-33	160.0	74.0	74.5

ENERGY ABSORPTION	CALCULATED TEMPERATURE(F)	/	TEMPERATURE (F)	CALCULATED ENERGY ABSORPTION(FT-LB)
10.0	-32.0	/	-30.0	10.3
15.0	-4.8	/	-20.0	11.8
20.0	11.2	/	-10.0	13.7
25.0	22.9	/	.0	16.3
30.0	32.5	/	10.0	19.6
35.0	40.9	/	20.0	23.6
40.0	48.5	/	30.0	28.6
45.0	55.7	/	40.0	34.4
50.0	62.7	/	50.0	41.0
55.0	69.9	/	60.0	48.1
60.0	77.5	/	70.0	55.1
65.0	86.2	/	80.0	61.6
70.0	97.9	/	90.0	66.9
		/	100.0	70.7
		/	110.0	72.9
		/	120.0	74.0

Appendix D, Table 2C

CHARPY V-NOTCH TEST RESULTS FOR LONGITUDINAL SHELL-PLATE SPECIMENS TAKEN FROM CALLAO PLATE K-5.
CALCULATIONS FOR LATERAL EXPANSION DATA OF LT. ORIENTATION, STA. CHARPY SPECIMENS.
*SEE IDENTIFICATION CODES IN FIGURES 7 AND 15.

SPECIMEN	TEMPERATURE(F)	OBSERVED LATERAL EXPANSION (MILS)	CALCULATED LATERAL EXPANSION (MILS)
STA-34*	-100.0	3.5	4.7
STA-22	-50.0	2.0	7.7
STA-21	-50.0	2.0	7.7
STA-35	-10.0	14.0	13.7
STA-36	-10.0	22.0	13.7
STA-28	15.0	12.0	20.4
STA-37	15.0	20.0	20.4
STA-38	40.0	30.0	29.8
STA-39	40.0	33.0	29.8
STA-29	60.0	30.0	38.7
STA-30	60.0	37.0	38.7
STA-24	80.0	51.0	47.7
STA-23	80.0	56.0	47.7
STA-26	120.0	54.0	59.3
STA-25	120.0	54.0	59.3
STA-32	160.0	64.0	61.3
STA-33	160.0	64.0	61.3

LATERAL EXPANSION(MILS)	CALCULATED TEMPERATURE(F)	/	TEMPERATURE (F)	CALCULATED LATERAL EXPANSION(MILS)
5.0	-91.7	/	-90.0	5.1
10.0	-30.7	/	-80.0	5.5
15.0	-4.4	/	-70.0	6.1
20.0	13.7	/	-60.0	6.8
25.0	28.1	/	-50.0	7.7
30.0	40.5	/	-40.0	8.8
35.0	51.8	/	-30.0	10.1
40.0	62.7	/	-20.0	11.7
45.0	73.8	/	-10.0	13.7
50.0	85.7	/	.0	16.1
55.0	100.2	/	10.0	18.9
60.0	126.2	/	20.0	22.1
		/	30.0	25.7
		/	40.0	29.8
		/	50.0	34.2
		/	60.0	38.7
		/	70.0	43.3
		/	80.0	47.7
		/	90.0	51.6
		/	100.0	54.9

Appendix D, Table 3A

DYNAMIC -TEAR TEST RESULTS FOR LONGITUDINAL SHELL-PLATE SPECIMENS TAKEN FROM CALLAO PLATE K-5.
CALCULATIONS FOR SHEAR FRACTURE APPEARANCE DATA OF LT, SDTL*, DYNAMIC-TEAR SPECIMENS.
*SEE IDENTIFICATION CODES IN FIGURES 7 AND 15.

SPECIMEN	TEMPERATURE(F)	OBSERVED SHEAR FRACTURE (%)	CALCULATED SHEAR FRACTURE (%)
SDTL-23*	-50.0	.0	.1
SDTL-32	.0	.0	1.0
SDTL-20	30.0	5.0	3.9
SDTL-35	30.0	5.0	3.9
SDTL-27	60.0	10.0	13.8
SDTL-21	80.0	20.0	29.5
SDTL-36	80.0	25.0	29.5
SDTL-29	120.0	75.0	84.3
SDTL-22	120.0	98.0	84.3
SDTL-30	160.0	100.0	100.0
SDTL-34	160.0	100.0	100.0
SDTL-24	200.0	100.0	100.0
SDTL-33	300.0**	100.0	100.0

% SHEAR FRACTURE	CALCULATED TEMPERATURE(F)	/	TEMPERATURE (F)	CALCULATED SHEAR FRACTURE(%)
2.0	15.0	/	20.0	2.5
5.0	35.7	/	30.0	3.9
10.0	52.1	/	40.0	6.0
15.0	62.1	/	50.0	9.2
50.0	96.2	/	60.0	13.8
85.0	120.6	/	70.0	20.4
90.0	125.4	/	80.0	29.5
95.0	131.9	/	90.0	41.4
98.0	138.5	/		

** Specimens tested at temperatures between 300 and 1300 F had 100 percent shear fracture appearances.

Appendix D, Table 3B

DYNAMIC -TEAR TEST RESULTS FOR LONGITUDINAL SHELL-PLATE SPECIMENS TAKEN FROM CALLAO PLATE K-5.
CALCULATIONS FOR ENERGY ABSORPTION DATA OF LT, SDTL*, DYNAMIC-TEAR ENERGY/10.
*SEE IDENTIFICATION CODES IN FIGURES 7 AND 15.

SPECIMEN	TEMPERATURE(F)	OBSERVED ENERGY ABSORPTION(FT-LB)	CALCULATED ENERGY ABSORPTION(FT-LB)
SDTL-23*	-50.0	5.6	5.7
SDTL-32	.0	4.6	6.3
SDTL-20	30.0	7.6	8.3
SDTL-35	30.0	9.5	8.3
SDTL-27	60.0	14.4	14.8
SDTL-21	80.0	20.8	25.0
SDTL-36	80.0	26.2	25.0
SDTL-29	120.0	53.5	61.6
SDTL-22	120.0	71.2	61.6
SDTL-30	160.0	74.7	74.6
SDTL-34	160.0	74.5	74.6
SDTL-24	200.0	70.6	74.0
SDTL-33	300.0	68.2	60.5

ENERGY ABSORPTION	CALCULATED TEMPERATURE(F)	/	TEMPERATURE (F)	CALCULATED ENERGY ABSORPTION(FT-LB)
10.0	41.8	/	50.0	11.8
15.0	60.5	/	60.0	14.8
20.0	71.7	/	70.0	19.1
25.0	80.0	/	80.0	25.0
30.0	86.8	/	90.0	32.7
35.0	92.7	/	100.0	41.9
40.0	98.0	/	110.0	52.1
45.0	103.1	/	120.0	61.6
50.0	108.0	/	130.0	68.8
55.0	112.9	/	140.0	72.8
60.0	118.2	/		
65.0	124.2	/		
70.0	132.3	/		

Appendix E

Impact Test Results for Transverse Shell-Plate Specimens Taken from Callao Plate K-5

Appendix E, Table 1A

CHARPY V-NOTCH TEST RESULTS FOR TRANSVERSE SHELL-PLATE SPECIMENS TAKEN FROM CALLAO PLATE K-5.
CALCULATIONS FOR SHEAR FRACTURE APPEARANCE DATA OF TS* ORIENTATION, SLD* CHARPY SPECIMENS.
*SEE IDENTIFICATION CODES IN FIGURES 7 AND 15.

SPECIMEN	TEMPERATURE(F)	OBSERVED SHEAR FRACTURE (%)	CALCULATED SHEAR FRACTURE (%)
SLD-73*	-100.0	.0	.0
SLD-62	-50.0	.0	.0
SLD-61	-50.0	.0	.0
SLD-74	-10.0	5.0	.0
SLD-75	-10.0	5.0	.0
SLD-68	15.0	10.0	.0
SLD-67	15.0	10.0	.0
SLD-76	40.0	30.0	29.6
SLD-77	40.0	25.0	29.6
SLD-70	60.0	80.0	84.4
SLD-69	60.0	85.0	84.4
SLD-64	80.0	100.0	99.5
SLD-63	80.0	100.0	99.5
SLD-66	120.0	100.0	100.0
SLD-65	120.0	100.0	100.0
SLD-72	160.0	100.0	100.0
SLD-71	160.0	100.0	100.0

% SHEAR FRACTURE	CALCULATED TEMPERATURE(F)	/	TEMPERATURE (F)	CALCULATED SHEAR FRACTURE(%)
2.0	24.1	/	30.0	7.9
5.0	27.7	/	40.0	29.6
10.0	31.3	/	50.0	59.8
15.0	34.0	/	60.0	84.4
50.0	46.8	/	70.0	96.3
85.0	60.3	/		
90.0	63.5	/		
95.0	68.2	/		
98.0	73.5	/		

Appendix E, Table 1B

CHARPY V-NOTCH TEST RESULTS FOR TRANSVERSE SHELL-PLATE SPECIMENS TAKEN FROM CALLAO PLATE K-5.
CALCULATIONS FOR ENERGY ABSORPTION DATA OF TS* ORIENTATION, SLD* CHARPY SPECIMENS.
*SEE IDENTIFICATION CODES IN FIGURES 7 AND 15.

SPECIMEN	TEMPERATURE(F)	OBSERVED ENERGY ABSORPTION(FT-LB)	CALCULATED ENERGY ABSORPTION(FT-LB)
SLD-73*	-100.0	4.0	6.3
SLD-62	-50.0	10.5	7.7
SLD-61	-50.0	6.5	7.7
SLD-74	-10.0	14.0	12.9
SLD-75	-10.0	15.5	12.9
SLD-68	15.0	18.0	20.9
SLD-67	15.0	19.5	20.9
SLD-76	40.0	30.0	34.1
SLD-77	40.0	27.0	34.1
SLD-70	60.0	42.0	45.7
SLD-69	60.0	55.5	45.7
SLD-64	80.0	48.0	52.9
SLD-63	80.0	54.0	52.9
SLD-66	120.0	55.0	54.8
SLD-65	120.0	50.0	54.8
SLD-72	160.0	44.0	45.3
SLD-71	160.0	46.5	45.3

ENERGY ABSORPTION	CALCULATED TEMPERATURE(F)	/	TEMPERATURE (F)	CALCULATED ENERGY ABSORPTION(FT-LB)
10.0	-26.2	/	-20.0	10.9
15.0	-1.8	/	-10.0	12.9
20.0	12.8	/	.0	15.5
25.0	23.7	/	10.0	18.9
30.0	33.0	/	20.0	23.2
35.0	41.4	/	30.0	28.3
40.0	49.7	/	40.0	34.1
45.0	58.6	/	50.0	40.2
50.0	69.7	/	60.0	45.7
		/	70.0	50.1
		/	80.0	52.9
		/	90.0	54.3

Appendix E, Table 1C

CHARPY V-NOTCH TEST RESULTS FOR TRANSVERSE SHELL-PLATE SPECIMENS TAKEN FROM CALLAO PLATE K-5.
CALCULATIONS FOR LATERAL EXPANSION DATA OF TS* ORIENTATION, SLD* CHARPY SPECIMENS.
*SEE IDENTIFICATION CODES IN FIGURES 7 AND 15.

SPECIMEN	TEMPERATURE(F)	OBSERVED LATERAL EXPANSION (MILS)	CALCULATED LATERAL EXPANSION (MILS)
SLD-73*	-100.0	1.5	3.0
SLD-62	-50.0	8.0	5.3
SLD-61	-50.0	4.0	5.3
SLD-74	-10.0	12.0	11.4
SLD-75	-10.0	14.0	11.4
SLD-68	15.0	15.0	19.2
SLD-67	15.0	16.0	19.2
SLD-76	40.0	29.0	30.2
SLD-77	40.0	28.0	30.2
SLD-70	60.0	37.0	39.7
SLD-69	60.0	47.0	39.7
SLD-64	80.0	44.0	46.3
SLD-63	80.0	47.0	46.3
SLD-66	120.0	50.0	49.3
SLD-65	120.0	51.0	49.3
SLD-72	160.0	43.0	42.5
SLD-71	160.0	42.0	42.5

LATERAL EXPANSION(MILS)	CALCULATED TEMPERATURE(F)	/	TEMPERATURE (F)	CALCULATED LATERAL EXPANSION(MILS)
5.0	-53.9	/	-50.0	5.3
10.0	-16.5	/	-40.0	6.3
15.0	3.0	/	-30.0	7.6
20.0	17.2	/	-20.0	9.3
25.0	28.9	/	-10.0	11.4
30.0	39.5	/	.0	14.1
35.0	49.8	/	10.0	17.3
40.0	60.8	/	20.0	21.1
45.0	74.8	/	30.0	25.5
		/	40.0	30.2
		/	50.0	35.1
		/	60.0	39.7
		/	70.0	43.5
		/	80.0	46.3
		/	90.0	48.1

Appendix E, Table 2A

CHARPY V-NOTCH TEST RESULTS FOR TRANSVERSE SHELL-PLATE SPECIMENS TAKEN FROM CALLAO PLATE K-5.
CALCULATIONS FOR SHEAR FRACTURE APPEARANCE DATA OF TL• ORIENTATION, SLC• CHARPY SPECIMENS.
•SEE IDENTIFICATION CODES IN FIGURES 7 AND 15.

SPECIMEN	TEMPERATURE(F)	OBSERVED SHEAR FRACTURE (%)	CALCULATED SHEAR FRACTURE (%)
SLC-54•	-100.0	.0	.0
SLC-45	-50.0	.0	.7
SLC-44	-50.0	.0	.7
SLC-55	-10.0	5.0	4.9
SLC-56	-10.0	5.0	4.9
SLC-51	15.0	20.0	14.3
SLC-50	15.0	20.0	14.3
SLC-57	40.0	20.0	35.0
SLC-58	40.0	20.0	35.0
SLC-42	60.0	70.0	60.4
SLC-41	60.0	60.0	60.4
SLC-47	80.0	85.0	85.1
SLC-46	80.0	90.0	85.1
SLC-49	120.0	98.0	99.9
SLC-48	120.0	100.0	99.9
SLC-53	160.0	100.0	100.0
SLC-52	160.0	100.0	100.0

% SHEAR FRACTURE	CALCULATED TEMPERATURE(F)	/	TEMPERATURE (F)	CALCULATED SHEAR FRACTURE(%)
2.0	-29.1	/	-20.0	3.1
5.0	-9.8	/	-10.0	4.9
10.0	6.2	/	.0	7.7
15.0	16.2	/	10.0	11.7
50.0	52.3	/	20.0	17.4
85.0	79.9	/	30.0	25.1
90.0	85.4	/	40.0	35.0
95.0	93.1	/	50.0	47.0
98.0	101.1	/	60.0	60.4
		/	70.0	73.7
		/	80.0	85.1
		/	90.0	93.2

Appendix E. Table 2B

CHARPY V-NOTCH TEST RESULTS FOR TRANSVERSE SHELL-PLATE SPECIMENS TAKEN FROM CALLAO PLATE K-5.
CALCULATIONS FOR ENERGY ABSORPTION DATA OF TL* ORIENTATION, SLC* CHARPY SPECIMENS.
*SEE IDENTIFICATION CODES IN FIGURES 7 AND 15.

SPECIMEN	TEMPERATURE(F)	OBSERVED ENERGY ABSORPTION(FT-LB)	CALCULATED ENERGY ABSORPTION(FT-LB)
SLC-54*	-100.0	2.0	3.3
SLC-45	-50.0	2.5	5.8
SLC-44	-50.0	6.0	5.8
SLC-55	-10.0	11.0	12.0
SLC-56	-10.0	13.0	12.0
SLC-51	15.0	18.0	18.0
SLC-50	15.0	18.0	18.0
SLC-57	40.0	22.0	24.7
SLC-58	40.0	25.0	24.7
SLC-42	60.0	33.5	29.6
SLC-41	60.0	27.0	29.6
SLC-47	80.0	31.0	33.4
SLC-46	80.0	32.0	33.4
SLC-49	120.0	36.5	37.1
SLC-48	120.0	38.0	37.1
SLC-53	160.0	37.5	37.8
SLC-52	160.0	38.0	37.8

ENERGY ABSORPTION	CALCULATED TEMPERATURE(F)	/	TEMPERATURE (F)	CALCULATED ENERGY ABSORPTION(FT-LB)
5.0	-59.3	/	-50.0	5.8
10.0	-20.1	/	-40.0	6.9
15.0	3.3	/	-30.0	8.3
20.0	22.7	/	-20.0	10.0
25.0	41.3	/	-10.0	12.0
30.0	61.8	/	.0	14.2
35.0	91.5	/	10.0	16.7
		/	20.0	19.3
		/	30.0	22.0
		/	40.0	24.7
		/	50.0	27.2
		/	60.0	29.6
		/	70.0	31.7
		/	80.0	33.4
		/	90.0	34.8
		/	100.0	35.9
		/	110.0	36.6
		/	120.0	37.1

Appendix E, Table 2C

CHARPY V-NOTCH TEST RESULTS FOR TRANSVERSE SHELL-PLATE SPECIMENS TAKEN FROM CALLAO PLATE K-5.
CALCULATIONS FOR LATERAL EXPANSION DATA OF TL* ORIENTATION, SLC* CHARPY SPECIMENS.
*SEE IDENTIFICATION CODES IN FIGURES 7 AND 15.

SPECIMEN	TEMPERATURE(F)	OBSERVED LATERAL EXPANSION (MILS)	CALCULATED LATERAL EXPANSION (MILS)
SLC-54*	-100.0	1.5	1.5
SLC-45	-50.0	2.0	1.5
SLC-44	-50.0	4.5	1.5
SLC-55	-10.0	1.3	4.8
SLC-56	-10.0	1.2	4.8
SLC-51	15.0	16.0	15.1
SLC-50	15.0	15.0	15.1
SLC-57	40.0	24.0	23.7
SLC-58	40.0	20.0	23.7
SLC-42	60.0	34.0	28.8
SLC-41	60.0	26.0	28.8
SLC-47	80.0	32.0	32.5
SLC-46	80.0	32.0	32.5
SLC-49	120.0	37.0	36.8
SLC-48	120.0	37.0	36.8
SLC-53	160.0	39.0	38.6
SLC-52	160.0	38.0	38.6

LATERAL EXPANSION(MILS)	CALCULATED TEMPERATURE(F)	/	TEMPERATURE (F)	CALCULATED LATERAL EXPANSION(MILS)
5.0	-9.5	/	.0	8.9
10.0	2.6	/	10.0	13.1
15.0	14.8	/	20.0	17.0
20.0	28.4	/	30.0	20.5
25.0	44.6	/	40.0	23.7
30.0	65.9	/	50.0	26.4
35.0	99.7	/	60.0	28.8
		/	70.0	30.8
		/	80.0	32.5
		/	90.0	33.9
		/	100.0	35.0
		/	110.0	36.0
		/	120.0	36.8
		/	130.0	37.4
		/	140.0	37.9
		/	150.0	38.3
		/	160.0	38.6
		/	170.0	38.9
		/	180.0	39.1
		/	190.0	39.3

Appendix E, Table 3A

DYNAMIC-TEAR TEST RESULTS FOR TRANSVERSE SHELL-PLATE SPECIMENS TAKEN FROM CALLAO PLATE K-5.
CALCULATIONS FOR SHEAR FRACTURE APPEARANCE DATA OF TL, SDTT*, DYNAMIC-TEAR SPECIMENS.
*SEE IDENTIFICATION CODES IN FIGURES 7 AND 15.

SPECIMEN	TEMPERATURE(F)	OBSERVED SHEAR FRACTURE (%)	CALCULATED SHEAR FRACTURE (%)
SDTT-10*	-50.0	.0	.2
SDTT-1	.0	.0	1.8
SDTT-2	30.0	8.0	6.6
SDTT-17	30.0	8.0	6.6
SDTT-16	60.0	20.0	21.3
SDTT-7	60.0	15.0	21.3
SDTT-3	80.0	30.0	41.3
SDTT-18	80.0	50.0	41.3
SDTT-12	120.0	90.0	91.6
SDTT-5	120.0	95.0	91.6
SDTT-14	160.0	100.0	100.0
SDTT-4	200.0	100.0	100.0
SDTT-6	300.0**	100.0	100.0

% SHEAR FRACTURE	CALCULATED TEMPERATURE(F)	/	TEMPERATURE (F)	CALCULATED SHEAR FRACTURE(%)
2.0	1.8	/	10.0	2.9
5.0	23.2	/	20.0	4.4
10.0	40.1	/	30.0	6.6
15.0	50.6	/	40.0	9.9
50.0	86.7	/	50.0	14.7
85.0	112.9	/	60.0	21.3
90.0	118.0	/	70.0	30.1
95.0	125.0	/	80.0	41.3
98.0	132.3	/	90.0	54.6

** Specimens tested at temperatures between 300 and 1300 F had 100 percent shear fracture appearances.

Appendix E, Table 3B

DYNAMIC-TEAR TEST RESULTS FOR TRANSVERSE SHELL-PLATE SPECIMENS TAKEN FROM CALLAO PLATE K-5.
CALCULATIONS FOR ENERGY ABSORPTION DATA OF TL, SDTT*, DYNAMIC-TEAR ENERGY/10.
*SEE IDENTIFICATION CODES IN FIGURES 7 AND 15.

SPECIMEN	TEMPERATURE(F)	OBSERVED ENERGY ABSORPTION(FT-LB)	CALCULATED ENERGY ABSORPTION(FT-LB)
SDTT-10*	-50.0	5.2	5.2
SDTT-1	.0	5.7	5.8
SDTT-2	30.0	7.3	7.6
SDTT-17	30.0	8.9	7.6
SDTT-16	60.0	13.3	12.9
SDTT-7	60.0	10.8	12.9
SDTT-3	80.0	15.9	19.6
SDTT-18	80.0	23.8	19.6
SDTT-12	120.0	32.7	34.4
SDTT-5	120.0	35.9	34.4
SDTT-14	160.0	37.8	37.6
SDTT-4	200.0	37.5	37.7
SDTT-6	300.0	35.5	35.5

ENERGY ABSORPTION	CALCULATED TEMPERATURE(F)	/	TEMPERATURE (F)	CALCULATED ENERGY ABSORPTION(FT-LB)
10.0	47.1	/	50.0	10.6
15.0	67.1	/	60.0	12.9
20.0	81.1	/	70.0	15.9
25.0	93.3	/	80.0	19.6
30.0	105.9	/	90.0	23.6
35.0	122.9	/	100.0	27.7
		/	110.0	31.5
		/	120.0	34.4
		/	130.0	36.2

Appendix F

Charpy V-Notch Test Results for Heat-Affected Zone Specimens Taken from Weldments from the Callao Accident

Appendix F, Table 1A

CHARPY V-NOTCH TEST RESULTS FOR HEAT-AFFECTED ZONE SPECIMENS TAKEN FROM WELDMENTS FROM THE CALLAO ACCIDENT.

CALCULATIONS FOR SHEAR FRACTURE APPEARANCE DATA OF TL•HAZ••OF HEAD PLATE K-2, HJ•SPECIMENS.
•SEE IDENTIFICATION CODES IN FIGURES 5&15.
•• HEAT-AFFECTED ZONE.

SPECIMEN	TEMPERATURE(F)	OBSERVED SHEAR FRACTURE (%)	CALCULATED SHEAR FRACTURE (%)
HJ-13•	-100.0	.0	.8
HJ-2	-50.0	20.0	21.0
HJ-1	-50.0	25.0	21.0
HJ-12	-10.0	45.0	55.9
HJ-11	-10.0	40.0	55.9
HJ-16	-5.0	75.0	60.3
HJ-17	-5.0	70.0	60.3
HJ-8	15.0	80.0	76.2
HJ-7	15.0	80.0	76.2
HJ-14	50.0	85.0	93.3
HJ-15	50.0	90.0	93.3
HJ-4	80.0	99.0	98.6
HJ-3	80.0	95.0	98.6
HJ-6	120.0	100.0	99.9
HJ-5	120.0	100.0	99.9
HJ-19	120.0	100.0	99.9
HJ-9	160.0	100.0	100.0
HJ-10	160.0	100.0	100.0

% SHEAR FRACTURE	CALCULATED TEMPERATURE(F)	/	TEMPERATURE (F)	CALCULATED SHEAR FRACTURE(%)
2.0	-91.4	/	-90.0	2.3
5.0	-79.8	/	-80.0	4.9
10.0	-67.8	/	-70.0	8.9
15.0	-58.9	/	-60.0	14.3
50.0	-16.5	/	-50.0	21.0
85.0	29.3	/	-40.0	28.9
90.0	40.2	/	-30.0	37.6
95.0	56.3	/	-20.0	46.7
98.0	74.3	/	-10.0	55.9
		/	.0	64.6
		/	10.0	72.6
		/	20.0	79.6
		/	30.0	85.3
		/	40.0	89.9
		/	50.0	93.3
		/	60.0	95.8
		/	70.0	97.5

Appendix F, Table 1B

CHARPY V-NOTCH TEST RESULTS FOR HEAT-AFFECTED ZONE SPECIMENS TAKEN FROM WELDMENTS FROM THE CALLAO ACCIDENT.

CALCULATIONS FOR ENERGY ABSORPTION DATA OF
TL•HAZ••OF HEAD PLATE K-2, HJ•SPECIMENS.
•SEE IDENTIFICATION CODES
IN FIGURES 5&15.
•• HEAT-AFFECTED ZONE.

SPECIMEN	TEMPERATURE(F)	OBSERVED ENERGY ABSORPTION(FT-LB)	CALCULATED ENERGY ABSORPTION(FT-LB)
HJ-13•	-100.0	5.0	5.5
HJ-2	-50.0	14.0	14.8
HJ-1	-50.0	18.5	14.8
HJ-12	-10.0	27.0	26.7
HJ-11	-10.0	15.5	26.7
HJ-16	-5.0	28.5	28.2
HJ-17	-5.0	28.5	28.2
HJ-8	15.0	38.5	33.7
HJ-7	15.0	36.0	33.7
HJ-14	50.0	39.5	41.3
HJ-15	50.0	41.0	41.3
HJ-4	80.0	48.0	45.4
HJ-3	80.0	42.0	45.4
HJ-6	120.0	54.0	48.2
HJ-5	120.0	52.5	48.2
HJ-19	120.0	42.0	48.2
HJ-9	160.0	49.0	49.1
HJ-10	160.0	45.0	49.1

ENERGY ABSORPTION	CALCULATED TEMPERATURE(F)	/	TEMPERATURE (F)	CALCULATED ENERGY ABSORPTION(FT-LB)
10.0	-69.6	/	-60.0	12.2
15.0	-49.4	/	-50.0	14.8
20.0	-32.2	/	-40.0	17.7
25.0	-15.7	/	-30.0	20.7
30.0	1.2	/	-20.0	23.7
35.0	19.9	/	-10.0	26.7
40.0	42.7	/	.0	29.6
45.0	76.1	/	10.0	32.4
		/	20.0	35.0
		/	30.0	37.4
		/	40.0	39.5
		/	50.0	41.3
		/	60.0	42.9
		/	70.0	44.3
		/	80.0	45.4
		/	90.0	46.3
		/	100.0	47.1
		/	110.0	47.7
		/	120.0	48.2
		/	130.0	48.5

Appendix F, Table 1C

CHARPY V-NOTCH TEST RESULTS FOR HEAT-AFFECTED ZONE SPECIMENS TAKEN FROM WELDMENTS FROM THE CALLAO ACCIDENT.

CALCULATIONS FOR LATERAL EXPANSION DATA OF
TL*HAZ**OF HEAD PLATE K=2, HJ*SPECIMENS.
*SEE IDENTIFICATION CODES
IN FIGURES 5&15.
** HEAT-AFFECTED ZONE.

SPECIMEN	TEMPERATURE(F)	OBSERVED LATERAL EXPANSION (MILS)	CALCULATED LATERAL EXPANSION (MILS)
HJ-13*	-100.0	4.0	4.3
HJ-2	-50.0	15.0	15.6
HJ-1	-50.0	21.5	15.6
HJ-12	-10.0	30.0	27.9
HJ-11	-10.0	19.5	27.9
HJ-16	-5.0	29.0	29.5
HJ-17	-5.0	28.0	29.5
HJ-8	15.0	37.5	35.4
HJ-7	15.0	38.5	35.4
HJ-14	50.0	43.0	43.9
HJ-15	50.0	43.0	43.9
HJ-4	80.0	51.0	48.6
HJ-3	80.0	44.0	48.6
HJ-6	120.0	57.0	51.7
HJ-5	120.0	49.0	51.7
HJ-19	120.0	50.0	51.7
HJ-9	160.0	51.0	52.7
HJ-10	160.0	46.0	52.7

LATERAL EXPANSION(MILS)	CALCULATED TEMPERATURE(F)	/	TEMPERATURE (F)	CALCULATED LATERAL EXPANSION(MILS)
5.0	-95.8	/	-90.0	6.0
10.0	-71.1	/	-80.0	8.0
15.0	-52.0	/	-70.0	10.3
20.0	-35.2	/	-60.0	12.8
25.0	-19.2	/	-50.0	15.6
30.0	-3.3	/	-40.0	18.5
35.0	13.5	/	-30.0	21.6
40.0	32.5	/	-20.0	24.8
45.0	56.0	/	-10.0	27.9
50.0	93.9	/	.0	31.0
		/	10.0	34.0
		/	20.0	36.8
		/	30.0	39.4
		/	40.0	41.8
		/	50.0	43.9
		/	60.0	45.7
		/	70.0	47.3
		/	80.0	48.6
		/	90.0	49.6
		/	100.0	50.5

Appendix F, Table 2A

CHARPY V-NOTCH TEST RESULTS FOR HEAT-AFFECTED ZONE SPECIMENS TAKEN FROM WELDMENTS FROM THE CALLAO ACCIDENT.

CALCULATIONS FOR SHEAR FRACTURE APPEARANCE DATA OF TL*HAZ**OF SHELL PLATE K-8,HK*SPECIMENS.
*SEE IDENTIFICATION CODES IN FIGURES 10 AND 15.
** HEAT-AFFECTED ZONE.

SPECIMEN	TEMPERATURE(F)	OBSERVED SHEAR FRACTURE (%)	CALCULATED SHEAR FRACTURE (%)
HK-11*	-100.0	.0	.0
HK-2	-50.0	10.0	.0
HK-1	-50.0	5.0	.0
HK-16	-30.0	15.0	13.3
HK-17	-30.0	15.0	13.3
HK-12	-10.0	40.0	41.6
HK-13	-10.0	30.0	41.6
HK-8	15.0	80.0	71.4
HK-7	15.0	85.0	71.4
HK-14	50.0	85.0	92.4
HK-15	50.0	85.0	92.4
HK-4	80.0	90.0	98.1
HK-3	80.0	95.0	98.1
HK-6	120.0	100.0	99.8
HK-5	120.0	100.0	99.8
HK-10	160.0	100.0	100.0
HK-9	160.0	100.0	100.0

% SHEAR FRACTURE	CALCULATED TEMPERATURE(F)	/	TEMPERATURE (F)	CALCULATED SHEAR FRACTURE(%)
2.0	-40.7	/	-40.0	2.5
5.0	-37.2	/	-30.0	13.3
10.0	-32.6	/	-20.0	27.2
15.0	-28.7	/	-10.0	41.6
50.0	-3.8	/	.0	54.9
85.0	33.2	/	10.0	66.4
90.0	43.5	/	20.0	75.8
95.0	59.7	/	30.0	83.1
98.0	79.1	/	40.0	88.5
		/	50.0	92.4
		/	60.0	95.1
		/	70.0	96.9

Appendix F, Table 2B

CHARPY V-NOTCH TEST RESULTS FOR HEAT-AFFECTED ZONE SPECIMENS TAKEN FROM WELDMENTS FROM THE CALLAO ACCIDENT.

CALCULATIONS FOR ENERGY ABSORPTION DATA OF
TL•HAZ••OF SHELL PLATE K-8,HK•SPECIMENS.
•SEE IDENTIFICATION CODES
IN FIGURES 10 AND 15.
•• HEAT-AFFECTED ZONE.

SPECIMEN	TEMPERATURE(F)	OBSERVED ENERGY ABSORPTION(FT-LB)	CALCULATED ENERGY ABSORPTION(FT-LB)
HK-11•	-100.0	6.5	6.5
HK-2	-50.0	14.5	13.0
HK-1	-50.0	11.5	13.0
HK-16	-30.0	22.0	21.5
HK-17	-30.0	23.0	21.5
HK-12	-10.0	25.5	28.2
HK-13	-10.0	26.5	28.2
HK-8	15.0	37.5	34.3
HK-7	15.0	37.0	34.3
HK-14	50.0	38.0	39.6
HK-15	50.0	38.0	39.6
HK-4	80.0	39.0	42.2
HK-3	80.0	45.0	42.2
HK-6	120.0	44.0	44.0
HK-5	120.0	42.0	44.0
HK-10	160.0	47.5	44.8
HK-9	160.0	41.5	44.8

ENERGY ABSORPTION	CALCULATED TEMPERATURE(F)	/	TEMPERATURE (F)	CALCULATED ENERGY ABSORPTION(FT-LB)
10.0	-56.6	/	-50.0	13.0
15.0	-45.6	/	-40.0	17.4
20.0	-33.8	/	-30.0	21.5
25.0	-20.2	/	-20.0	25.1
30.0	-3.6	/	-10.0	28.2
35.0	18.5	/	.0	30.9
40.0	53.4	/	10.0	33.3
		/	20.0	35.3
		/	30.0	37.0
		/	40.0	38.4
		/	50.0	39.6
		/	60.0	40.6
		/	70.0	41.5
		/	80.0	42.2
		/	90.0	42.8
		/	100.0	43.3
		/	110.0	43.7
		/	120.0	44.0
		/	130.0	44.3
		/	140.0	44.5

Appendix F, Table 2C

CHARPY V-NOTCH TEST RESULTS FOR HEAT-AFFECTED ZONE SPECIMENS TAKEN FROM WELDMENTS FROM THE CALLAO ACCIDENT.

CALCULATIONS FOR LATERAL EXPANSION DATA OF
TL•HAZ••OF SHELL PLATE K-8,HK•SPECIMENS.
•SEE IDENTIFICATION CODES
IN FIGURES 10 AND 15.
•• HEAT-AFFECTED ZONE.

SPECIMEN	TEMPERATURE(F)	OBSERVED LATERAL EXPANSION (MILS)	CALCULATED LATERAL EXPANSION (MILS)
HK-11•	-100.0	6.0	6.0
HK-2	-50.0	14.0	13.2
HK-1	-50.0	12.0	13.2
HK-16	-30.0	22.5	20.9
HK-17	-30.0	24.0	20.9
HK-12	-10.0	26.0	28.0
HK-13	-10.0	26.0	28.0
HK-8	15.0	36.0	35.1
HK-7	15.0	37.0	35.1
HK-14	50.0	41.0	41.7
HK-15	50.0	37.5	41.7
HK-4	80.0	40.0	44.8
HK-3	80.0	46.0	44.8
HK-6	120.0	48.0	46.8
HK-5	120.0	44.0	46.8
HK-10	160.0	50.0	47.6
HK-9	160.0	45.0	47.6

LATERAL EXPANSION(MILS)	CALCULATED TEMPERATURE(F)	/	TEMPERATURE (F)	CALCULATED LATERAL EXPANSION(MILS)
10.0	-58.9	/	-50.0	13.2
15.0	-45.3	/	-40.0	17.0
20.0	-32.3	/	-30.0	20.9
25.0	-18.7	/	-20.0	24.6
30.0	-3.6	/	-10.0	28.0
35.0	14.5	/	.0	31.1
40.0	39.0	/	10.0	33.9
45.0	82.6	/	20.0	36.3
		/	30.0	38.4
		/	40.0	40.2
		/	50.0	41.7
		/	60.0	42.9
		/	70.0	44.0
		/	80.0	44.8
		/	90.0	45.5
		/	100.0	46.0
		/	110.0	46.5
		/	120.0	46.8
		/	130.0	47.1
		/	140.0	47.3

Appendix G

Charpy V-Notch Test Results for Weld-Metal Specimens

Appendix G, Table 1A

CHARPY V-NOTCH TEST RESULTS FOR WELD-METAL SPECIMENS TAKEN FROM THE CALLAO ACCIDENT.

CALCULATIONS FOR SHEAR FRACTURE APPEARANCE DATA OF LT•LONGITUDINAL WELD-METAL SPECIMENS, WL•
•SEE IDENTIFICATION CODES IN FIGURES 13 & 15.

SPECIMEN	TEMPERATURE(F)	OBSERVED SHEAR FRACTURE (%)	CALCULATED SHEAR FRACTURE (%)
WL-14•	-100.0	.0	.4
WL-2	-50.0	2.0	2.1
WL-1	-50.0	2.0	2.1
WL-8	15.0	20.0	15.8
WL-7	15.0	20.0	15.8
WL-18	40.0	20.0	31.1
WL-19	40.0	35.0	31.1
WL-9	60.0	40.0	49.7
WL-17	60.0	50.0	49.7
WL-16	100.0	90.0	89.7
WL-15	100.0	85.0	89.7
WL-6	120.0	98.0	98.3
WL-13	120.0	100.0	98.3
WL-12	160.0	100.0	100.0

% SHEAR FRACTURE	CALCULATED TEMPERATURE(F)	/	TEMPERATURE (F)	CALCULATED SHEAR FRACTURE(%)
2.0	-51.8	/	-50.0	2.1
5.0	-23.1	/	-40.0	2.9
10.0	-.5	/	-30.0	4.0
15.0	13.2	/	-20.0	5.5
50.0	60.3	/	-10.0	7.5
85.0	93.8	/	.0	10.2
90.0	100.4	/	10.0	13.7
95.0	109.3	/	20.0	18.2
98.0	118.4	/	30.0	24.0
		/	40.0	31.1
		/	50.0	39.8
		/	60.0	49.7
		/	70.0	60.6
		/	80.0	71.5
		/	90.0	81.6

Appendix G, Table 1B

CHARPY V-NOTCH TEST RESULTS FOR WELD-METAL SPECIMENS TAKEN FROM THE CALLAO ACCIDENT.

CALCULATIONS FOR ENERGY ABSORPTION DATA OF LT-LONGITUDINAL WELD-METAL SPECIMENS, WL-
-SEE IDENTIFICATION CODES IN FIGURES 13&15.

SPECIMEN	TEMPERATURE(F)	OBSERVED ENERGY ABSORPTION(FT-LB)	CALCULATED ENERGY ABSORPTION(FT-LB)
WL-14-	-100.0	6.5	6.5
WL-2	-50.0	8.0	8.9
WL-1	-50.0	10.0	8.9
WL-8	15.0	43.5	37.5
WL-7	15.0	52.0	37.5
WL-18	40.0	33.5	47.6
WL-19	40.0	49.0	47.6
WL-9	60.0	54.5	54.6
WL-17	60.0	45.0	54.6
WL-16	100.0	63.0	65.3
WL-15	100.0	61.0	65.3
WL-6	120.0	71.0	69.2
WL-13	120.0	77.0	69.2
WL-12	160.0	73.0	74.7

ENERGY ABSORPTION	CALCULATED TEMPERATURE(F)	/	TEMPERATURE (F)	CALCULATED ENERGY ABSORPTION(FT-LB)
10.0	-46.8	/	-40.0	12.6
15.0	-34.3	/	-30.0	16.9
20.0	-23.1	/	-20.0	21.4
25.0	-12.4	/	-10.0	26.1
30.0	-1.6	/	.0	30.7
35.0	9.4	/	10.0	35.3
40.0	20.9	/	20.0	39.6
45.0	33.2	/	30.0	43.7
50.0	46.5	/	40.0	47.6
55.0	61.3	/	50.0	51.2
60.0	78.3	/	60.0	54.6
65.0	98.6	/	70.0	57.7
70.0	124.7	/	80.0	60.5
		/	90.0	63.0
		/	100.0	65.3
		/	110.0	67.4
		/	120.0	69.2
		/	130.0	70.9
		/	140.0	72.3
		/	150.0	73.6

Appendix G, Table 1C

CHARPY V-NOTCH TEST RESULTS FOR WELD-METAL SPECIMENS TAKEN FROM THE CALLAO ACCIDENT.

CALCULATIONS FOR LATERAL EXPANSION DATA OF LT-LONGITUDINAL WELD-METAL SPECIMENS, WL-
*SEE IDENTIFICATION CODES IN FIGURES 13&15.

SPECIMEN	TEMPERATURE(F)	OBSERVED LATERAL EXPANSION (MILS)	CALCULATED LATERAL EXPANSION (MILS)
WL-14*	-100.0	4.0	4.0
WL-2	-50.0	7.0	8.2
WL-1	-50.0	9.0	8.2
WL-8	15.0	41.0	34.2
WL-7	15.0	48.0	34.2
WL-18	40.0	33.5	44.3
WL-19	40.0	42.0	44.3
WL-9	60.0	55.0	51.1
WL-17	60.0	43.0	51.1
WL-16	100.0	59.0	61.0
WL-15	100.0	56.0	61.0
WL-6	120.0	67.0	64.2
WL-13	120.0	68.0	64.2
WL-12	160.0	66.0	66.0

LATERAL EXPANSION(MILS)	CALCULATED TEMPERATURE(F)	/	TEMPERATURE (F)	CALCULATED LATERAL EXPANSION(MILS)
5.0	-64.1	/	-60.0	5.7
10.0	-44.0	/	-50.0	8.2
15.0	-30.0	/	-40.0	11.3
20.0	-17.8	/	-30.0	15.0
25.0	-6.2	/	-20.0	19.1
30.0	5.2	/	-10.0	23.3
35.0	16.8	/	.0	27.7
40.0	28.9	/	10.0	32.1
45.0	41.9	/	20.0	36.4
50.0	56.5	/	30.0	40.4
55.0	73.5	/	40.0	44.3
60.0	94.9	/	50.0	47.9
		/	60.0	51.1
		/	70.0	54.0
		/	80.0	56.7
		/	90.0	59.0
		/	100.0	61.0
		/	110.0	62.7
		/	120.0	64.2
		/	130.0	65.4

Appendix G, Table 2A

CHARPY V-NOTCH TEST RESULTS FOR WELD-METAL SPECIMENS TAKEN FROM THE CALLAO ACCIDENT.

CALCULATIONS FOR SHEAR FRACTURE APPEARANCE DATA OF TL. TRANSVERSE WELD-METAL SPECIMENS, WM.
*SEE IDENTIFICATION CODES IN FIGURES 10 AND 15.

SPECIMEN	TEMPERATURE(F)	OBSERVED SHEAR FRACTURE (%)	CALCULATED SHEAR FRACTURE (%)
WM-37*	-100.0	.0	2.2
WM-22	-50.0	5.0	6.6
WM-21	-50.0	5.0	6.6
WM-36	-30.0	10.0	10.0
WM-35	-30.0	10.0	10.0
WM-38	-15.0	20.0	13.5
WM-39	-15.0	15.0	13.5
WM-40	-5.0	20.0	16.5
WM-27	15.0	25.0	24.0
WM-28	15.0	20.0	24.0
WM-29	60.0	50.0	50.6
WM-30	60.0	35.0	50.6
WM-23	80.0	70.0	65.5
WM-24	80.0	55.0	65.5
WM-25	120.0	98.0	90.9
WM-26	120.0	90.0	90.9
WM-31	160.0	100.0	99.5
WM-32	160.0	100.0	99.5
WM-33	212.0	100.0	100.0
WM-34	212.0	100.0	100.0

% SHEAR FRACTURE	CALCULATED TEMPERATURE(F)	/	TEMPERATURE (F)	CALCULATED SHEAR FRACTURE(%)
5.0	-62.9	/	-60.0	5.3
10.0	-29.9	/	-50.0	6.6
15.0	-9.7	/	-40.0	8.1
50.0	59.2	/	-30.0	10.0
85.0	108.5	/	-20.0	12.2
90.0	118.1	/	-10.0	14.9
95.0	131.2	/	.0	18.1
98.0	144.6	/	10.0	21.9
		/	20.0	26.3
		/	30.0	31.4
		/	40.0	37.2
		/	50.0	43.6
		/	60.0	50.6
		/	70.0	57.9
		/	80.0	65.5
		/	90.0	72.9

Appendix G, Table 2B

CHARPY V-NOTCH TEST RESULTS FOR WELD-METAL SPECIMENS TAKEN FROM THE CALLAO ACCIDENT.

CALCULATIONS FOR ENERGY ABSORPTION DATA OF TL. TRANSVERSE WELD-METAL SPECIMENS, WM.
*SEE IDENTIFICATION CODES IN FIGURES 10 AND 15.

SPECIMEN	TEMPERATURE(F)	OBSERVED ENERGY ABSORPTION(FT-LB)	CALCULATED ENERGY ABSORPTION(FT-LB)
WM-37*	-100.0	5.0	9.2
WM-22	-50.0	15.0	13.6
WM-21	-50.0	9.0	13.6
WM-36	-30.0	18.0	16.3
WM-35	-30.0	18.0	16.3
WM-38	-15.0	27.0	18.7
WM-39	-15.0	23.0	18.7
WM-40	-5.0	20.5	20.5
WM-27	15.0	19.5	24.7
WM-28	15.0	20.0	24.7
WM-29	60.0	37.5	36.5
WM-30	60.0	35.0	36.5
WM-23	80.0	42.0	42.2
WM-24	80.0	39.5	42.2
WM-25	120.0	55.0	52.4
WM-26	120.0	51.0	52.4
WM-31	160.0	62.0	58.3
WM-32	160.0	58.0	58.3
WM-33	212.0	59.0	60.1
WM-34	212.0	59.5	60.1

ENERGY ABSORPTION	CALCULATED TEMPERATURE(F)	/	TEMPERATURE (F)	CALCULATED ENERGY ABSORPTION(FT-LB)
10.0	-88.5	/	-80.0	10.7
15.0	-39.1	/	-70.0	11.5
20.0	-7.9	/	-60.0	12.5
25.0	16.1	/	-50.0	13.6
30.0	36.5	/	-40.0	14.9
35.0	54.8	/	-30.0	16.3
40.0	72.4	/	-20.0	17.9
45.0	90.1	/	-10.0	19.6
50.0	109.5	/	.0	21.5
55.0	133.9	/	10.0	23.6
60.0	200.3	/	20.0	25.9
		/	30.0	28.3
		/	40.0	30.9
		/	50.0	33.6
		/	60.0	36.5
		/	70.0	39.3
		/	80.0	42.2
		/	90.0	45.0
		/	100.0	47.6
		/	110.0	50.1

Appendix G, Table 2C

CHARPY V-NOTCH TEST RESULTS FOR WELD-METAL SPECIMENS TAKEN FROM THE CALLAO ACCIDENT.

CALCULATIONS FOR LATERAL EXPANSION DATA OF TL. TRANSVERSE WELD-METAL SPECIMENS, WM. *SEE IDENTIFICATION CODES IN FIGURES 10 AND 15.

SPECIMEN	TEMPERATURE (F)	OBSERVED LATERAL EXPANSION (MILS)	CALCULATED LATERAL EXPANSION (MILS)
WM-37*	-100.0	2.0	7.4
WM-22	-50.0	15.5	12.8
WM-21	-50.0	9.0	12.8
WM-36	-30.0	17.0	15.9
WM-35	-30.0	17.0	15.9
WM-38	-15.0	27.0	18.8
WM-39	-15.0	23.5	18.8
WM-40	-5.0	18.0	20.9
WM-27	15.0	20.0	25.7
WM-28	15.0	19.0	25.7
WM-29	60.0	39.0	38.3
WM-30	60.0	34.0	38.3
WM-23	80.0	44.0	44.1
WM-24	80.0	40.0	44.1
WM-25	120.0	59.0	53.8
WM-26	120.0	54.0	53.8
WM-31	160.0	61.0	58.9
WM-32	160.0	56.0	58.9
WM-33	212.0	61.0	60.3
WM-34	212.0	59.0	60.3

LATERAL EXPANSION (MILS)	CALCULATED TEMPERATURE (F)	TEMPERATURE (F)	CALCULATED LATERAL EXPANSION (MILS)
10.0	-71.9	-70.0	10.2
15.0	-35.5	-60.0	11.4
20.0	-9.1	-50.0	12.8
25.0	12.4	-40.0	14.3
30.0	31.3	-30.0	15.9
35.0	48.7	-20.0	17.8
40.0	65.7	-10.0	19.8
45.0	83.1	.0	22.0
50.0	102.2	10.0	24.4
55.0	124.4	20.0	27.0
60.0	185.3	30.0	29.6
		40.0	32.5
		50.0	35.4
		60.0	38.3
		70.0	41.3
		80.0	44.1
		90.0	46.9
		100.0	49.5
		110.0	51.8
		120.0	53.8

Appendix H

Results of Elevated-Temperature Dynamic-Tear Test of Head-Plate K-1

Appendix H, Table 1B

(See Appendix B, Table 3A for Corresponding Results of Shear Fracture Appearance)

RESULTS OF ELEVATED-TEMPERATURE DYNAMIC-TEAR TESTS OF HEAD PLATE K-1 FROM THE CALLAO ACCIDENT.
*SEE IDENTIFICATION CODES IN FIGURES 4 AND 15.

CALCULATIONS FOR ENERGY ABSORPTION DATA OF LONGITUDINAL (LT)* SPECIMENS.

SPECIMEN	TEMPERATURE(F)	OBSERVED ENERGY ABSORPTION(FT-LB)	CALCULATED ENERGY ABSORPTION(FT-LB)
HDTL-69*	-50.0	51.0	51.0
HDTL-58	.0	91.0	59.7
HDTL-56	.0	57.0	59.7
HDTL-55	30.0	58.0	216.9
HDTL-71	30.0	334.0	216.9
HDTL-60	60.0	420.0	459.1
HDTL-72	60.0	530.0	459.1
HDTL-57	80.0	415.0	572.0
HDTL-70	80.0	652.0	572.0
HDTL-59	120.0	662.0	650.1
HDTL-61	120.0	646.0	650.1
HDTL-64	160.0	602.0	614.1
HDTL-65	200.0	609.0	600.6
HDTL-62	300.0	589.0	590.7
HDTL-67	500.0	554.0	553.8
HDTL-66	888.0	459.0	459.0
HDTL-63	1278.0	859.0	859.0

ENERGY ABSORPTION	CALCULATED TEMPERATURE(F)	/	TEMPERATURE (F)	CALCULATED ENERGY ABSORPTION(FT-LB)
55.0	-2.9	/	.0	59.7
95.0	11.0	/	10.0	90.7
135.0	18.4	/	20.0	144.7
170.0	23.7	/	30.0	216.9
210.0	29.1	/	40.0	299.3
250.0	34.1	/	50.0	382.7
290.0	38.9	/	60.0	459.1
330.0	43.6	/	70.0	523.0
370.0	48.4	/	80.0	572.0
410.0	53.4	/	90.0	606.6
450.0	58.7	/	100.0	629.1
490.0	64.6	/	110.0	642.6
530.0	71.3	/	120.0	650.1
570.0	79.5	/	130.0	653.9
610.0	91.3	/	140.0	655.7
650.0	119.8	/		

Appendix H, Table 2B

(See Appendix C, Table 5A for Corresponding Results of Shear Fracture Appearance)

RESULTS OF ELEVATED-TEMPERATURE DYNAMIC-TEAR TESTS OF HEAD PLATE K-1 FROM THE CALLAO ACCIDENT.
*SEE IDENTIFICATION CODES IN FIGURES 4 AND 15.

CALCULATIONS FOR ENERGY ABSORPTION DATA OF TRANSVERSE (TL)* SPECIMENS.

SPECIMEN	TEMPERATURE(F)	OBSERVED ENERGY ABSORPTION(FT-LB)	CALCULATED ENERGY ABSORPTION(FT-LB)
HDTT-45*	-50.0	53.0	53.3
HDTT-53	.0	44.0	55.3
HDTT-52	30.0	61.0	60.2
HDTT-39	30.0	56.0	60.2
HDTT-49	60.0	33.0	74.6
HDTT-38	80.0	106.0	96.6
HDTT-54	80.0	108.0	96.6
HDTT-47	100.0	158.0	137.4
HDTT-42	120.0	214.0	204.8
HDTT-37	140.0	251.0	294.8
HDTT-44	160.0	421.0	375.4
HDTT-40	200.0	408.0	414.4
HDTT-46	300.0	407.0	419.9
HDTT-50	500.0	444.0	420.3
HDTT-48	691.0	419.0	447.9
HDTT-41	890.0	394.0	373.5
HDTT-51	1084.0	204.0	212.2
HDTT-43	1279.0	494.0	492.7

ENERGY ABSORPTION	CALCULATED TEMPERATURE(F)	/	TEMPERATURE (F)	CALCULATED ENERGY ABSORPTION(FT-LB)
55.0	-3.5	/	.0	55.3
75.0	60.6	/	10.0	56.4
95.0	78.9	/	20.0	57.9
110.0	87.9	/	30.0	60.2
130.0	97.1	/	40.0	63.4
150.0	104.5	/	50.0	68.0
170.0	110.7	/	60.0	74.6
190.0	116.3	/	70.0	83.8
210.0	121.3	/	80.0	96.6
230.0	125.9	/	90.0	114.0
250.0	130.4	/	100.0	137.4
270.0	134.7	/	110.0	167.5
290.0	139.0	/	120.0	204.8
310.0	143.3	/	130.0	248.2
330.0	147.8	/	140.0	294.8
350.0	152.7	/	150.0	339.3
370.0	158.3	/	160.0	375.4
390.0	165.5	/	170.0	398.9
410.0	179.7	/	180.0	410.2
		/	190.0	413.8

Appendix I

Results of Elevated-Temperature Dynamic-Tear Tests of Shell-Plate K-5

Appendix I, Table 1B

(See Appendix D, Table 3A for Corresponding Results of Shear Fracture Appearance)

RESULTS OF ELEVATED-TEMPERATURE DYNAMIC-TEAR TESTS OF SHELL PLATE K-5 FROM THE CALLAO ACCIDENT.
*SEE IDENTIFICATION CODES IN FIGURES 7 AND 15

CALCULATIONS FOR ENERGY ABSORPTION DATA OF LONGITUDINAL (LT)* SPECIMENS.

SPECIMEN	TEMPERATURE (F)	OBSERVED ENERGY ABSORPTION (FT-LB)	CALCULATED ENERGY ABSORPTION (FT-LB)
SDTL-23*	-50.0	56.0	56.9
SDTL-32	.0	46.0	63.7
SDTL-20	30.0	76.0	83.4
SDTL-35	30.0	97.0	83.4
SDTL-27	60.0	144.0	148.2
SDTL-21	80.0	208.0	249.6
SDTL-36	80.0	262.0	249.6
SDTL-29	120.0	535.0	618.4
SDTL-22	120.0	712.0	618.4
SDTL-30	160.0	747.0	745.8
SDTL-34	160.0	745.0	745.8
SDTL-24	200.0	706.0	709.7
SDTL-33	300.0	682.0	680.4
SDTL-31	500.0	714.0	714.9
SDTL-26	682.0	664.0	663.4
SDTL-28	884.0	477.0	477.3
SDTL-19	1085.0	464.0	463.9
SDTL-25	1277.0	894.0	894.0

ENERGY ABSORPTION	CALCULATED TEMPERATURE (F)	/	TEMPERATURE (F)	CALCULATED ENERGY ABSORPTION (FT-LB)
95.0	38.5	/	40.0	97.4
135.0	56.1	/	50.0	118.1
175.0	66.7	/	60.0	148.2
210.0	73.6	/	70.0	190.9
250.0	80.1	/	80.0	249.6
290.0	85.6	/	90.0	326.3
330.0	90.4	/	100.0	419.7
370.0	94.9	/	110.0	522.1
410.0	99.0	/	120.0	618.4
450.0	103.0	/	130.0	690.8
490.0	106.9	/	140.0	730.1
530.0	110.8	/	150.0	743.5
570.0	114.8	/		
610.0	119.0	/		
650.0	123.9	/		
690.0	129.9	/		
730.0	140.0	/		

Appendix I, Table 2B

(See Appendix E, Table 3B for Corresponding Results of Shear Fracture Appearance)

RESULTS OF ELEVATED-TEMPERATURE DYNAMIC-TEAR TESTS OF SHELL PLATE K-5 FROM THE CALLAO ACCIDENT.
*SEE IDENTIFICATION CODES IN FIGURES 7 AND 15.

CALCULATIONS FOR ENERGY ABSORPTION DATA OF TRANSVERSE (TL)* SPECIMENS.

SPECIMEN	TEMPERATURE(F)	OBSERVED ENERGY ABSORPTION(FT-LB)	CALCULATED ENERGY ABSORPTION(FT-LB)
SDTT-10*	-50.0	52.0	52.3
SDTT-1	.0	57.0	57.7
SDTT-2	30.0	73.0	75.6
SDTT-17	30.0	89.0	75.6
SDTT-16	60.0	133.0	128.3
SDTT-7	60.0	108.0	128.3
SDTT-3	80.0	159.0	193.8
SDTT-18	80.0	238.0	193.8
SDTT-12	120.0	327.0	342.9
SDTT-5	120.0	359.0	342.9
SDTT-14	160.0	378.0	376.3
SDTT-4	200.0	375.0	376.5
SDTT-6	300.0	355.0	352.5
SDTT-8	500.0	344.0	349.2
SDTT-11	684.0	344.0	337.7
SDTT-9	892.0	284.0	288.3
SDTT-13	1088.0	259.0	257.2
SDTT-15	1273.0	369.0	369.3

ENERGY ABSORPTION	CALCULATED TEMPERATURE(F)	/	TEMPERATURE (F)	CALCULATED ENERGY ABSORPTION(FT-LB)
55.0	-12.2	/	-10.0	55.4
75.0	29.4	/	.0	57.7
95.0	44.5	/	10.0	61.4
110.0	52.3	/	20.0	67.1
130.0	60.6	/	30.0	75.6
150.0	67.5	/	40.0	87.9
170.0	73.5	/	50.0	105.1
190.0	79.0	/	60.0	128.3
210.0	84.1	/	70.0	157.9
230.0	89.0	/	80.0	193.8
250.0	93.8	/	90.0	234.2
270.0	98.6	/	100.0	275.6
290.0	103.6	/	110.0	313.3
310.0	109.0	/	120.0	342.9
330.0	115.2	/	130.0	362.0
350.0	123.1	/	140.0	371.7
370.0	137.5	/	150.0	375.4